MAÍSA QUINTILIANO ALVES

UNVEILING THE FUTURE OF LAND RECLAMATION FOR MINING AREAS: PLANT SPECIES RESPONSES TO CLIMATE CHANGE-RELATED EVENTS IN THE BRAZILIAN LEGAL AMAZON

Thesis submitted to the Agricultural Engineering Graduate Program of the Universidade Federal de Viçosa in partial fulfillment of the requirements for the degree of *Doctor Scientiae*.

Adviser: Rubens Alves de Oliveira

Co-advisers: Carlos A. Brasileiro de Alencar
Fernando Franca da Cunha
Rafael Gomes Viana
Paulo Roberto Cecon

VIÇOSA - MINAS GERAIS
2024

Ficha catalográfica elaborada pela Biblioteca Central da Universidade Federal de Viçosa - Campus Viçosa

T
A474u
2024

Alves, Maísa Quintiliano, 1992-
Unveiling the future of land reclamation for mining areas: plant species responses to climate change-related events in Brazilian Legal Amazon / Maísa Quintiliano Alves. – Viçosa, MG, 2024.
1 tese eletrônica (117 f.): il. (algumas color.).

Texto em inglês.
Inclui apêndices.
Orientador: Rubens Alves de Oliveira.
Tese (doutorado) - Universidade Federal de Viçosa, Departamento de Engenharia Agrícola, 2024.
Inclui bibliografia.
DOI: https://doi.org/10.47328/ufvbbt.2024.337
Modo de acesso: World Wide Web.

1. Mudanças climáticas. 2. Secas. 3. Recuperação ecológica - Amazônia. 4. Minas e recursos minerais - Amazônia.
I. Oliveira, Rubens Alves de , 1961-. II. Universidade Federal de Viçosa. Departamento de Engenharia Agrícola. Programa de Pós-Graduação em Engenharia Agrícola. III. Título.

CDD 22. ed. 551.5253

Bibliotecário(a) responsável: Alice Regina Pinto Pires CRB-6/2523

MAÍSA QUINTILIANO ALVES

UNVEILING THE FUTURE OF LAND RECLAMATION FOR MINING AREAS: PLANT SPECIES RESPONSES TO CLIMATE CHANGE-RELATED EVENTS IN THE BRAZILIAN LEGAL AMAZON

Thesis submitted to the Agricultural Engineering Graduate Program of the Universidade Federal de Viçosa in partial fulfillment of the requirements for the degree of *Doctor Scientiae*.

APPROVED: April 29, 2024.

Assent:

Documento assinado digitalmente
gov.br
MAISA QUINTILIANO ALVES
Data: 15/07/2024 20:00:57-0300
Verifique em https://validar.iti.gov.br

Maísa Quintiliano Alves
Author

Documento assinado digitalmente
gov.br
RUBENS ALVES DE OLIVEIRA
Data: 15/07/2024 14:51:11-0300
Verifique em https://validar.iti.gov.br

Rubens Alves de Oliveira
Adviser

To God and to my parents.

ACKNOWLEDGEMENTS

To God, who gave me everything, who taught me what I needed to learn, who supported me when I had no strength left, who showed me that a new day always comes.

To my father, Lindolfo Alves Filho, my eternal and best friend, who taught me to believe that anything is possible, who helped me breathe when the air was lacking, who carried me when I couldn't walk, who taught me what true love is and never left me alone in any moment of this journey, even when he was no longer physically present. To you, I owe everything.

To my mother, Olga Maria Quintiliano Alves, an example of strength, perseverance, struggle, and self-love, a role model of a woman, my greatest treasure, who made me continue when I wanted to give up, who did the impossible so that I could follow this path, who often thought of me before herself. I am a part of you; thank you for giving me life and teaching me how to live it.

To my friends and boyfriend, who are my joy, who reminded me of who I was when I felt lost, who were present in the most difficult moments of my life. I know I chose the best human beings to share this life with me.

To my mentors, for empathy, patience, autonomy, trust, and friendship. I am immensely grateful for all the knowledge and opportunities provided.

To my colleagues at work in Pará, for the laughter that helped me endure the worst days and for sharing the good days with me. Thank you for all the support, for sharing a bit of your story with me, and for making me feel loved when I was far from home.

To the Federal University of Viçosa, for granting me the invaluable opportunity to explore and cultivate my potential, thereby experiencing the most enriching days of my life.

To the Conselho Nacional de Desenvolvimento Científico e Tecnológico (CNPq), the Fundação de Amparo à Pesquisa do Estado de Minas Gerais (FAPEMIG), and the Coordenação de Aperfeiçoamento de Pessoal de Nível Superior (CAPES) for fostering scientific progress.

To Vale S.A., for funding the project that led to this thesis and for giving me the opportunity to experience so many unique and enriching experiences throughout my education.

To the Coordenação de Aperfeiçoamento de Pessoal de Nível Superior (CAPES), to granting the scholarship.

This study was financed in part by the Coordenação de Aperfeiçoamento de Pessoal de Nível Superior – Brasil (CAPES) – Finance Code 001.

“Imagination is more important than knowledge”

(Albert Einstein)

ABSTRACT

ALVES, Maísa Quintiliano, D.Sc., Universidade Federal de Viçosa, April, 2024. **Unveiling the future of land reclamation for mining areas: plant species responses to climate change-related events in the Brazilian Legal Amazon**. Adviser: Rubens Alves de Oliveira. Co-advisers: Carlos Augusto Brasileiro de Alencar, Fernando Franca da Cunha, Rafael Gomes Viana and Paulo Roberto Cecon.

The increase in atmospheric CO_2 concentrations triggers a transient response in climate, leading to global temperature rise. As the climate warms, extreme events intensify. Given the global significance of the Amazon and the increasing efforts for environmental recovery in the region, this study aimed to understand the relationship between local land-use changes and the occurrence of extreme climate events in an area influenced by mining activities within the Brazilian Legal Amazon. Additionally, it sought to assess the impact of water deficit on the photosynthesis and growth of fast-growing species used in the reclamation of mining areas, growing under elevated atmospheric CO_2 levels. Results suggested that large-scale deforestation has a regional impact occasionally outweighing local effect. Significant trends reveal a general pattern of drought that has been more intense in the north of the study area, regardless of land cover, whether preserved or deforested. Moreover, the dry season is getting drier, but the wet season is not getting wetter over the entire area, and extreme events are becoming more frequent. Regarding the impact on vegetation, our findings do not provide substantial evidence that the assessed species used in the reclamation of mining areas in the region will be profoundly impacted by the rise in atmospheric CO_2 and intense drought events—particularly concerning plant growth and biomass production. Nonetheless, they might be affected by extreme heat. Ultimately, notable attention is directed towards a considerable reduction in the emergence of Pigeon pea individuals, which declined by half in resource-rich environments (elevated atmospheric CO_2 and irrigation). This decline is likely a consequence of interspecific competition within the chambers and may indicate a shift in the composition of developing vegetation.

Keywords: Climate-change. Drought. Land-reclamation. The-Amazon. Mining.

RESUMO

ALVES, Maísa Quintiliano, D.Sc., Universidade Federal de Viçosa, abril de 2024. **Revelando o futuro da recuperação de áreas degradadas na mineração: respostas de espécies vegetais a eventos relacionados às mudanças climáticas na Amazônia Legal Brasileira**. Orientador: Rubens Alves de Oliveira. Coorientadores: Carlos Augusto Brasileiro de Alencar, Fernando Franca da Cunha, Rafael Gomes Viana e Paulo Roberto Cecon.

O aumento nas concentrações atmosféricas de CO_2 desencadeia uma resposta transitória no clima, resultando no aumento da temperatura global. À medida que o clima se aquece, eventos extremos se intensificam. Em razão da importância global da Amazônia e os crescentes esforços de recuperação ambiental na região, este estudo teve como objetivo compreender a relação entre mudanças locais no uso da terra e a ocorrência de eventos climáticos extremos em uma área influenciada por atividades de mineração na Amazônia Legal brasileira. Além disso, buscou avaliar o impacto do déficit hídrico na fotossíntese e no crescimento de espécies de crescimento rápido usadas na recuperação de áreas de mineração, sob elevados níveis de CO_2. Os resultados sugerem que o desmatamento em larga escala tem um impacto regional que ocasionalmente supera os efeitos locais. Tendências significativas revelam um padrão geral de seca mais intensa na parte norte da área de estudo, independentemente da cobertura do solo, seja preservada ou desmatada. Ademais, a estação seca está se tornando mais seca, mas a estação chuvosa não está se tornando mais úmida em toda a área, e eventos extremos estão se tornando mais frequentes. No que tange os impactos na vegetação, nossos achados não fornecem evidências substanciais de que as espécies avaliadas utilizadas na recuperação de áreas de mineração na região serão profundamente impactadas pelo aumento de CO_2 atmosférico e eventos intensos de seca, especialmente no que diz respeito ao crescimento vegetal e à produção de biomassa. No entanto, elas podem ser afetadas pelo calor extremo. Finalmente, chamamos atenção para uma redução considerável na emergência de indivíduos de Feijão-guandu, que diminuíram pela metade em ambientes com plena disponibilidade de recursos (CO_2 atmosférico elevado e água). Essa diminuição é provavelmente uma consequência da competição interespecífica dentro das câmaras e pode indicar uma mudança na composição da vegetação em desenvolvimento.

Palavras-chave: Mudanças-climáticas; Seca; Recuperação-de-areas-degradadas; Amazônia; Mineração.

SUMMARY

1. INTRODUCTION

In the pre-industrial period, the atmospheric CO_2 concentration was around 280 ppm (FAN et al., 2020). From 1850 to 2019, human activities released circa 2400 $GtCO_2$ into the atmosphere, increasing the concentration to 410 ppm. In the worst-case emissions scenario, atmospheric CO_2 concentration is expected to reach 700 ppm before 2070. As a transient climate response (i.e., greenhouse effect), the temperature has risen, warming thus the global surface in 1.09°C (relative to 1850–1900) (ARIAS et al., 2023). As the climate warms, the severity of extreme events, both dry and wet, intensifies.

The Sixth Assessment Report of the Intergovernmental Panel on Climate Change (IPCC) has illustrated that there is strong evidence linking human activities to climate change. Changes in land use plays a leading role in carbon emissions in Brazil, where deforestation to establish pastures plays a leading role in threatening the environmental sustainability in the southeastern Brazilian Amazon (GATTI et al. 2021; HASE UETA et al. 2023).

Due to global warming, in the eastern Amazon, particularly, the dry season is generally getting drier, with the increase of consecutive dry days (LUCAS et al., 2021; MU & JONES, 2022; SANTOS et al., 2020). Additionally, the wet season is also getting wetter in certain areas, accompanied eventually by more intense rainfall. Changes in the water cycle are likely to result in greater variability in soil moisture. Some regions in the eastern Amazon are foreseen to experience agricultural and ecological droughts, impacting local vegetation (ARIAS et al., 2023).

In this region, ongoing projects and a novel proposal for a bold large-scale restoration, the “Arc of restoration” (DA CRUZ et al. 2021; TORRES 2022), have attracted worldwide attention. Actions of this size can generate positive environmental impacts that go beyond the borders of the country. However, climate change potentially affects plants’ growth and survival, including seedlings and newly recruited trees (OMETTO et al. 2022). Thus, understanding how the local climate has been affected by changes in land use and the local pattern of these changes, is crucial for the feasibility of Arc of deforestation initiative in a region of global importance.

Potential impacts of climate change on tropical forest biomes must be considered in the early designing step of restoration projects, but such impacts are still uncertain. It is pressing, thus, to understand how plants used in restoration physio- and morphologically respond to rising CO_2 and temperature, likely accompanied by water deficit. There is a consensus that plants can adapt (i.e., acclimate/downregulate) to moderate temperature increases in tropical biomes, but inconsistencies regarding how well they can acclimate and

whether their grow rate increases as a result of the CO_2 fertilization effect are pointed out (OMETTO et al., 2022).

All considered, the **general objective** of this study is to assess the impact of water deficits resulting from an increase in extreme precipitation events on the photosynthesis and growth of fast-growing species utilized in the reclamation of mining areas within the Brazilian Legal Amazon. To achieve this objective, it is imperative to first understand the relationship between local land use change and the occurrence of extreme precipitation events.

As a guiding framework, we explore two **hypotheses**:

- Local shifts in land use and land cover in the eastern Brazilian Legal Amazon are impacting the local climate by increasing the frequency of extreme precipitation events.

- Changes in precipitation patterns and the increasing occurrence of extreme precipitation events, as well as the increase in atmospheric CO_2 impair the establishment and development of fast-growing species used in the reclamation of mining areas in the eastern Brazilian Legal Amazon.

The findings of this research, conducted under conditions of elevated atmospheric CO_2, provide valuable insights for prospective restoration and reforestation initiatives that must account for the effects of climate change.

2. LITERATURE REVIEW

2.1. Carbon dioxide and climate change

In the pre-industrial period, the atmospheric CO_2 concentration was around 280 ppm (FAN et al., 2020). From 1850 to 2019, human activities released circa 2400 $GtCO_2$ into the atmosphere, increasing the concentration to 410 ppm. In the worst-case emissions scenario, atmospheric CO_2 concentration is expected to reach 700 ppm before 2070. As a transient climate response (i.e., greenhouse effect), the temperature has risen attendant to CO_2 levels, nearly 1.65°C per 1000 PgC, warming thus the global surface in 1.09°C (relative to 1850–1900) (ARIAS et al., 2023).

As the climate warms, the severity of extreme events, both dry and wet, intensifies. While annual precipitation is expected to increase with rising temperatures in South America, its distribution will experience a great geographical variation driven by changes in circulation

patterns. This raises significant concerns, as aridity is expected to increase in traditionally moist regions and important carbon sinks, such as the Amazon basin. Conversely, there are predictions of catastrophic floods, particularly in urban areas (ARIAS et al., 2023).

In this section, it is imperative to underscore that while CO_2 do not hold the highest Global Warming Potential (GWP) among the Greenhouse Gases (GHG), it holds paramount significance due to its prevalence in the atmosphere, rendering it the most hazardous. Therefore, CO_2 is typically used as reference to express the forcing radiation of accumulated concentration of further GHG to a certain time-horizon in the future (see Table 1) (FOSTER et al., 2007).

Table 1 – Lifetimes, and global warming potentials (GWP) of Greenhouse Gases (GHG) relative to CO_2 in a time horizon of 20, 100 and 500 years.

Compound	**Chemical formula**	**Lifetime in Atmosphere (years)**	**Global Warming Potential**		
			20-year	**100-year**	**500-year**
Carbon dioxide	CO_2	variable	1	1	1
Methane	CH_4	10.8	67	23	6.9
Nitrous oxide	N_2O	114	291	298	153
HFC-23	CHF_3	270	12,000	14,800	12,200
HCFC-22	$CHClF_2$	12	5,200	1,800	550
Sulphur hexafluoride	SF_6	3,200	16,300	23,900	34,900
PFC-116	C_2F_6	10,000	8,600	12,200	18,200

Summarized and adapted from Foster et al. (2007).

The water vapor, the most influential greenhouse gas in the Earth's atmosphere, which contributes to approximately half of the current greenhouse effect, is not indicated in Foster et al. (2007)'s list. One reason is that, although water exhibits greater radiative flux than other GHG, CO_2 included, water can condense and precipitate. Consequently, water vapor has a mean lifespan of less than two weeks, in contrast to years or more for other greenhouse gases, rendering its 100-year GWP negligible (SHERWOOD; DIXIT; SALOMEZ, 2018).

Action plans have been elaborated worldwide aiming the GHG emissions mitigation. Those plans are specific to each country, but Brazil can particularly benefit from climate action, as it has several competitive advantages, such as low-carbon energy supply and renewable energy potential. In the country, agriculture and deforestation pose the greatest sources of carbon emission. Interestingly, reaching zero illegal deforestation, restoring/reforesting degraded areas and improving pasture management are critical actions for the country to reach

the so-called net zero CO_2 emission by 2050, i.e., when CO_2 removals exceed anthropogenic emissions (THE WORLD BANK GROUP, 2023).

2.2. Land use land cover changes contribution to greenhouse gases emissions

The Sixth Assessment Report of the Intergovernmental Panel on Climate Change (IPCC) has illustrated that there is strong evidence linking human activities to climate change. Notably, factors such as aerosol emissions and significant alterations in land use, particularly deforestation, are identified as key contributors to this impactful global phenomenon (2021). As aforementioned, changes in land use plays a leading role in carbon emissions in Brazil. Despite its impact on the destruction of trees that sequester significant carbon, deforestation is also associated with fires and the introduction of cattle herds, contributing to the release of methane into the atmosphere.

2.3. The Amazon and mining activity in the eastern Pará

Land use land cover in eastern Amazon region has been changing over the years according to the implementation of different development programs, which were far from sustainable. Current human occupation in the region began in 1890 with subsistence farming and plant extractivism (Rubber tree latex and Brazil nuts). Between 1950-1970, the "Amazon Operation" project was implemented, intending to transform the entire Amazon into a large producer of grains, meat, timber, and sugarcane. It came with the development of many logging centers and deforestation in Maranhão. Years later, several economical and settlement projects were developed, encouraging logging, large-scale farming, and industrial mining in the entire region (MAGALHÃES et al., 2016; SANT'ANA JÚNIOR; ALVES, 2017).

The region's mineral potential was revealed in 1967 but the exploration booster only happened in the 1980s with the implementation of the Iron Ore project. The EFC, built in 1985, provided ore transportation and the expansion of mining. Currently, the railroad of approximately 1,000 km connects the S11D project, in Canaã dos Carajás (PA), to the Terminal da Madeira port, in São Luiz (MA). Mining activity and the railroad construction deeply impacted the settlement dynamic and the environment in the region, but the cattle raising is pointed out as the larger source of impact due to its extension (CRISTO; SANTOS; MATLABA, 2022a; MAGALHÃES et al., 2016). Due to prolonged and extensive deforestation

over the years, this segment of the Legal Amazon is associated with the so-called “Arc of deforestation”, the most deforested area in this biome (CAVALCANTE et al. 2019).

Presently, the regional economy is based on cattle raising and mining (MAGALHÃES et al., 2016). Some authors discussed the regional social vulnerability, highlighting worse conditions in Maranhão municipalities, due also to its historical development process. Land conflicts, the violence driven by the polarization between native people and the capitalism expansion, and the increasing occurrence of severe violation of human rights, such as analogous-to-slavery labor regime, are examples of social impacts associated with land use changes in the territory (CELENTANO et al., 2017; CRISTO; SANTOS; MATLABA, 2022a, 2022b; SANT’ANA JÚNIOR; ALVES, 2017).

2.4. Amazon climate patterns and forecasts in the context of climate change

The climate of South America (SA) is intricately shaped by both large- and local-scale circulation mechanisms, playing a pivotal role in determining the considerable spatial and temporal variability of rainfall across the Amazon region (MU and JONES 2022). This area witnesses substantial fluctuations in rainfall, characterized by a pronounced dry season in the southern Amazon and an absence of a dry season in the northwest region (MARENGO et al. 2018). Notably, the eastern part is significantly influenced by the El Niño/Southern Oscillation (ENSO), the Intertropical Convergence Zone (ITCZ), and sea surface temperatures (SSTs) (Haghtalab et al. 2020).

Recent observations indicate general downward trends in precipitation and rising air temperatures in South America, accompanied by a heightened frequency of extreme events in the Amazon (LUCAS et al. 2021; ARIAS et al. 2023; BOCHOW and BOERS 2023). Particularly, Haghtalab et al. (2020)’s evaluation of precipitation trends across the Amazon basin revealed a significant drying trend in the eastern region, albeit excluding the area influenced by the Amazon's deforestation. Similarly, trends in extreme precipitation and temperature events in Maranhão, situated between the Amazon and the Cerrado, unveil varying climate changes in the eastern Amazon. Close to our study area, negative trends in some precipitation indices, such as maximum five-day precipitation, were observed, along with an increase in consecutive dry days.

Mu and Jones (2022) also demonstrated distinct spatial distribution of rainfall trends during the rainy season in the Brazilian Legal Amazon. They highlighted significant areas experiencing negative precipitation trends over the Arc of Deforestation, particularly during the

dry season. In our study area's proximity, similar heterogeneity in trends was documented. Negative trends in some precipitation indices, like maximum precipitation in five days, and an increase in consecutive dry days were noticed (LUCAS et al. 2021; SANTOS et al. 2020).

Finally, in line with the latest IPCC report on climate change (2023), the region is anticipated to experience a rise in average temperatures, increased drought conditions, and heightened occurrences of extreme heat. Moreover, a reduction in both total and average precipitation is projected, along with an intensification of precipitation events. Projections also indicate a surge in the intensity and frequency of meteorological droughts in the eastern Amazon, which may profoundly affect the local vegetation.

2.5. Pivotal physiological processes in plants

2.5.1. Leaf respiration

Two cellular processes drive plants' growth: respiration and photosynthesis. The net result between those processes reflects the growth rate. **Respiration** is pivotal for survival and development of plants as it provides energy and carbon precursors for biosynthesis (SLOT; KITAJIMA, 2015). During this physiological process, plants undergo oxygen consumption and sugar oxidation to acquire energy, which is transiently stored in the form of Adenosine Triphosphate (ATP) for subsequent utilization in various cellular processes (eq.1). The oxygen serves as final electrons acceptor, being reduced to water, and the sugar is oxidated to CO_2 throughout controlled reactions. The respiration process outputs are, thus, CO_2 and water, which are exactly the input of photosynthesis (eq.2) (TAIZ et al., 2017).

$$C_6H_{12}O_6 + 6\,H_2O + 6\,O_2 \rightarrow 12\,H_2O + 6\,CO_2 + Energia \qquad (1)$$

$$6\,CO_2 + 12\,H_2O \rightarrow C_6H_{12}O_6 + 6\,O_2 + 6\,H_2O \qquad (2)$$

2.5.2. Photosynthesis

As the name suggests, **photosynthesis** is the synthesis of complex organic compounds using the energy that came from light (*photo*). It takes place in two sequential stages, the light-dependent reactions and Calvin-Benson Cycle. In the first stage water hydrolysis provides electrons for the electron transport chain during the first stage of photosynthesis, supporting the generation of high energetic molecules: Nicotinamide Adenine Dinucleotide Phosphate (NADPH) and ATP (Fig.1) (TAIZ et al., 2017).

Figure 1 – Initial stage of photosynthesis: The light-dependent reactions take place in thylakoid membrane of the chloroplasts in plant cells. It starts with the hydrolysis of water molecules releasing electrons that are excited by the energy of light in Photosystems I (P680) and II (P700). The electrons are transported along a chain of important proteins, enzymes and lipidic molecules in a cyclic or acyclic pathway, generating energetic molecules (ATP and NADPH), which are used in the second stage of photosynthesis to assimilate the atmospheric carbon and promote the regeneration of RuBP

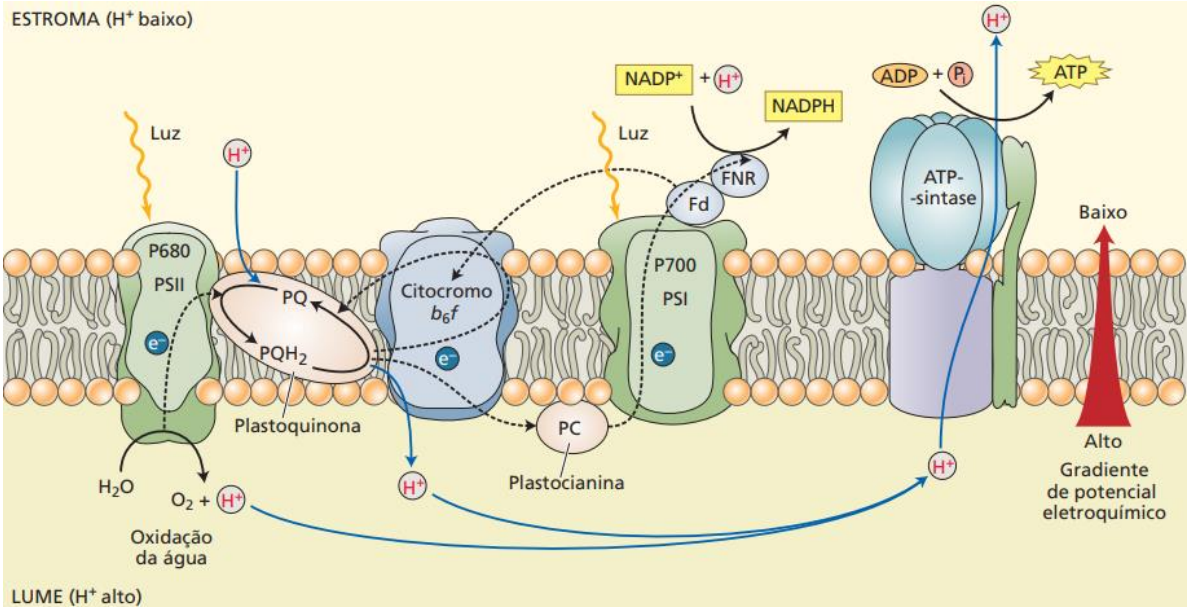

Taiz et al. (2017)

2.5.2.1. C_3 Photosynthesis

During the second stage of photosynthesis, a key enzyme of Calvin-Benson Cycle, Ribulose-1,5-bisphosphate carboxylase/oxygenase (RuBisCo), uses the Ribulose-1,5-bisphosphate (RuBP) as a substrate to fixate the CO_2 taken from atmosphere into 3-phosphoglycerate (PGA). It is known as a carboxylation reaction. Through a series of sequential reactions using those energetic coins previously generated in the first stage, the PGA is converted to 1,3-bisphosphoglycerate (PGAL), a precursor of glucose molecule. An important step of the cycle is the regeneration of RuBP, which takes place after the generation of PGAL at an energetic cost, ensuring the continuality of the cycle (TAIZ et al., 2017) (Fig.2).

Figure 2 – Second stage of photosynthesis: The light-independent reactions (Calvin-Benson Cycle) occur in stromal matrix of the chloroplasts in C_3 plants and in the bundle sheath cells in C_4 species. It starts with RuBP carboxylation catalyzed by RuBisCo, followed by a reduction reaction generating PGAL, precursor of glucose. The final step is the regeneration of RuBP from further PGAL molecules at energetic cost, supporting the continuity of the cycle

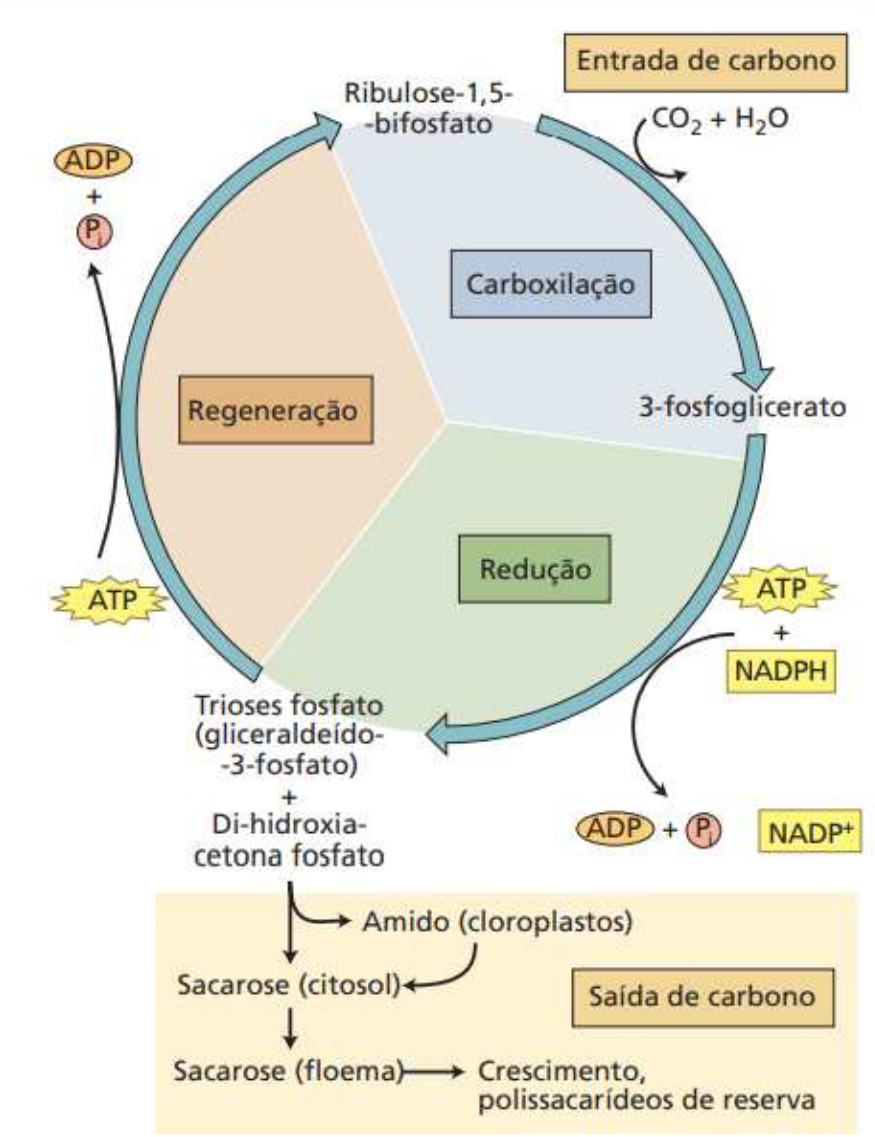

Taiz et al. (2017)

2.5.2.2. Photorespiration

During the Calvin-Benson Cycle, RuBisCo can fixate the atmospheric O_2 instead of CO_2 by catalyzing the oxygenation reaction of RuBP. The carbon release in the form of CO_2 is the result of this counterproductive process known as **photorespiration**, which reduces photosynthetic efficiency, as it competes with photosynthesis for the same substrate (RuBP) and consumes energy. Although counterproductive, photorespiration brings up some positive

implications, assisting the metabolism of nitrogen (N), sulphur (S), and C1 carbon, plants immunity and acclimation to abiotic stresses (JIANG et al., 2023; TIMM; HAGEMANN, 2020). Environmental factors such as high temperatures and low levels of atmospheric CO_2 stimulate photorespiration among the great majority of plants. Warmer environments usually tilt the balance away from photosynthesis and toward photorespiration, as under those conditions the CO_2 solubility exhibits a great decrease, the oxygenase activity of RuBisCo overrides the carboxylase activity, and stomates close to retain water, reducing CO_2 concentration around the active site of RuBisCo by consequence (TAIZ et al., 2017).

Most plants (~85 % of all known plants) carry out photosynthesis through the **C_3 pathway**, generating a 3-carbon compound (PGA) as the first step of carbon fixation, as aforementioned. In those plants the Calvin-Benson cycle takes place in the stromal matrix of chloroplasts. Hundreds of millions of years ago, when the earliest plants emerged, the Earth's atmosphere appeared to have CO_2 concentrations approximately four to five times greater than present-day levels. Thus, photosynthesis is now limited by the current CO_2 concentration (~0,04%), which is significantly lower than the optimal range. As CO_2 levels increase, it stimulates photosynthesis due to the rising concentration gradient from air to leaf and reduction in the photorespiration rates (ZISKA; BUNCE, 2006).

Contrarily to CO_2 levels, the temperature progressive increase negatively impact photosynthesis limiting CO_2 assimilation. It occurs due to solubility reduction of CO_2, leading to the predominance of the oxygenase activity of RuBisCo over the carboxylase activity. In another words, in C_3 species the temperature increase is associated with higher (lower) photorespiration (photosynthesis) rates (TAIZ et al., 2017). Key environmental factors that affect photosynthesis will be further elaborated in the upcoming sections of this review.

The ratio of transpired water to photosynthetically assimilated carbon (transpiration rate) in C_3 plants is about 400:1 molecule/molecule, reflecting a water use efficiency (WUE) of 1/400 (i. e., 0,0025). Such relatively low WUE is explained by the lower CO_2 diffusion coefficient compared to water, the resistance provided by membranes throughout CO_2 diffusion in plants and the high concentration of water vapor within the leaf against the low concentration of atmospheric CO_2, which produces significant differences in the magnitude of gradients (TAIZ et al., 2017). Ultimately, photorespiration per se accounts for the reduced energy and water use efficiency in C_3 plants.

As we see, C_3 species require a substantial volume of water, especially in warm and dry environments, where plants face a functional dilemma: the decrease in stomatal aperture. This mechanism is necessary to mitigate transpiration and water loss, but it also barriers the

CO_2 input and O_2 output, limiting photosynthesis and increasing photorespiration (TAIZ et al., 2017). As an adaptative response to environmental stimulus, drought included, plants developed two different mechanisms that precede the Calvin-Benson cycle to increase the CO_2 concentration around RuBisCo and reduce photorespiration occurrence: the **C_4 Metabolism** (C_4) and the **Crassulacean Acid Metabolism** (CAM) (ZISKA; BUNCE, 2006). The latter will not be addressed in this thesis as it does not fall within its scope.

2.5.2.3. C_4 Photosynthesis

Plants with **C_4** photosynthetic metabolism have a 4-carbon compound as the first stable product of carbon fixation in the Calvin-Benson cycle. They are the tropical grasses, including some of the world's most productive crops, such as Maize (*Zea mays*), Sugarcane (*Saccharum ssp.*) and Sorghum (*Sorghum bicolor*). Apart rare exceptions, leaves of C_4 plants exhibit the Kranz anatomy, in which the bundle sheath cells are arranged in a circle around the vascular tissues, accompanied by an outer layer of mesophyll cells (TAIZ et al., 2017) (Fig.3).

Figure 3 – Anatomic differences between C_3 and C_4 leaves. In C_4 leaves, the bundle sheath cells are arranged in a circle around the vascular tissues, accompanied by an outer layer of mesophyll cells

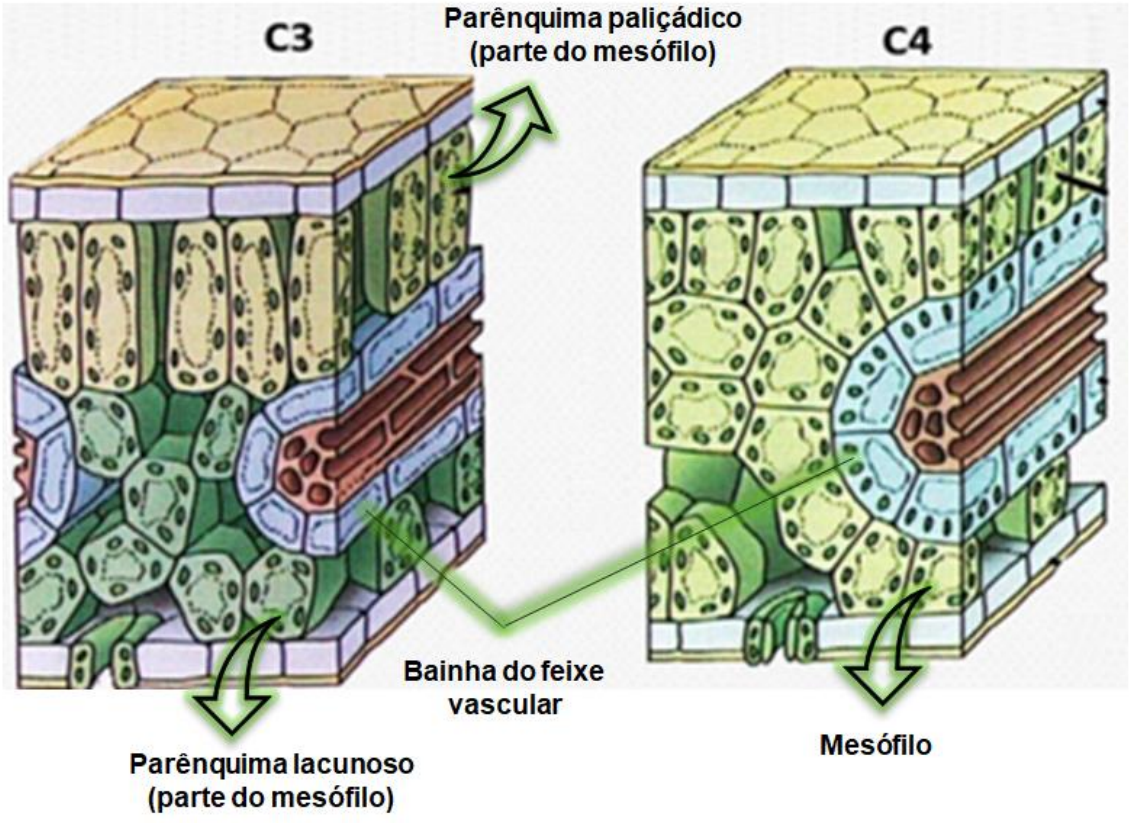

Adapted from Taiz et al. (2017)

Anatomic adaptations in leaves have established a diffusion barrier that segregates the Calvin-Benson cycle from a preceding step. Therefore, the carbon assimilation stage of photosynthesis in C_4 species starts with the generation of a 4-carbon acid (oxaloacetate, malate, or aspartate) through the fixation of CO_2 into a 3-carbon substrate (Phosphoenolpyruvate – PEP), which is catalyzed by the Phosphoenolpyruvate carboxylase (PEPCase) within mesophyll cells. The 4-carbon acid crosses the diffusion barrier and CO_2 is released through decarboxylation reactions within bundle sheath cells establishing a high carbon concentration (10 times the atmospheric concentration) around the active sites of RuBisCo. From then on, the CO_2 is reduced to carbohydrates in the Calvin-Benson cycle as in C_3 plants, and the 3-carbon product of decarboxylation (e.g., pyruvate) returns to mesophyll cells for PEP regeneration (SILVA; ALVES; ZINGARETTI, 2020a; TAIZ et al., 2017) (Fig. 4).

Figure 4 – Carbon assimilation in C_4 species. During the carbon assimilation stage, atmospheric C02 is reduced to carbonic acid followed by a carboxylation reaction catalyzed by PEPCase, producing a 4-carbon acid within mesophyll cells. The acid crosses a diffusion barrier towards the bundle sheath cells, where the acid is decarboxylated releasing the CO_2 to be fixated by RuBisCo in the Calvin-Benson cycle

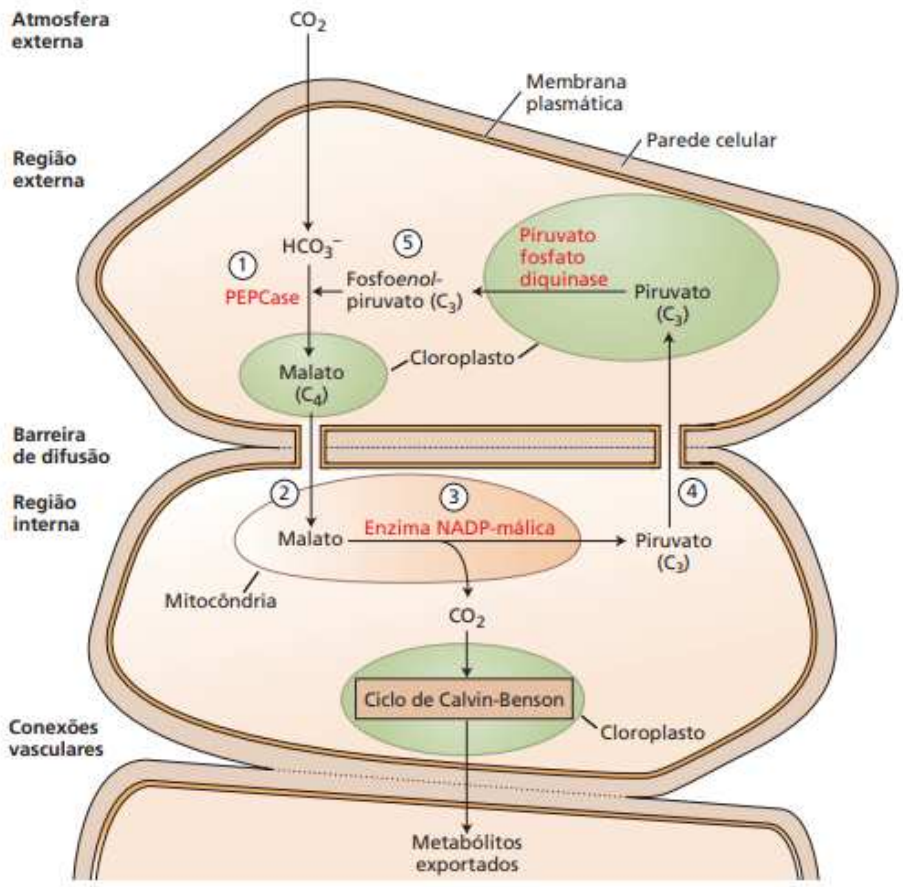

Taiz et al. (2017)

Theoretically, increased CO_2 levels should pose little effect in C_4 photosynthesis, due to natural capacity of C_4 plants in concentrate CO_2 close to saturation around RuBisCo active sites at moderate temperatures (20-30 °C) (SAGE, 2002). However, specific information about the response mechanism of C_4 species to elevated CO_2 remains unclear. Some research findings have been contradicting theoretical expectations, indicating an increase in photosynthesis in C_4 plants in response to rising CO_2 levels (ZISKA; BUNCE, 2006).

As aforementioned, the effects of high temperatures are mainly manifested in CO_2 solubility, reducing its levels in leaves. Taking this into consideration, two pivotal characteristics of C_4 plants enable the maintenance of photosynthesis rates at higher temperatures: (1) high CO_2 concentration within bundle sheath, which restricts photorespiration; and (2) a sufficiently high affinity between PEPCase and its substrate (HCO_3^-), enabling the saturation of PEPCase binding sites and a reduction in stomatal opening to store water (TAIZ et al., 2017).

At this point of the discussion, it is already reasonable to presume a higher WUE in C_4 plants. What actually happens is that C_4 photosynthesis induces lower CO_2 concentrations within the intercellular airspaces, which stimulates CO_2 absorption. So, functional processes in these plants can operate with tinier stomatal aperture, reducing water loss through transpiration. The result is a transpiration rate of circa 150:1 CO_2 molecules/ water molecules (i. e., WUE of 0,0067) (TAIZ et al., 2017).

2.6. Plants typical response to abiotic factors

Plant development is primarily affected by light (solar radiation), atmospheric CO_2 and O_2, temperature, water (air humidity and soil moisture) and content and availability of nutrients and toxins. Some of them will be briefly discussed below.

2.6.1. Light

Light quantity (excess and scarcity) is a typical factor that stimulates acclimatization in many species. Usually, sun leaves can be thicker and exhibit a thicker palisade layer whereas shade leaves may be thinner, have more chlorophyll at each reaction site and display lower transpiration rates. When, for instance, shade leaves are abruptly exposed to direct sunlight, the capacity of light-independent reactions to convert the excessive energy into sugar molecules may be exceeded. This can result in the generation of reactive oxygen species (ROS) accounting for cellular damage.

2.6.2. Temperature

Plants' response to **temperature** variation assumes an asymmetric bell-shaped curve on a graph of temperature *vs.* photosynthesis rate (Fig.5). Maximum photosynthesis occurs within a narrow temperature range, known as the thermal optimum, beyond which reversible and irreversible damages can compromise plant development. Thermal plasticity can be observed even at an intraspecific level, as individuals of the same species grown in warmer conditions manifest higher photosynthetic rates than those cultivated in cooler environments. This adjustment capacity (acclimatization) allows plants to perform photosynthesis in extremely harsh conditions, far beyond their natural limits.

Figure 5 – Photosynthetic assimilation rate (A) as a function of temperature (T) at current atmospheric CO_2 concentrations. Plants of C_4 species exhibit enhanced carbon assimilation rates at elevated temperatures. Conversely, C_3 species often display a broad and flared plateau in their A/T response curve, primarily due to the influence of photorespiration

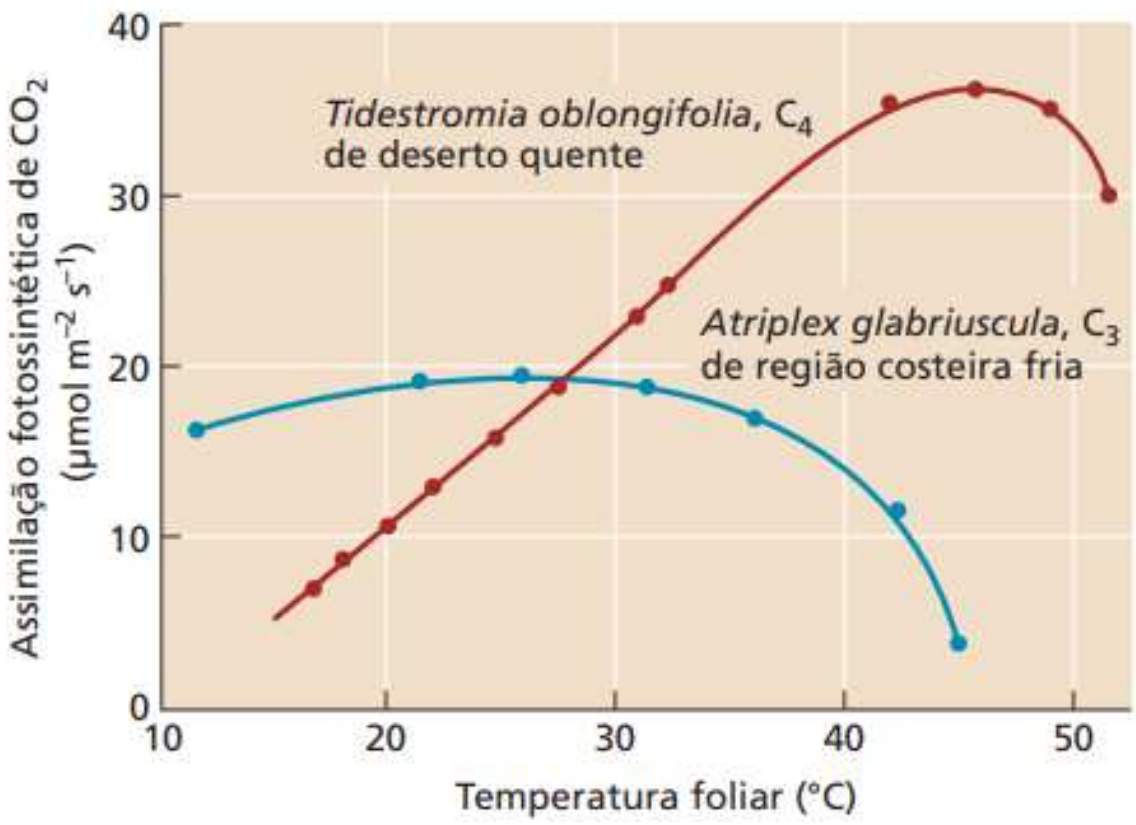

Taiz et al. (2017)

At current atmosphere, with CO_2 concentration around 400 ppm and under favorable light and water conditions, the photosynthetic thermal optimum in C_3 species ranges typically between 20-35 °C (SAGE; WAY; KUBIEN, 2008), with a wide peak in the mid-20 °C, whereas it usually occurs between 30-40 °C in C_4 species (MASSAD; TUZET; BETHENOD, 2007). The reason behind the difference between C_3 and C_4 thermal optimum is well known and explained: photorespiration increases with temperature in C_3 species as a reflection of (1) the reduction of CO_2 solubility and concentration within plant's leaf (C_i) and (2) the predominance of the RuBisCo's oxygenase activity, due to the decreased affinity of RuBisCo for CO_2. In C_4 species, this effect is not observed due to the concentration mechanism that maintains CO_2 near-saturation within plant's leaves, ensuring a higher affinity of RuBisCo for CO_2. Due to this characteristic, C_4 plants are predominantly found in tropical lands, where they display a higher carbon assimilation rate (TAIZ et al., 2017).

In conditions of light saturation and under current CO_2 levels, distinct mechanisms are constantly pointed out as possible controllers of the net carbon assimilation as temperature rises. They are: (1) P_i regeneration capacity; (2) RuBisCo capacity (to consume RuBP); (3) Electron transport capacity and (4) RuBisCo activase perfomance. Sage and Kubien (2007) depicted the variation in carbon assimilation in a C_3 species (tobacco) across a temperature range (A/T curve) under intermediate levels of CO_2 (300 ppm) (Fig. 6a). Although the net CO_2 assimilation response to temperature indeed varies among species, modulated response curves of most other C_3 plants typically exhibit a similar shape (e.g., sweet potato – Fig. 6b, bean, Eucalyptus, soybean, chili pepper, tomato and rice).

Figure 6 – Likely biochemical controlling mechanism of photosynthesis in C_3 plants. Net CO_2 assimilation (A) as function of temperature (T) in leaves of tobacco at intercellular partial pressure of CO_2 (Ci) of 300 µbar **(a)** and responses of A to T in leaves of sweet potato at different Ci (140, 250 and 500 µbar) **(b)**. The graphs show controlling mechanisms over photosynthesis in C_3 species with increasing temperatures. Under moderate CO_2 levels (250-300 ppm), this process initiates with Pi regeneration at low temperatures, transitions to RuBisCo capacity at moderate temperatures, and subsequently involves electron transport capacity (closely associated with RuBP regeneration) at higher temperatures

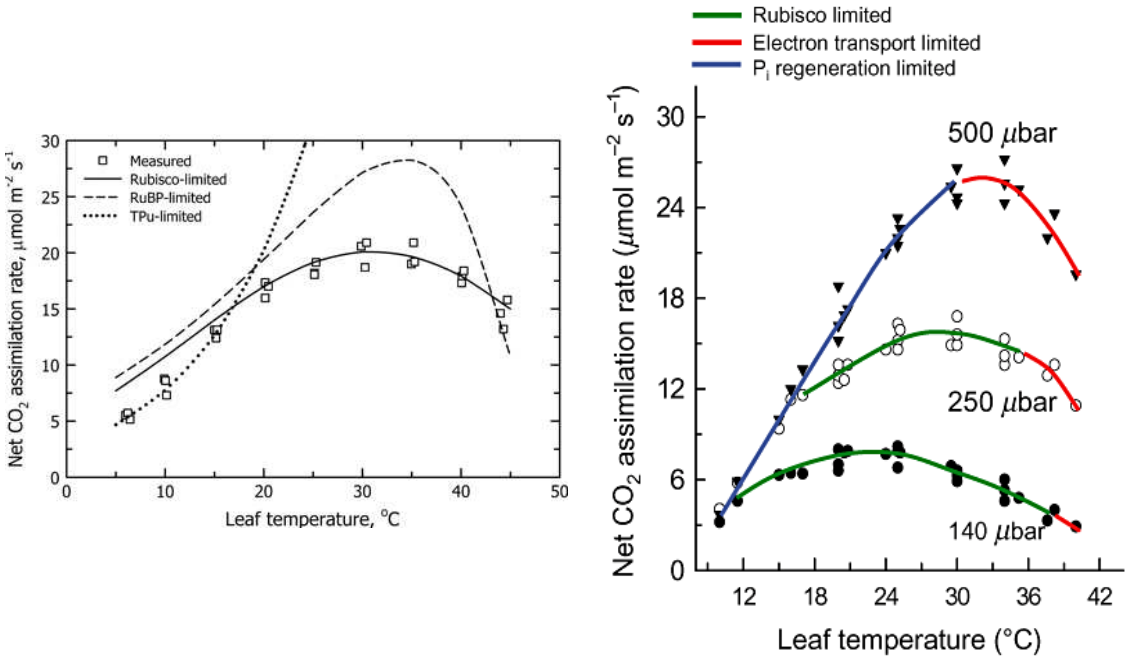

(a) (b)

Sage & Kubien (2007) and Sage et al. (2008)

Regarding C_3 species, in the initial slope of the A/T response curve, at low temperatures, **P_i regeneration capacity** limits carbon assimilation, as the capacity of sucrose synthesis at expensive of ATP consumption is temperature dependent. For tobacco, it occurs until 18 °C, when **RuBisCo capacity** takes place as primary restrictor mechanism. At very high temperatures (40 °C, for tobacco), the **electron transport capacity** (highly associated with **RuBP regeneration**) seems to limit carbon assimilation, but the cause of its decline above the thermal optimum remains obscure. A leading hypothesis is that high temperatures stimulate cyclic electron transport in the first stage of photosynthesis (light-dependent reactions), causing a reduction in NADPH usually produced by linear transport (SAGE; KUBIEN, 2007).

The **RuBisCo activase (Rac)** is an important enzyme that ensures the catalytic activity of RuBisCo removing inhibitors from its reaction sites. Evidence has pointed to Rac's role in

limiting carbon assimilation at elevated temperatures: (1) the decline in RuBisCo activation coincides with increased RuBP pools, RuBP/PGA ratios and reduced carbon assimilation; (2) the acclimation to higher temperatures lead to higher stability of Rac accompanied by carbon assimilation increments and, (3) irreversible denaturation of Rac's subunits at supra-optimum temperatures (SAGE; KUBIEN, 2007; SAGE; WAY; KUBIEN, 2008).

In **C_4** plants, the regulatory mechanisms limiting carbon assimilation are still unclear, especially at supra-optimal temperatures. The CO_2 concentration mechanism in **C_4** species enhances the efficiency of RuBisCo enzymes, resulting in lower RuBisCo content compared to C_3 species. Hence, at lower temperatures (<20°C), carbon assimilation in **C_4** plants is constrained primarily by RuBisCo capacity. Under these conditions, increased CO_2 solubility occurs; however, the limited RuBisCo content is insufficient to efficiently capture all available carbon dioxide molecules. At moderated temperatures (about 20-45°C), the main limitation on carbon assimilation is still uncertain, but **PEPCase capacity** is one possibility. Finally, above 45°C, RuBisCo activation may become limiting in C_4 as well as in C_3 plants (SAGE, 2002; SAGE; KUBIEN, 2007).

Besides photosynthesis, temperature increments also impacts plants' respiration rates, which rises exponentially as a short-term response to the increased demand of cellular maintenance (SLOT; KITAJIMA, 2015). In the context of global warming, the respiration-temperature association raises critical and fair concerns about forests becoming net carbon sources rather than sinks, as respiration surge has the potential to negatively impact the development of plants or even render their survival untenable (GATTI et al., 2021; OMETTO et al., 2022).

2.6.3. Carbon dioxide

Leaf photosynthesis, respiration and plants' biochemical composition are very responsive to rising atmospheric CO_2. Although CO_2 is the main responsible for the global warming effect, which can damage plants though excessive temperature enhancement, it has been investigated if it also benefits vegetation, especially C_3 species, through the so-called "CO_2 **fertilization effect**" (FAN et al., 2020). Under appropriated light, water and nutrient conditions, C_3 photosynthesis is stimulated with atmospheric CO_2, due to enhanced concentration of the gas in RuBisCo's active reaction sites, endorsing carboxylation (SAGE; KUBIEN, 2007). Some of the effects of the CO_2 fertilization, which is still under discussion, include the enhancement of photosynthesis rates, plant growth, and grain yield (FAN et al., 2020).

In a manner analogous to temperature, different mechanisms limit photosynthesis as CO_2 increases. Under conditions of moderate temperature and low Ci (internal CO_2 concentration), the primary limiting factor is the restricted concentration of CO_2 molecules, which stimulates oxygenation reactions. Therefore, it is also appropriate to state that RuBisCo capacity limits photosynthesis at low Ci (SAGE; KUBIEN, 2007). As Ci increases, the RuBP regeneration capacity usually becomes the constraining factor. It occurs because light-dependent reactions cannot increase NADHP and ATP production to meet the elevated demand. It is interesting, however, that high CO_2 concentrations impose a reduction in stomatic conductivity in C_3 plants, mitigating transpiration (i.e., water losses), which can increase the WUE (TAIZ et al., 2017).

Theoretically, photosynthesis saturates at about 100-200 ppm in C_4 plants. This allows C_4 plants to have less RuBisCo content and show high carbon assimilation under low Ci. Therefore, significant effects of rising CO_2 on C_4 photosynthesis are not expected, as at the current CO_2 concentration RuBisCo's reaction sites are already saturated restricting photorespiration. Contrastingly, increasing Ci is expected to stimulate C_3 photosynthesis over a wider CO_2 range (Fig.7) (TAIZ et al., 2017). Nevertheless, research findings on CO_2 fertilization effect often contradict theoretical expectations, pointing to significant enhancement of photosynthesis in C_4 plants (SILVA; ALVES; ZINGARETTI, 2020b; WAND et al., 2001; ZISKA; BUNCE, 2006).

Figure 7 – Photosynthetic responses to rising atmospheric carbon dioxide. Net carbon assimilation rate as function of internal leaf CO_2 concentration in *Tidestromia oblongifolia* (C_4) and *Larrea tridentata* (C_3)

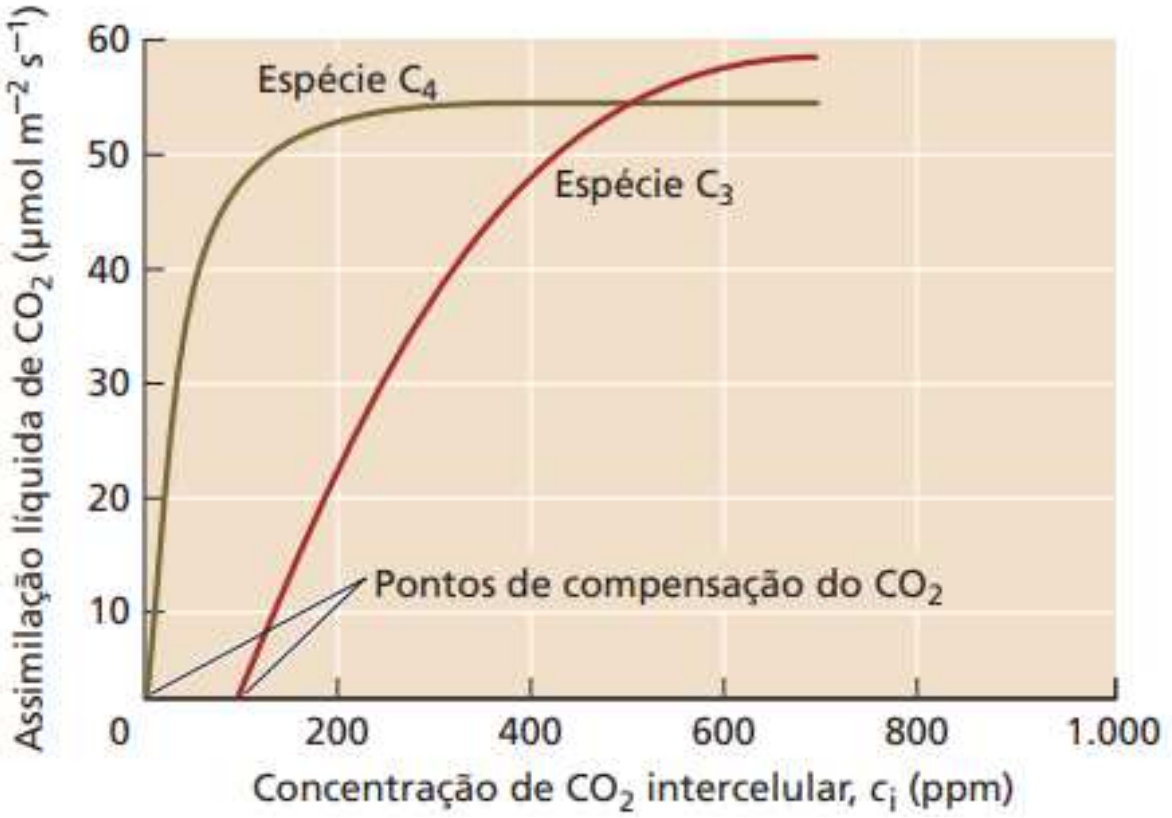

Taiz et al. (2017)

2.6.4. Water

Besides its relevance in various biochemical processes, such as cellular division, nutrients absorption and transport and root development, **water** also assumes an important role in photosynthesis. Electrons and protons are released though water hydrolysis, supporting the energetic molecules production (ATP and NADPH) during light-dependent reactions (TAIZ et al., 2017). Hence, drought has the potential to constrain primary productivity, thereby posing a risk to various biomes, especially tropical forests by affecting their functions and structure (OMETTO et al., 2022). The response of plants to drought varies not only with the characteristics of the drought event itself, including its duration and severity, but also on plant-specific attributes such as species, growth form, and developmental stage (FAN et al., 2020; ZHANG et al., 2018).

As aforementioned, besides controlling CO_2 flux, the stomatal apparatus in plants also regulate the water flux. Due to their mechanism of CO_2 concentration within bundle sheath cells (Fig.8), C_4 plants display lower CO_2 concentration in intercellular airspaces, stimulating

atmospheric CO_2 absorption (TAIZ et al., 2017). Therefore, under the current CO_2 levels and favorable water conditions, WUE is generally expected to be higher in C_4 species, as they can operate with a tinny stomatal aperture, which prevents water loss. However, this anticipation does not necessarily hold true under drought stress. In a robust meta-analysis, Zhang et al. (2018) observed that drought induces divergent responses in WUE, with a decrease in C_4 plants, especially under severe drought, and an increase in C_3 plants. Evern though, WUE is not necessarily higher in C_3 than in C_4 species. It is also noteworthy that certain C_4 plants exhibit increased WUE as an adaptive response to severe drought conditions, a phenomenon also observed in desertic species. These varied responses reveal the plasticity of WUE in C_4 plants.

Figure 8 – Distinguishing the gas exchange mechanisms in C_3 and C_4 Plants: In C_3 species, CO2 is promptly captured and utilized in the Calvin-Benson cycle. Conversely, C4 species temporarily store CO2 within mesophyll cells, enhancing carbon use efficiency. This unique feature enables C4 plants to maintain thinner stomatal apertures, facilitating gas exchange with reduced water loss

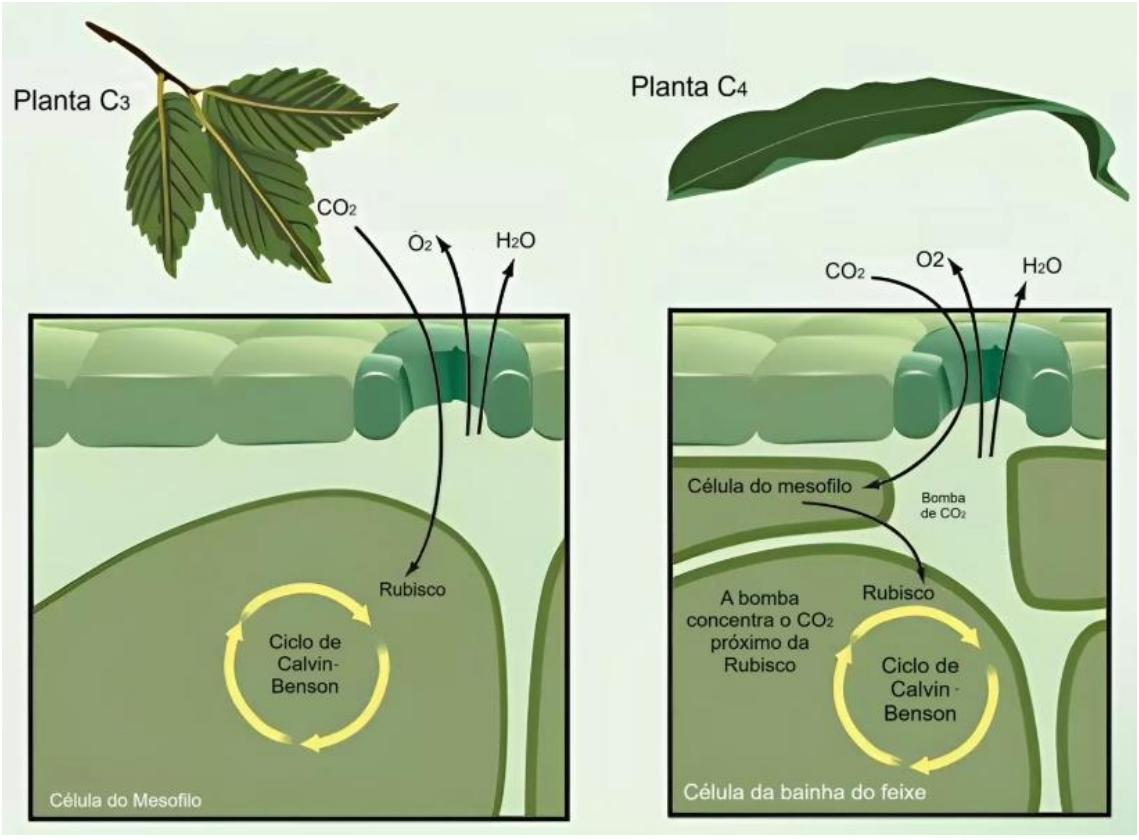

Accessed at https://agroadvance.com.br/blog-plantas-C4-o-que-sao/

2.7. Acclimation (downregulation)

Deviations from normal limits in the quality and quantity of abiotic factors impose plant stress when it limits the plentiful growth and reproduction potential. To cope with these conditions, plants offset the stressors through **acclimation**, which entails mostly reversible modifications in the physiological or morphological characteristics of either young or mature leaves when exposed to challenging environmental factors. The plant's ability to adjust according to environmental changes is known as plasticity. When a persistent response spans generations and assumes a genetic character, it is referred to as **adaptation** (TAIZ et al., 2017).

Plants can acclimate in response to different abiotic factors, such as rising temperature and CO_2 levels, either occurring simultaneously or not. In fact, plant acclimatation can be different when multiple factors are acting instead of an individual factor. It is also common that one single environmental factor impacts the acclimation process of different physiological mechanisms, such as photosynthesis, respiration and stomatal conductance.

2.7.1. Temperature

Climate warming forecasts point to enhanced frequency of supra-optimal temperatures both in the short- (minutes to hours) and long-term (days to years). Long-term exposure of plants to warmer growth regime can lead them to acclimate, displaying stable or even elevated photosynthetic rates in the new regime (SAGE; WAY; KUBIEN, 2008).

The process of thermal acclimation is subject to variation across different species and growth environments. In C_3 plants, at current CO_2 levels and temperatures ranging 5–10 °C higher or lower, a shift in the thermal optimum is noticed toward the new growth temperature, accompanied by an increase in the net photosynthesis rate in the same direction. Conversely, the thermal optimum decreases in the opposite direction (Fig. 9) (SAGE; KUBIEN, 2007).

Figure 9 – Common pattern of thermal acclimation at current CO_2 levels in C_3 species. Different potential drives lead to net photosynthetic rates acclimating at cooler and warmer temperatures

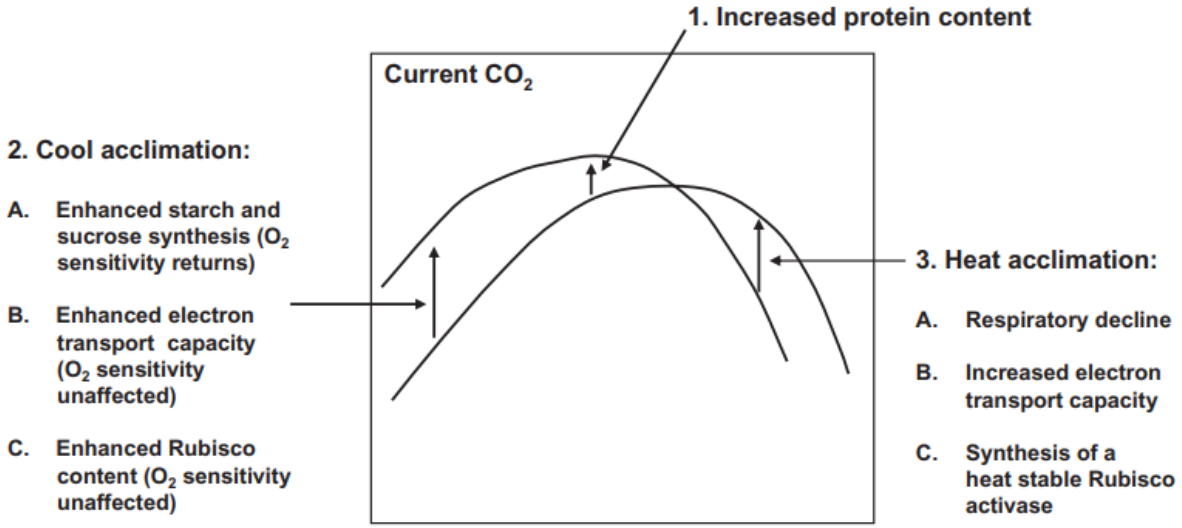

Sage & Kubien (2007)

As indicated in Fig. 9, the main potential drivers of heat acclimation in C_3 plants are reduced respiration rates, increased electron transport capacity and production of heat stable isoforms of Rac enzymes. Nevertheless, when the temperature is elevated enough to cause thermal stress, photoinhibition and protein denaturation are the main drivers of an extended decline in photosynthesis rates (SAGE; KUBIEN, 2007). It is also important to highlight that the capacity for thermal acclimation is apparently restricted in plants adapted to grow in extreme habitats (KEMP; WILLIAMS, 1980; KUBIEN; SAGE, 2004).

While the specific mechanisms governing thermal acclimation in C_4 plants remain unclear, certain general patterns of acclimation have been identified. In some instances, the thermal optimum shifts toward the growth temperature, yet with minimal changes observed in the net photosynthetic rate. Conversely, an alternative pattern of response entails net photosynthesis changes following thermal acclimation (SAGE; KUBIEN, 2007).

Leaf respiration can also acclimate to elevated temperatures. Plants' respiration rates rapidly increase with temperature (over minutes to hours), which potentially affects the global carbon balance (LEE; REICH; BOLSTAD, 2005). Therefore, a critical concern is how well plants can acclimate to limit carbon release, avoiding the shifting from a carbon sink to a source (OMETTO et al., 2022). Empirical evidence has indicated that thermal acclimation - occurring over a span of a few hours to days – typically leads to a reduction in respiration rates, although

the process is often not entirely homeostatic. However, longer exposures can deliver a greater degree of homeostasis, as plants have enough time to make complete adjustments. Conversely, greater temperature changes may reduce the degree of homeostasis achieved (SLOT; KITAJIMA, 2015).

Tjoelker et al. (2008) and Lee et al. (2005) reported intra- or interspecies variations in acclimation magnitude, whereas Campbell et al. (2007) found no relevant differences among different plant functional type. However, in a warming world, some general differences between warm and cold-biome plants regarding respiration acclimation must be pointed out. Firstly, complete homeostasis achievement poses a greater challenge to tropical plants compared to temperate ones, and not surprisingly, temperate species deliver a more complete acclimation of photosynthesis than tropical species. Secondly, whereas global warming may bring temperate species closer to their thermal optimum, it is possible that tropical plants are very close to their supra-optimal temperatures, being subjected to heat stress and subsequential increased respiratory demand (SLOT; KITAJIMA, 2015).

2.7.2. Carbon dioxide

Experimental studies have indicated that plant acclimation can also occur in the presence of elevated CO_2 levels (TAIZ et al., 2017). In the short term, increased CO_2 usually boosts photosynthesis, yet over time, plants often acclimate, leading to a decline in photosynthetic rates (ZISKA; BUNCE, 2006). When investigating woody plants' response to heightened CO_2, Mindela et a. (2022) found that acclimation is apparently age-dependent, i.e., acclimation is more frequent after long exposure to elevated CO_2.

In general, potential drivers for plants acclimation at elevated CO_2 include, at least, (1) gene repression and carbohydrate accumulation; (2) limited N uptake; (3) restricted RuBP regeneration capacity and (4) increased saccharide content (ZISKA; BUNCE, 2006). Although the acclimation led to unclear changes in plants' photosynthetic apparatus of C_4 species, some C_3 species acclimate by reducing the synthesis of certain photosynthetic enzymes, such as RuBisCo (MAROCO; EDWARDS; KU, 1999).

2.8. Field methodologies for assessing plant response to climate change

Open-Top Chambers (OTC) and Free-Air CO_2 Enrichment (FACE) experiments are pivotal field methodologies employed to assess plants' responses to climate change. OTC structures are enclosed by a translucent polycarbonate sheet, excluding the top of the chambers,

thereby passively warming the air and soil within (Fig.10). Typically, these chambers incorporate a controlled release system for CO_2 gas, aiming to simulate predicted atmospheric conditions as realistically as possible (REDDY et al., 2021). While OTC experiments are more cost-effective than FACE experiments and offer control over water content, they introduce a distinct microclimate featuring higher humidity, temperature, and light intensity due to the translucent plastic. This discrepancy is considered a drawback, as it deviates from a perfect simulation of real-world conditions (SILVA et al., 2020).

Figure 10 – Open-top chambers. This cost-effective methodology for field assessment of plants' responses to climate change involves structures enclosed by a translucent polycarbonate sheet, leaving the top of the chambers open to facilitate gas exchange. This design results in the establishment of a distinct microclimate within the chambers, characterized by elevated temperatures, humidity, and light intensity compared to the external environment. One-module structure **(a)**, two-modules structure **(b)**, pipes array for CO_2 release within the chamber – adapted from J.B.L. da Silva et al. (2020) **(c)** and chambers on field (REDDY et al., 2021) **(d)**

(a) (b)

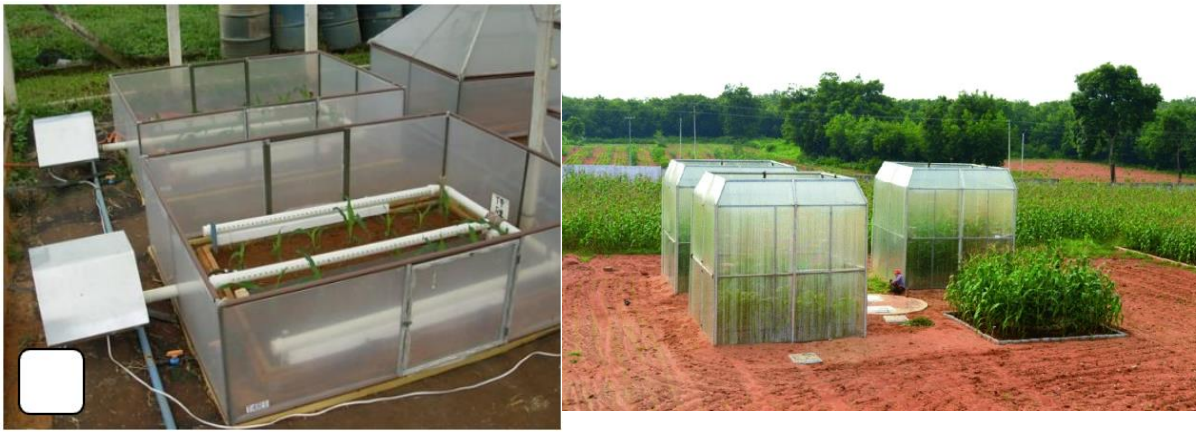

(c) (d)

Adapted from J.B.L. da Silva et al. (2020) and (REDDY et al., 2021)

Conversely, FACE experiments entail exposing expansive fields to elevated CO_2 levels by surrounding the area with CO_2 emitters, either in horizontal or vertical configurations (Fig. 11). This approach creates an environment with a high concentration of CO_2 (AINSWORTH; LONG, 2005). Despite its effectiveness in replicating realistic conditions, the operational costs associated with FACE experiments are considerably high, posing limitations on its widespread use, particularly in underdeveloped or developing nations (KUMAR et al., 2020).

Figure 11 - Free-Air CO_2 Enrichment. This advanced methodology for field assessment of plants' responses to climate change involves the explosion of expansive fields to elevated CO2 levels by surrounding the area with CO2 emitters, which results in an environment with high concentrations of CO2. FACE experiments in patches of deciduous forest (a) and in a crop (b)

(a) (b)

Taiz et al. (2017)

In the upcoming section, we will unveil and discuss responses garnered from experiments conducted globally, with a particular focus on tropical forests. Nevertheless, we can already highlight some pivotal and recurring insights (TAIZ et al., 2017):

- **C_3** species generally exhibit greater sensitivity to elevated CO_2 levels compared to **C_4** species, especially when water availability is assured. This heightened sensitivity results in a notable increase in the photosynthetic rate, often exceeding 20%, attributed to the elevated carbon concentration within mesophyll cells;
- On the other hand, photosynthesis and respiration exhibit thermal acclimation, manifesting lower rates than those predicted by modeling;

- At elevated CO_2 levels, it ceases to be a limiting factor, with nutrients availability becoming the primary constraint due to increased demand.

2.9. How do plants respond to climate change?

In a warming world, with elevated CO_2 concentrations followed by increasing temperatures and droughts geographically distributed, photosynthesis, respiration and growth rates must respond to changes in multiple and simultaneous abiotic factors (FAN et al., 2020; OMETTO et al., 2022). The collective impact of multiple stressors can alter plant physiology and productivity differently compared to when these stressors act independently (TAIZ et al., 2017). Moreover, plants may undergo modifications to either acclimate or adapt to these environmental changes (ZISKA; BUNCE, 2006). As such, the assessment of potential global warming impacts on plants necessitates a comprehensive modeling approach that accounts for the intricacies of various biomes, species, and photosynthetic pathways, as well as the potential for acclimation or adaptation. Nevertheless, global vegetation models often lack the incorporation of acclimation or fail to consider these specificities (SLOT; WINTER, 2017).

Tropical forests hold the majority of global biodiversity and are constantly threatened, either for deforestation or possible effects of climate change on forest structure, carbon storage and hydrology. The clarification of uncertainties concerning the CO_2 fertilization effect on plant growth (FAN et al., 2020; OMETTO et al., 2022) and acclimation limits in tropical species (OMETTO et al., 2022; SLOT; KITAJIMA, 2015) is imperative to enhance comprehension of the future of these ecosystems. It is widely agreed that plants may take advantage of the rising temperatures in global temperate zones by increasing CO_2 uptake, thereby boosting plan growth. However, tropical species usually exhibit incomplete acclimation to elevated temperatures compared to their response under moderate warming conditions. Therefore, tropical forests may experience diminished or no net gain of carbon under conditions of intense warming, as plants are often exposed to supra-optimal temperatures in the tropics (SLOT; WINTER, 2017).

In addition to CO_2 fertilization, models and observations suggest that various other factors influence the vegetation response to a CO_2-enriched atmosphere, such as nitrogen deposition and the length of the growing season (OMETTO et al., 2022). Anthropogenic activities, like deforestation, industry, and agriculture, contribute significantly to the release of nitrogen into the atmosphere, leading to detrimental effects when deposited on soil worldwide.

This process results in soil acidification, depleting base cations (Ca^{2+} and Mg^{2+}) and releasing toxic amounts of Al^{3+} (BOWMAN et al., 2008).

The assessment of plants' response to climate change can span various scales, ranging from cellular and leaf levels to entire plants and plant communities. At **cellular level**, the photorespiration reduction in C_3 plants may result in decreases in leaf content of its products, such as glycine, serine, and ammonium. It may also contribute to reductions in leaf proteins contents owing to the low nitrate photoreduction (ZISKA; BUNCE, 2006).

At the **single-leaf level**, acclimation significantly influences carbon dynamics, obscuring the interaction between physiological processes like photosynthesis and dark respiration and the escalating atmospheric CO_2 levels (CAMPBELL et al., 2007; SLOT; KITAJIMA, 2015; SLOT; WINTER, 2017; ZISKA; BUNCE, 2006). Furthermore, climate change affects leaf chemistry, often leading to an augmented C/N ratio, associated with increased carbohydrate, lignin, and cellulose content. Consequently, alongside the decrease in N assimilation due to reduced photorespiration, the elevated atmospheric CO_2 can increase leaf biomass, leading to a dilution of N concentrations. Conversely, rising temperatures may induce an increase in leaf N concentration. Therefore, when simultaneously applied, the individual impacts of increased CO_2 and high temperatures can to some extent counterbalance each other (WANG et al., 2023). Furthermore, stomatal regulation is also affected at leaf level. While C_3 plants typically experience a reduction in stomatal conductance with rising CO_2 levels, the limitation of photosynthesis due to stomatal factors decreases. The maintenance or increase of photosynthesis rates and carbon uptake are reported in water-stressed environments, revealing improved WUE (ZHANG et al., 2018). This positive effect is believed to be notable in **C_4** plants subjected to salinity and water deficit condition (ALLEN et al., 2011; ZISKA; BUNCE, 2006).

Individual plants' response to climate change have been widely studied. Under increased CO_2 concentrations, plant growth may be constrained not by a scarcity of CO_2, but rather by the availability of nutrients (TAIZ et al., 2017). Indeed, accelerated plant growth rates inevitably heighten the demand for nutrients. However, plant growth prevails primarily under conditions of nutrient scarcity, while in instances of abundance, this growth may not manifest. This behavior is ascribed to the heightened efficiency of nutrient utilization under scarcity conditions (Lal et al., 2022).

Ziska and Bouce (2006) highlighted multiple documented effects of global warming on individual plants, such as amplified plant growth, increased seed germination and emergence in herbaceous plants, greater tiller and leaf formation in both herbaceous and woody C_3, as well as some C_4 species, heightened root growth, improved fine-root colonization of fungi, increased

nodule formation, and enhanced floral and fruit production, along with elevated pollen synthesis. However, the authors pointed out the absence of a clear link between plants' responses at single-leaf (anatomical and physiological modifications) and at whole-plant level. For instance, the increase in tiller formation and growth rates occurs independently of leaf area and maturation. Another example involves the expansion of the soybean's leaf area at elevated CO_2 levels and rising temperatures, which leads to self-shading, potentially reducing the whole-plant photosynthetic rates. The authors also discussed the impact of dark respiration response on a whole-plant scale. They stressed that the ratio between the whole-plant respiration and photosynthesis does not necessarily increase proportionally to biomass, indicating a decrease in respiratory cost per unit tissue at increased CO_2 levels. Conversely, the reduction in stomatal conductance appears to be less effective in preventing water loss in whole plants compared to the leaf scale.

An important morphological response of plants to climate change involves photoassimilate partitioning. Typically, plants allocate additional carbon to structures related to a limiting resource (ZISKA; BUNCE, 2006). In an enriched CO_2 atmosphere, where CO_2 is no longer a limiting resource for photosynthesis and plant growth, nutrients and water availability emerge as the new limiting factors. Consequently, under such conditions, the root-to-shoot ratio generally increases (LAL et al., 2022; ZISKA; BUNCE, 2006). Conversely, this ratio is expected to decrease under warming conditions. As previously discussed, the introduction of the temperature factor to the equation may result in different plant responses.

According to Lal et al. (2022), the combined effect of elevated CO_2 and high-temperature stress has been found to have a detrimental impact on the photosynthetic assimilation of carbon, resulting in reduced nitrogen uptake and assimilation in plants. Nonetheless, the CO_2 fertilization effect may help maintain carbon balance. In general, evidence supporting CO_2 fertilization of growth in individual tropical species is either lacking or contentious. However, the increase in water use efficiency (WUE) under elevated CO_2, attributed to stomatal regulation, is widely documented, especially in C_3 plants experiencing severe drought conditions.

Additionally, there is a prevalent concern regarding the physiological responses, suggesting that heightened temperatures may lead tropical forests from serving as a carbon sink to becoming a carbon source due to excessive plant respiration. While some research indicates that thermal acclimation holds the potential of mitigating carbon release, there remains a possibility that plant functions are already approaching, or even surpassing, their thermal optimum limits (OMETTO et al., 2022).

Finally, plant responses to climate change can be evaluated on broader scales, including communities, ecosystems, a global scale, and within an evolutionary context. Within a community, plant-to-plant interactions, such as competition, play a crucial role yet are often overlooked in predictions (MAGALHÃES; AMOROSO; LARSON, 2021). Individual plants' responses to increasing CO_2 may differ from those grown in competition, as any resource affecting the growth of an individual also alters its competitive ability (MAGALHÃES; AMOROSO; LARSON, 2021; ZISKA; BUNCE, 2006). In **managed systems**, such as agricultural systems, the presence of any weed species appears to hinder the ability of the crop to respond either vegetatively or reproductively to enhanced CO_2. However, further studies are needed to confirm and explore these insights (ZISKA; BUNCE, 2006).

In **unmanaged systems**, such as forests, a warming climate indirectly impacts the coexistence of tree species by altering the dynamics of competitive interactions. Climate change is inducing natural species selection beginning with competition amongst individual trees (MAGALHÃES; AMOROSO; LARSON, 2021). It is widely recognized that individual plants offer limited insights into the responses of communities and ecosystems to climate change (POORTER; NAVAS, 2003; ZISKA; BUNCE, 2006). Inferences drawn about the responses of individual plants based on factors such as photosynthetic pathways, growth rates, and nutrient availability may not always be reliable (ZISKA; BUNCE, 2006). Assessing the response of communities poses a significant challenge due to the high biodiversity and the limited control over other critical abiotic resources, including water and nutrients. However, evaluating plants' response to rising CO_2 during early succession, when there is less competition among species, is less complex. Ziska and Bounce (2006) pointed out the greater biomass production of a C_3 sedge (*Scirpus olneyi*) over a C_4 grass (*Spartina patens*) in a marsh system at elevated CO_2. Conversely, in a dry, tallgrass prairie system, a dominant C_4 grass outcompeted a dominant C_3 species in response to elevated CO_2, primarily due to the C_4 species' higher drought tolerance.

A meta-analysis conducted by Poorter and Navas (2003) revealed differences between the responses of species growing in isolation and those in competition. At the individual plant level, fast-growing pioneer species demonstrated a robust response compared to slow-growing climax species. Interestingly, under competitive conditions, both fast- and slow-growing species responded similarly to elevated CO_2 levels. While significant differences were found between C_3 and C_4 species at high nutrient levels, with C_4 species demonstrating lower benefits under elevated CO_2, the situation differed in the case of competition at low nutrient levels. Under such circumstances, no discernible differences between C_3 and C_4 species were observed, likely due to the restricted CO_2 response of C_3 species at low nutrient levels. The authors

concluded that in environments with high nutrient availability, C_3 species might outcompete C_4 species, while nitrogen-fixing dicots could thrive in conditions of low nutrient availability.

At the **ecosystem scale**, responses to elevated CO_2 levels vary within grassland communities, with those possessing higher species richness demonstrating more significant growth responses. In forest ecosystems, young trees have exhibited a notable growth increase (~30%) at elevated CO_2 (~700 ppm) (ZISKA; BUNCE, 2006). Certain tropical forests may experience temporary physiological benefits in response to higher temperatures and shifts in precipitation patterns. Nevertheless, the declining resilience of these forests to such stressors has led to a reduction in the provision of essential ecosystem services, including regulation, support, provisioning, and cultural services (OMETTO et al., 2022). Notably, among ecosystems in South America, including grasslands and savannahs, forests exhibit a heightened sensitivity to climate variability stress due to their limited adaptive capacity outside their optimal climate niche compared to other ecosystems, with this adaptive capacity being inversely related to stand density (competition) (MAGALHÃES; AMOROSO; LARSON, 2021).

While high species density often corresponds to limited adaptive capacity, increased biodiversity can enhance an ecosystem's ability to withstand the impacts of climate change (OMETTO et al., 2022). Conversely, the reduced water availability, prompted by climate change, can accelerate the decline of forest resilience (MAGALHÃES; AMOROSO; LARSON, 2021). Furthermore, the invasion of ecosystems by non-native species stands as a significant driver of global biodiversity loss. Climate change has garnered significant attention for its role in facilitating biological invasions, enabling the spread of exotic species into previously uncolonized regions. Under stress, the growth of plants is typically reduced, leading to the reallocation of unused photosynthesized carbon toward the synthesis of secondary chemical compounds. This adaptive strategy allows plants to cope with stress while simultaneously increasing their allelopathic potential. Consequently, there is a possibility that exotic species, under the duress of climate change and intraspecific competition, may amplify their ability to impact native plant species through allelopathy, thereby augmenting the mortality of native species (MEDINA-VILLAR et al., 2020).

With respect to climate-related mortality and regeneration, prolonged droughts have played a leading role in promoting moist forest trees mortality since the 1980s, particularly softwood, pioneer and evergreen species. Nevertheless, findings from experimental research suggest that tree seedlings and saplings in tropical moist forests have the capacity to adapt photosynthetically to moderate levels of warming, with indications of increased growth rates

compared to mature trees. Additionally, certain seedlings in these forests demonstrate flexibility in response to recurring droughts, exhibiting accelerated growth during periods of favorable moisture conditions. Notably, in the Amazon forests, there has been an observable shift in the abundance of tree genera, with a notable increase in dry habitat-associated genera among newly recruited trees. Simultaneously, the mortality of genera linked with moist habitats has risen, particularly in regions where dry seasons have intensified, signaling a gradual transition toward a drier forest ecosystem (OMETTO et al., 2022).

The impact of climate change on forest systems raises concerns regarding their long-term capacity to serve as carbon sinks, effectively sequestering carbon. Uncertainties persist concerning the growth of plants resulted from CO_2 fertilization effect, the limits of photosynthetic and respiratory acclimation, the consequences of interactions between nitrogen pools and anticipated climatic factors in plant development, and the ecological ramifications of climate change. Furthermore, there is a growing impetus for large-scale and more integrative studies, particularly due to the demonstrated limitations of single-leaf analysis in providing insight into ecosystem responses.

REFERENCES

AINSWORTH, E. A.; LONG, S. P. What have we learned from 15 years of free-air CO 2 enrichment (FACE)? A meta-analytic review of the responses of photosynthesis, canopy properties and plant production to rising CO 2. **New Phytologist**, v. 165, n. 2, p. 351–372, 18 fev. 2005.

ALLEN, L. H. et al. Elevated CO_2 increases water use efficiency by sustaining photosynthesis of water-limited maize and sorghum. **Journal of Plant Physiology**, v. 168, n. 16, p. 1909–1918, nov. 2011.

ARIAS, P. A. et al. Technical Summary. Em: MASSON-DELMOTTE, V., et al. (Eds.). **Climate Change 2021 – The Physical Science Basis. Contribution of Working Group I to the Sixth Assessment Report of the Intergovernmental Panel on Climate Change**. Cambridge, United Kingdom and New York, NY, USA: Cambridge University Press, 2023. p. 35–144.

BOWMAN, W. D. et al. Negative impact of nitrogen deposition on soil buffering capacity. **Nature Geoscience**, v. 1, n. 11, p. 767–770, 2 nov. 2008.

CAMPBELL, C. et al. Acclimation of photosynthesis and respiration is asynchronous in response to changes in temperature regardless of plant functional group. **New Phytologist**, v. 176, n. 2, p. 375–389, 10 out. 2007.

CELENTANO, D. et al. Towards zero deforestation and forest restoration in the Amazon region of Maranhão state, Brazil. **Land Use Policy**, v. 68, p. 692–698, nov. 2017.

CRISTO, L. DE A.; SANTOS, M. A.; MATLABA, V. J. Land-Use Changes and Socioeconomic Conditions of Communities along the Carajás Railroad in Eastern Amazonia. **Sustainability**, v. 14, n. 9, p. 5132, 24 abr. 2022a.

CRISTO, L. DE A.; SANTOS, M. A.; MATLABA, V. J. Socioeconomic and Environmental Vulnerability Index in the Brazilian Amazon: The Case of the Carajás Railroad. **The Extractive Industries and Society**, v. 11, p. 101128, set. 2022b.

FAN, X. et al. Carbon dioxide fertilization effect on plant growth under soil water stress associates with changes in stomatal traits, leaf photosynthesis, and foliar nitrogen of bell pepper (Capsicum annuum L.). **Environmental and Experimental Botany**, v. 179, p. 104203, nov. 2020.

FOSTER, P. et al. Changes in Atmospheric Constituents and in Radiative Forcing. Em: SOLOMON, S. et al. (Eds.). **The Physical Science Basis. Contribution of Working Group I to the Fourth Assessment Report of the Intergovernmental Panel on Climate Change**. Cambridge, UK: Cambridge University Press, 2007. p. 129–234.

GATTI, L. V. et al. Amazonia as a carbon source linked to deforestation and climate change. **Nature**, v. 595, n. 7867, p. 388–393, 2021.

JIANG, X. et al. The role of photorespiration in plant immunity. **Frontiers in Plant Science**, v. 14, 1 fev. 2023.

KEMP, P. R.; WILLIAMS, G. J. A Physiological Basis for Niche Separation Between Agropyron Smithii (C_3) and Bouteloua Gracilis (C_4). **Ecology**, v. 61, n. 4, p. 846–858, ago. 1980.

KUBIEN, D. S.; SAGE, R. F. Low-temperature photosynthetic performance of a C_4 grass and a co-occurring C_3 grass native to high latitudes. **Plant, Cell & Environment**, v. 27, n. 7, p. 907–916, 7 jul. 2004.

KUMAR, R. et al. Free-Air CO_2 Enrichment (FACE) and Free-Air Temperature Increase (FATI) Effects on Trifolium repens L. in Temperate Himalayas. **International Journal of Plant Production**, v. 14, n. 1, p. 43–56, 19 mar. 2020.

LAL, M. K. et al. From source to sink: mechanistic insight of photoassimilates synthesis and partitioning under high temperature and elevated [CO_2]. **Plant Molecular Biology**, v. 110, n. 4–5, p. 305–324, 24 nov. 2022.

LEE, T. D.; REICH, P. B.; BOLSTAD, P. V. Acclimation of leaf respiration to temperature is rapid and related to specific leaf area, soluble sugars and leaf nitrogen across three temperate deciduous tree species. **Functional Ecology**, v. 19, n. 4, p. 640–647, 19 ago. 2005.

MAGALHÃES, J. G. DE S.; AMOROSO, M. M.; LARSON, B. C. What evidence exists on the effects of competition on trees' responses to climate change? A systematic map protocol. **Environmental Evidence**, v. 10, n. 1, p. 34, 11 dez. 2021.

MAGALHÃES, M. P. et al. A cultura tropical. Em: MARCOS PEREIRA MAGALHÃES (Ed.). **Amazônia Antropogênica**. Museu Emílio Goeldi ed. Belém: [s.n.]. p. 429.

MAROCO, J. P.; EDWARDS, G. E.; KU, M. S. B. Photosynthetic acclimation of maize to growth under elevated levels of carbon dioxide. **Planta**, v. 210, n. 1, p. 115–125, 5 nov. 1999.

MASSAD, R.-S.; TUZET, A.; BETHENOD, O. The effect of temperature on **C_4**-type leaf photosynthesis parameters. **Plant, Cell & Environment**, v. 30, n. 9, p. 1191–1204, 4 set. 2007.

MEDINA-VILLAR, S. et al. Environmental stress under climate change reduces plant performance, yet increases allelopathic potential of an invasive shrub. **Biological Invasions**, v. 22, n. 9, p. 2859–2881, 24 set. 2020.

MNDELA, M. et al. A global meta-analysis of woody plant responses to elevated CO_2: implications on biomass, growth, leaf N content, photosynthesis and water relations. **Ecological Processes**, v. 11, n. 1, p. 52, 26 ago. 2022.

OMETTO, J. P. , et al. Tropical Forests. Em: PÖRTNER, H.-O. et al. (Eds.). **Climate Change 2022: Impacts, Adaptation and Vulnerability. Contribution of Working Group II to the Sixth Assessment Report of the Intergovernmental Panel on Climate Change**. Cambridge, UK and New York, NY, USA,: Cambridge University Press, 2022. p. 2369–2410.
POORTER, H.; NAVAS, M. Plant growth and competition at elevated CO_2: on winners, losers and functional groups. **New Phytologist**, v. 157, n. 2, p. 175–198, 24 fev. 2003.
REDDY, K. S. et al. SCADA Based Rainfall Simulation and Precision Lysimeters with Open Top Climate Chambers for Assessing Climate Change Impacts on Resource Losses in Semi-arid Regions. Em: [s.l: s.n.]. p. 435–446.

SAGE, R. F. Variation in the kcat of Rubisco in C_3 and C_4 plants and some implications for photosynthetic performance at high and low temperature. **Journal of Experimental Botany**, v. 53, n. 369, p. 609–620, 1 abr. 2002.

SAGE, R. F.; KUBIEN, D. S. The temperature response of C_3 and C_4 photosynthesis. **Plant, Cell & Environment**, v. 30, n. 9, p. 1086–1106, set. 2007.

SAGE, R. F.; WAY, D. A.; KUBIEN, D. S. Rubisco, Rubisco activase, and global climate change. **Journal of Experimental Botany**, v. 59, n. 7, p. 1581–1595, maio 2008.

SANT'ANA JÚNIOR, H. A. DE; ALVES, E. DE J. P. MINING-RAILROAD-PORT: "AT THE END OF THE LINE", A CITY IN QUESTION. **Vibrant: Virtual Brazilian Anthropology**, v. 14, n. 2, 7 dez. 2017.

SILVA, J. B. L. DA et al. Desenvolvimento de estrutura experimental para estudos de mudanças climáticas em culturas agrícolas. **Brazilian Journal of Animal and Environmental Research**, v. 3, n. 3, p. 2258–2264, 2020.

SILVA, R. G. DA; ALVES, R. DE C.; ZINGARETTI, S. M. Increased [CO_2] Causes Changes in Physiological and Genetic Responses in **C_4** Crops: A Brief Review. **Plants**, v. 9, n. 11, p. 1567, 13 nov. 2020a.

SILVA, R. G. DA; ALVES, R. DE C.; ZINGARETTI, S. M. Increased [CO_2] Causes Changes in Physiological and Genetic Responses in **C_4** Crops: A Brief Review. **Plants**, v. 9, n. 11, p. 1567, 13 nov. 2020b.

SLOT, M.; KITAJIMA, K. General patterns of acclimation of leaf respiration to elevated temperatures across biomes and plant types. **Oecologia**, v. 177, n. 3, p. 885–900, 7 mar. 2015.

SLOT, M.; WINTER, K. Photosynthetic acclimation to warming in tropical forest tree seedlings. **Journal of Experimental Botany**, v. 68, n. 9, p. 2275–2284, 1 abr. 2017.

TAIZ, L. et al. **Fisiologia e desenvolvimento vegetal**. 6. ed. Porto Alegre: artmed, 2017.
THE WORLD BANK GROUP. **Brazil: Country Climate and Development Report**. Washington: [s.n.].

TIMM, S.; HAGEMANN, M. Photorespiration—how is it regulated and how does it regulate overall plant metabolism? **Journal of Experimental Botany**, v. 71, n. 14, p. 3955–3965, 6 jul. 2020.

TJOELKER, M. G. et al. Coupling of respiration, nitrogen, and sugars underlies convergent temperature acclimation in Pinus banksiana across wide-ranging sites and populations. **Global Change Biology**, v. 14, n. 4, p. 782–797, 20 abr. 2008.

WAND, S. J. E. et al. Responses of wild C_4 and C_3 grass (Poaceae) species to elevated atmospheric CO 2 concentration: a meta-analytic test of current theories and perceptions. **Global Change Biology**, v. 5, n. 6, p. 723–741, 24 ago. 1999.

WANG, G. et al. Nitrogen supply influences photosynthetic acclimation of yellow birch (Betula costata Trautv.) to the combination of elevated CO_2 and warmer temperature. **New Forests**, 16 out. 2023.

ZHANG, J. et al. The Responses of Plant Leaf CO_2/H_2O Exchange and Water Use Efficiency to Drought: A Meta-Analysis. **Sustainability**, v. 10, n. 2, p. 551, 21 fev. 2018.

ZISKA, L. H.; BUNCE, J. A. Plant Responses to Rising Atmospheric Carbon Dioxide. Em: **Plant Growth and Climate Change**. [s.l.] Wiley, 2006. p. 17–47.

CHAPTER 1 – LAND USE LAND COVER CHANGES AND EXTREME PRECIPITATION EVENTS ALONG CARAJÁS RAILROAD IN THE EASTERN BRAZILIAN AMAZON*

Maísa Quintiliano Alves[1], Flávio Justino[2], Rubens Alves de Oliveira[3], Carlos Augusto Brasileiro de Alencar[4], Francisco Cássio Gomes Alvino[5] and Renan Rodrigues Coelho[6]

ABSTRACT

The importance and vulnerability of municipalities in the eastern Amazon led to the evaluation of the distribution of seasonal precipitation and extreme events over protected and deforested sites along the Carajás Railroad (EFC) based on three datasets: Brazilian Daily Weather Gridded Data (BR-DWGD), European Reanalysis (ERA5-Land), and Climate Hazards Group InfraRed Precipitation with Station (CHIRPS). The main purpose is the understanding of the relationship between local land use change and the occurrence of extreme climate events. Results suggested that large-scale deforestation has a regional impact occasionally outweighing local effect. Significant trends reveal a general pattern of drought that has been more intense in the north of the study area, regardless of land cover, whether preserved or deforested. Moreover, the dry season is getting drier, but the wet season is not getting wetter over the entire area, as Carajás National Forest and Curionópolis (southern sector) deliver positive and accentuated trends in the rainy season. Extreme events are becoming more frequent. The number of consecutive dry days has increased in the north revealing an extension of dry periods, whereas, the maximum one-day precipitation has soared in the south indicating the intensification of rainfall. CHIRPS provides stronger correlations with the standard dataset (BR-DWGD), as both furnish primary data based on rain gauges observations. It also outperforms ERA5-Land in annual and seasonal analyses, which does not invalidate the latter as a great alternative to use in data-poor locations. Ultimately, further research and technology implementation were recommended to improve reforestation efforts given the reported results.

Keywords: Extreme-precipitation-events. Extreme-events. Climate-change. ERA5-land. CHIRPS. Climate-products.

* Manuscript submitted for publication in Theoretical and Applied Climatology in September 2023. The final version, published on June 2024, includes improvements (https://doi.org/10.1007/s00704-024-05061-y).

1-5 Authors affiliation: Universidade Federal de Viçosa, Agricultural Engineering Department, Viçosa, Brazil.
6 Author affiliation: Vale S.A., Carajás Industrial Complex, Parauapebas, Brazil.

1. INTRODUCTION

The Sixth Assessment Report of the Intergovernmental Panel on Climate Change (IPCC) has demonstrated that climate change has been influenced among others by human activities, aerosol emissions, and changes in land use (2021). The initiation of a mining project can induce substantial change in land use, especially in the Amazon region, where the largest tropical forest is located and where ferruginous rupestrian grasslands also occur, both holding enormous biodiversity and endemism (DA SILVA et al. 2005; GIULIETTI et al. 2019; SCHAEFER et al. 2023). In addition, the Amazon Rainforest exerts a significant influence on global water cycles and climate dynamics (CELENTANO et al. 2017), making it especially important in the context of climate change.

One of the largest iron ore exploration projects of the world (S11D project) is in Brazilian Amazon (MATLABA et al. 2019). It constitutes the Northern System: a set of several extraction sites, processing plants, and a logistical operation mainly responsible for transporting ore from municipalities of Pará to a port in Maranhão (Porto da Madeira). The ore is transported by the Carajás Railroad (Estrada de Ferro Carajás – EFC), crossing municipalities that have been undergoing a complex development process since the mid-twentieth century related to projects and policies to encourage farming and, later, the mining activity (MAGALHÃES et al. 2016). The heterogeneous development along the EFC led to a regional economy based on cattle raising and mining and contributed to the social vulnerability of several municipalities, many of them with little infrastructure (CELENTANO et al. 2017; SANT'ANA JÚNIOR AND ALVES 2017; CRISTO et al. 2022). Furthermore, millions of hectares of land have shifted from tropical forests into urban, agricultural, mining, and chiefly pasture areas (MAPBIOMAS 2022).

Deforestation to establish pastures plays a leading role in threatening the environmental sustainability in the southeastern Brazilian Amazon (GATTI et al. 2021; HASE UETA et al. 2023). The region is associated with the so-called "Arc of deforestation", the most deforested area in this biome (CAVALCANTE et al. 2019). Despite this, Sant'Ana Júnior & Alves (2017) identified 28 conservation units along the EFC, which hold the preservation of the remaining native vegetation in the region. Eight of them are conservation federal units, such as Carajás National Forest (Carajás FLONA) and Gurupi Nature Reserve (Gurupi REBio). The latter is a biological reserve practically surrounded by deforestation. How does such forest remnant influence the local climate? Efforts have been conducted to comprehend the climatic effects of changes in land use on a local, regional, and global scale. The resulting findings assist

policy makers in supporting vulnerable populations, mitigating emissions, and promoting atmosphere carbon removal (IPCC 2021).

Ongoing projects and a novel proposal for a bold large-scale restoration, the “Arc of restoration” (DA CRUZ et al. 2021; TORRES 2022), have attracted worldwide attention. Actions of this size can generate positive environmental impacts that go beyond the borders of the country. However, climate change potentially affects plants growth and survival, including seedlings and newly recruited trees (OMETTO et al. 2022). Thus, understanding how the local climate has been affected by changes in land use and the local pattern of these changes, is crucial for the feasibility of Arc of deforestation initiative in a region of global importance.

South America's (SA) climate is significantly influenced by both large- and local-scale circulation mechanisms, which are crucial to dictate the high spatial and temporal variability of rainfall across the Amazon (MU and JONES 2022). This region experiences large fluctuations of rainfall, highlighted by a pronounced dry season in the southern Amazon, but absent dry season in the northwest part (MARENGO et al. 2018). Particularly, the eastern part is notably affected by the El Niño/Southern Oscillation (ENSO), the Intertropical Convergence Zone (ITCZ) and sea surface temperatures (SSTs) (HAGHTALAB et al. 2020). Currently, general downward trends in precipitation and increasing in air temperatures have been reported in SA, as well as a high frequency of extreme events in the Amazon (LUCAS et al. 2021; ARIAS et al. 2023; BOCHOW and BOERS 2023).

Despite the growing understanding about the effects of deforestation on large scale climate, Haghtalab et. al (2020) have emphasized the need for high-resolution precipitation analysis to capture the spatio-temporal variability. In this sense, by using high-resolution gridded precipitation from 1982 to 2018 they identified significant drying trends in eastern Amazon, but their study did not explore climatic characteristics and trends across the EFC's. Likewise, Mu and Jones (2022) revealed the distinct spatial distribution of rainfall trends during the rainy season in the Brazilian Legal Amazon, highlighting significant areas that have experienced negative precipitation trends over the Arc of Deforestation, in particular during the dry season. In the vicinity of the current study area, similar heterogeneity in trends was documented. Moreover, negative trends for some precipitation indices, such as maximum precipitation in five days, and an upward trend in consecutive dry days have been noticed (LUCAS et al. 2021; SANTOS et al. 2020). Santos et al. (2020) found enhanced dry conditions across the Amazon and Cerrado transition using weather stations data, with a large spatial-temporal variation in trends of extreme precipitation and temperature events, which demonstrate that climate is changing in a different manner depending on the location in eastern

Amazon. Moreover, Avila-Diaz et al. (2020) found significant warming patterns with increasing (decreasing) trends in warm (cold) extremes for the 1980-2016 interval. For precipitation indices, observations show an increase in consecutive dry days and a reduction of consecutive wet days over most parts of Brazil.

The aforementioned results useful serve to justify the need for more studies on climate events over this strategic and vulnerable region, to enhance the understanding of the human activities on climate. These changes may deeply impact the livelihoods of people, the environment as well as the efficiency of biome recovery. The data availability in the region is limited, especially due to the low density of precipitation gauge network (BAKER et al. 2021). Hence, high-quality gridded climatic products, satellite-based or reanalysis products, are essential to assess the rainfall regime (SILVA JUNIOR et al. 2018; HAGHTALAB et al. 2020, ZANDLER et al. 2020; REDA et al. 2021; FESSEHAYE et al. 2022).

Therefore, this study aims to assess the distribution of seasonal precipitation and extreme events from 1980 to 2020 over selected locations along the EFC, using three different climate variables datasets: BR-DWGD, ERA5-Land and CHIRPS. The purpose of analyses is to evaluate the datasets performances, but primary to understand the relationship between local land use change and extreme climate events occurrence, by assessing differences of climatic patterns in preserved sites (conservation unities) and deforested areas.

2. MATERIALS AND METHODS

2.1. Characterization of the study area

2.1.1. Location

This study focuses on a set of 28 municipalities along the EFC in northern Brazil (central point: 47.6905°W, 4.7293°S), an area hereafter referred to as the Northern System's domain. Five municipalities are in the state of Pará and 23 in Maranhão, representing the area of influence of the EFC. They comprise a transition between two biomes, being mostly within the Amazon, although some are also part of the Cerrado (Fig. 1a). Furthermore, the study area covers part of the drainage area of Tocantins - Araguaia and Atlântico Nordeste Ocidental basins.

Figure 1 – The Northern System's domain: location (central point: 47.6905°W, 4.7293°S); geopolitical boundaries (Pará state-PA and Maranhão state-MA); biomes (the Amazon – slightly transparent green and Cerrado – slightly transparent orange); federal conservation unities within its boundaries (Igarapé Gelado APA – vibrant orange, Carajás FLONA – vibrant green, Itacaiunas FLONA – a shade of greenish yellow; Tapirapé-Aquiri FLONA – blue, Campos Ferruginosos PARNA – a shade of bluish purple, Gurupi REBIO (red), Tapirapé REBIO – pink and Ciriaco RESEX – beige) **(a)**; climate types (Am – tropical monsoonal zones, Aw – tropical with dry winters and Af – tropical without dry season) and basins (Amazônica – green, Tocantins-Araguaia – pink and Atlântico Nordeste Ocidental – light blue) **(b)**

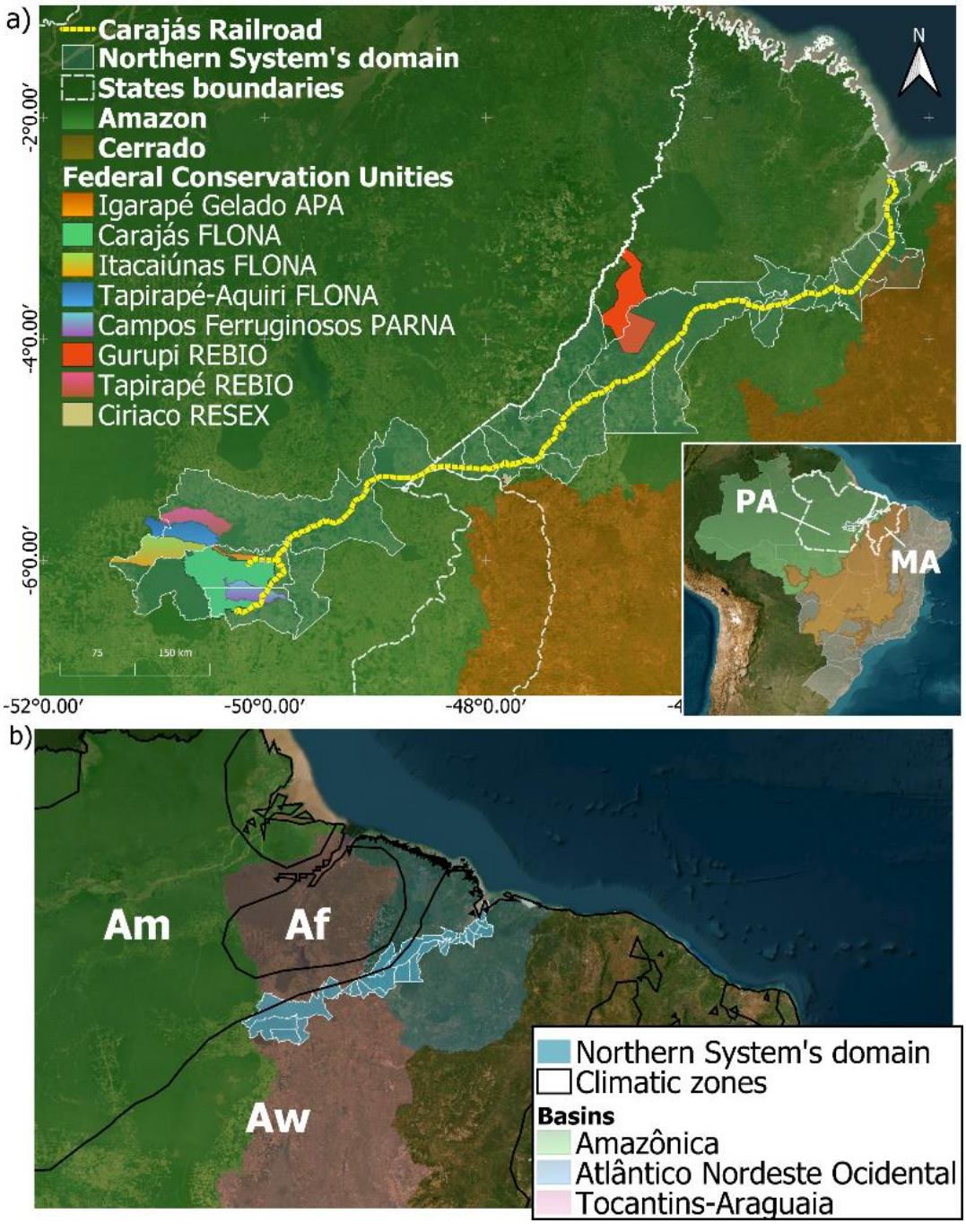

Own authorship

2.1.2. Climate

The regional climate is major classified as tropical with dry winters (Köppen-Geiger classification: Aw), although some municipalities partially fall in the tropical monsoonal zones and tropical without dry season (Köppen-Geiger classification: Am and Af, respectively) (Fig. 1b). The Am-type climate is wet and warm, with the monsoon period between February and May. The mean annual rainfall is about 2,500-2,800 mm, and the mean annual temperature is over 26 °C with few seasonal variation (ALVARES et al. 2013; PAIVA et al. 2020). The Aw-type is warm and wet markedly seasonal with dry winters. The rainy season lasts from November to May and the dry season from June to October, with rainfall of below 60 mm in the driest month (FERNANDES et al. 2018).

2.2. Land use and land cover data and sites selection

We assessed 36 years (1985-2021) of data on land use land cover in the Northern System's domain using updated statistics from the seventh collection of the Mapbiomas project (2022). Mapbiomas is a collaborative network accounted for the annual mapping of land cover land use in the Brazilian territory, among other activities. The mapping is based on a pixel-by-pixel classification of 30m resolution images from the Landsat satellite using robust machine learning algorithms on the Google Earth Engine platform. More details on the mapping methodology are available at https://mapbiomas.org/visao-geral-da-metodologia. Updated geospatial data of conservation units managed by the Instituto Chico Mendes de Biodiversidade (ICMBio) in the study area was obtained at https://www.gov.br/icmbio/pt-br/assuntos/dados_geoespaciais.

In this study, we identified major usage classes based on their extension in the territory. Taking 1985 as the base year, we also obtained the variation percentages for each land use in 1986, 1991, 1996, 2001, 2006, 2011, 2016 and 2021. This assessment enables the visualization of the land use class with the highest growth within the study area.

We assumed deforestation as the loss of forest formation area. Therefore, in addition to the Northern System's total area domain, municipalities with more than 50% of their area deforested by 2021 (base year: 1985) were selected for local climate studies, namely: Santa Inês (Maranhão), Curionópolis (Pará), Tufilândia (Maranhão), Monção (Maranhão) and São Francisco do Brejão (Maranhão). With the same purpose, we also selected two conservation

unities, Gurupi REBio (Maranhão) and Carajás FLONA (Pará), one in the north and the other in the south of the study area.

Gurupi REBio is the only integrated protected area in Maranhão, created in 1988 with ca. 270,000 ha to preserve prime lumber and other important forest species. This unit comprises areas of the Centro Novo do Maranhão, São João do Caru, and Bom Jardim. Within it, only the indirect use of natural resources is allowed (PAIVA et al. 2020). On the other hand, Carajás FLONA is a sustainable use unit in Pará established in 1998 with ca. 400,000 ha, covering part of municipalities of Parauapebas, Canaã dos Carajás e Água Azul do Norte. Collecting, extracting, and using forest natural resources is allowed, as long as the maintenance of ecological processes is assured (MAGALHÃES et al. 2016).

In this study, we assessed only a fraction of Gurupi REBio that intersects with the municipalities of the Northern System's domain (96,473.77 ha). Deforested Area and Conservation Unity sites are hereafter referred to as "DA" and "CU", respectively.

2.3. Precipitation data

We used daily data of three products to assess precipitation variations. The first, known as BR-DWGD, comprises a daily updated gridded precipitation data set (0.1°), obtained by spatial interpolation from observational data from 11,473 rain gauges and 1,252 weather stations, covering the Brazilian territory with a temporal coverage of 61 years (1961-2022) (XAVIER et al. 2022). More details at https://sites.google.com/site/alexandrecandidoxavierufes/brazilian-daily-weather-gridded-data?authuser=0.

The second product is the ERA5-Land, the fifth generation of European Reanalysis, which provides hourly high-resolution land data, covering the period from 1950 to the near-present, updated daily with a five-days latency. As the name suggests, it is a global reanalysis data set for the land component, with a spatial resolution of approximately 9 km (~0.08°) (MUÑOZ-SABATER et al. 2021). Further information at https://www.ecmwf.int/en/era5-land.

The third dataset is the CHIRPS, a quasi-global (50°S-50°N) and high-resolution (0.05°) dataset of blended gauge-satellite precipitation estimates. It comprises gridded precipitation time series with 41 years of coverage (1981 to near-present), low bias and latency (FUNK et al. 2015). More information at https://www.chc.ucsb.edu/data/chirps.

2.4. Precipitation pattern assessment

We acquired precipitation data from 1981 to 2020 in netCDF format and processed them using the ncdf4 package version 1.20 (PIERCE 2022) in software R version 4.2.2 (R CORE TEAM 2022). In ArcGIS Pro® version 2.8, we created a regular-gridded square box (0.1°) covering the polygon of the Northern System's domain and intersected the mid-points of its cells with the polygons of the study sites, obtaining what we called of "extraction points" (Fig. S1 – Appendix). Due to their size, we evaluated Santa Inês and Tufilândia as a single area, which allowed the intersection of grid points in a satisfactory amount. We used the coordinates of intersected points to extract the rainfall information from netCDF files using the raster package version 3.6-3 (HIJMANS 2022).

We assessed the variations of annual and monthly mean precipitation for each study site (selected areas) over the 1981-2020 period. We also compared the performance of the databases at annual, monthly, and seasonal scale, by calculations of correlation. The BR-DWGD includes a high number of rain gauges and weather stations within Brazilian territory, thus, it is assumed as the standard data in this study.

Trends and their magnitude were assessed by the Mann-Kendall test – M-K (MANN 1945; KENDALL 1975), and the Sen's slope estimator (SEN 1968), respectively, at 95% and 99% significance levels. Both are nonparametric methods widely used to detect trends and magnitudes of deviations in temporal series of climate data. The M-K assumes under the null hypothesis (Ho) no trend in climate extremes, whereas the alternative (Ha) lies on the evidence of monotonic trend, either increasing or decreasing (WIJNGAARD et al. 2003; MARTÍNEZ et al. 2009; AVILA-DIAZ et al. 2020). The tests were applied to the spatial average of the points for each study site, using the Kendall package version 2.2.1 (MCLEOD 2022) in R.

2.5. Extreme precipitation climate indices

Precipitation data assessment provides information about extreme events, such as their frequency, magnitude, and duration. All this information can be summarized in 11 extreme precipitation climate indices recommended by the world-renowned Expert Team on Climate Change Detection and Indices (ETCCDI). Those six used in this study (Table 1, in bold) were calculated in the Climate Data Operators – CDO software using precipitation data provided by the BR-DWGD and the ERA5-Land datasets.

Table 1 – Extreme precipitation indices recommended by ETCCDI. The indices used in this study are highlighted in bold.

Index	Index definition	Units
CDD	**Maximum number of consecutive dry days**	**days**
CWD	**Maximum number of consecutive wet days**	**days**
RX1day	**Annual maximum one-day precipitation**	**mm**
RX5day	**Annual maximum consecutive five-day precipitation**	**mm**
R10mm	**Annual count of days when daily precipitation ≥10 mm**	**days**
R20mm	**Annual count of days when daily precipitation ≥20 mm**	**days**
Rnmm	Annual count of days when daily precipitation ≥n mm	days
RCPTOT	Annual total precipitation in wet days	mm
R95p	Annual total precipitation from days >95th percentile	mm
R99p	Annual total precipitation from days >99th percentile	mm
SDII	The ratio of annual total precipitation to the number of wet days	mm/day

We prepared maps displaying the spatial distribution of the five-year averages of the indices from 1981 to 2020 using the ordinary kriging function in the ArcGIS PRO ® software version 2.8. Details on definitions of the core indices and calculation methodology are available at http://etccdi.pacificclimate.org/list_27_indices.shtml and https://guilherme.readthedocs.io/en/latest/pages/tutoriais/cdo.html, respectively.

Trends and their magnitude were assessed by the Mann-Kendall test – M-K (MANN 1945; KENDALL 1975) and the Sen's slope estimator (SEN 1968), respectively, at 95% and 99% significance levels, applied to the spatial average of the extraction points for each study site using the Kendall package version 2.2.1 (MCLEOD 2022) in R.

Breakpoints detection is used to investigate discontinuities in the rainfall time series. They are based on homogeneity tests capable of detecting a rupture in the climate series (mean shifts), giving information on the year of the break. The Pettit test (PETTITT 1979) is widely used for this purpose. This method supposes under the null hypothesis (Ho) data independency and identical distribution, whereas the alternative hypothesis (Ha) leads to accepting the presence of breaks is the series (MARTÍNEZ et al., 2009; WIJNGAARD et al., 2003). Here, we conducted the tests at 95 and 99% significance level using the trend package version 1.1.4 (POHLERT 2020) in R (AVILA-DIAZ et al., 2020).

3. RESULTS

3.1. Land use and land cover assessment

Data assessment outcomes revealed the dramatic change in land use land cover over the study area since 1985. Most of forest formation areas shifted to pasture, mainly in the central-eastern portion of the Northern System's domain. Despite their important presence, forests are mostly fragmented, except within the boundaries of federal conservation unities. The importance of protected areas stands out in this scenario, with a clear contribution to the preservation of the remaining greenness (Fig. 2a).

Some land use classes have uninterruptedly increased over the years in the region. Assessments considering 1985 as base year revealed that this is the case of mining, urban areas, and mainly temporary crops, with impressive increases of 400%, 220% and 60,000% in 2021, respectively. Pasture class has shown a certain stability or even a slight downward trend in recent years. Even so, it has more than doubled (137%) since 1985. Land use and land cover classes with decreasing trends mostly represent natural landscapes, such as savannas, mangroves, beaches and dunes, wetlands, and forests, evidencing natural environments degradation. The outcomes pointed to a loss of about 40% of the forest formation area over the years (Fig. 2b).

Despite the sharp increase of mining, urban and temporary crops areas, the extension of pasture and forest classes is still far greater than the others. In 2021, they represented about 3 million ha each, although forests were almost five times larger than pasture areas in 1985.

The annual extent of forest formation decreased until 2008-2009 and pastures increased. From then on, the figures point to a stability with small variations for both classes (Fig. 2c).

In five municipalities, deforestation exceeded 50% in 2021 with respect to the year 1985, namely: Santa Inês (63,7%), Curionópolis (58,8%), Tufilândia (52,7%), Monção (51,6%) and São Francisco do Brejão (50,4%), in descending order of deforestation magnitude (Fig. 3a). They are located mainly in Maranhão state, except for Curionópolis, which is very close to conservation areas in Pará (Fig. 3b).

Fig. 2 Classes of land use land cover in Northern System's domain: Classes in 1985 and 2021 **(a)**, relative areas (growth or reduction) of classes observed in 1986, 1991, 1996, 2001, 2006, 2011, 2016 and 2021, based on year 1985 **(b)**, and forest (green) and pasture (orange) area over time **(c)** (Database: Mapbiomas, 2022)

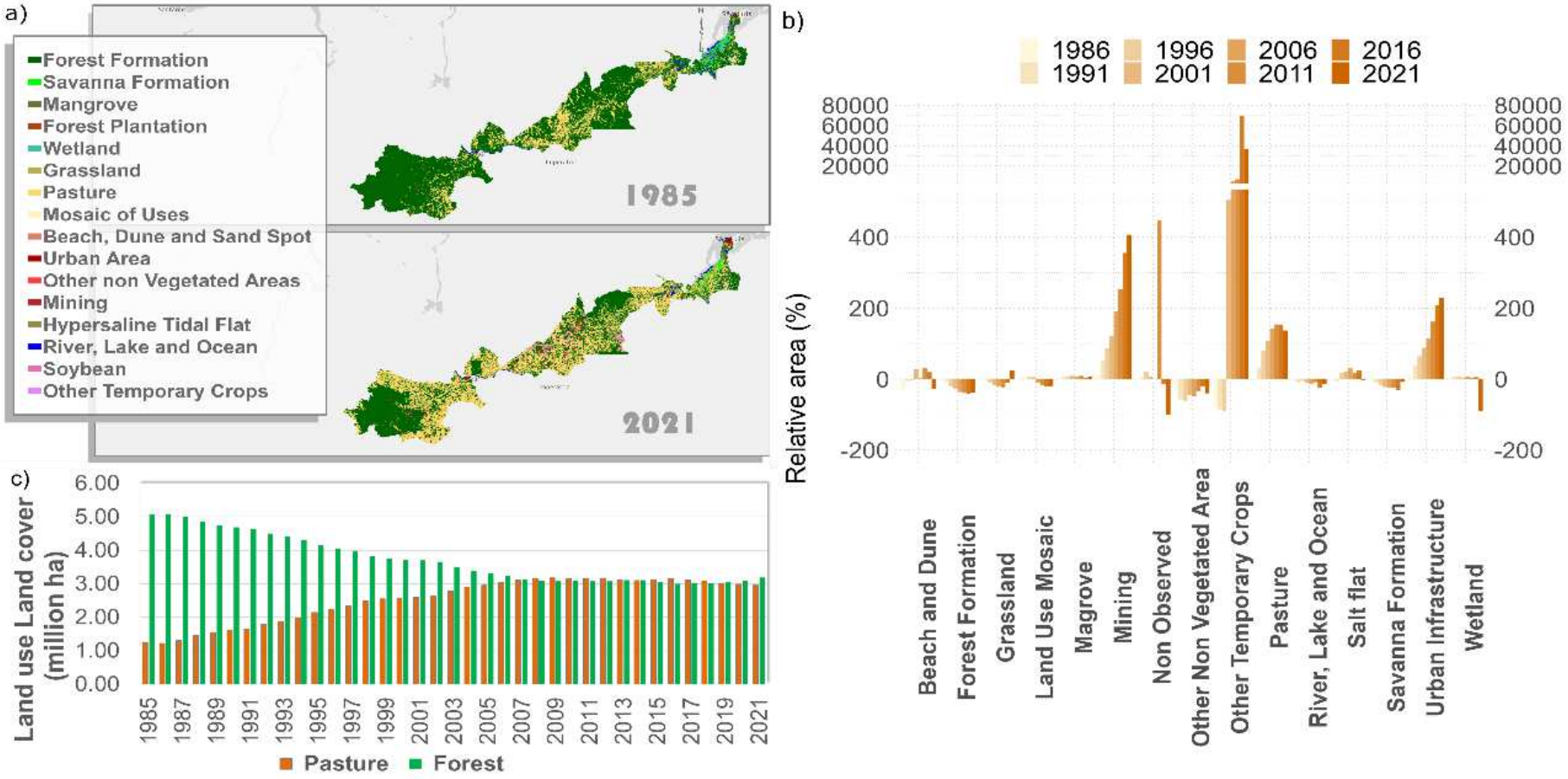

Own authorship

Fig. 3 Extension of forest formation in 1985 (dark green line) and 2021 (light green line) and its equivalent percentage loss (deforestation rate – orange bars) over this time interval in the Northern System's domain, being tagged the five municipalities with deforestation greater than 50% in 2021, which were selected for climate assessments in this study (Database: Mapbiomas, 2022) **(a)**. Location of the selected municipalities (pink) and conservation unities (Gurupi REBio – blue and Carajás FLONA – green) **(b)**

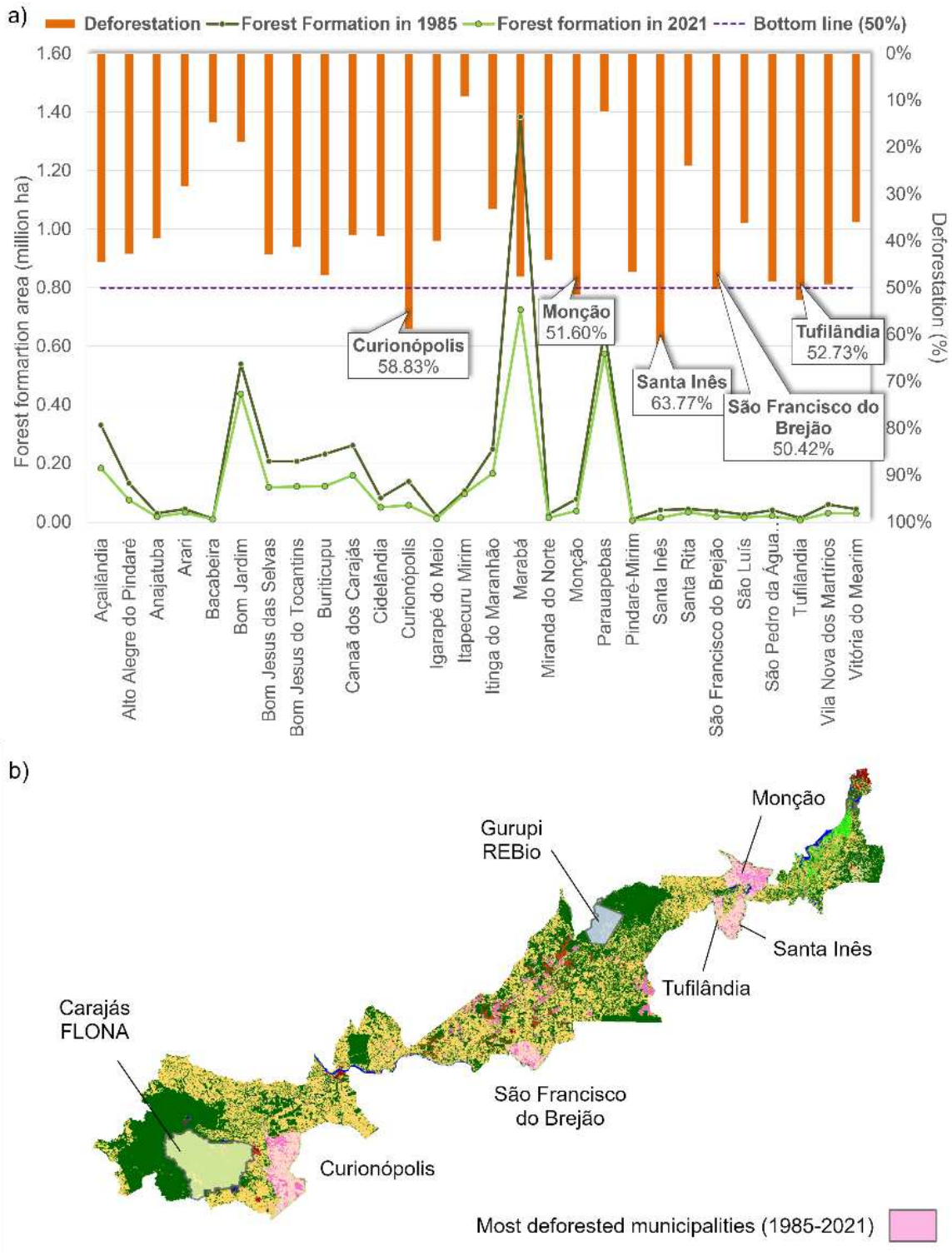

Own authorship

3.2. Land use and land cover data and sites selection

Figure 4 shows the annual precipitation over the study region based on the three datasets. An important spatial-temporal variability is noted for the Northern System's domain, as several authors have already reported for the region (De Souza et al. 2014; Alves et al. 2017; Santos et al. 2020). Slight differences are noticed among those datasets. The BR-DWGD usually exhibits lower averaged values but higher variability, as shown by the blue dots, with respect to CHIRPS and ERA5-LAND. Such variability is even more pronounced over northern sector sites in Maranhão (Fig. 4d, e, g).

Fig. 4 Climatology: Annual precipitation variations of sites under study using 40-years (1981-2020) of data provided by BR-DWGD (white boxes), ERA5-Land (grey boxes) and CHIRPS (black boxes) datasets. The blue dots represent the annual individual observations

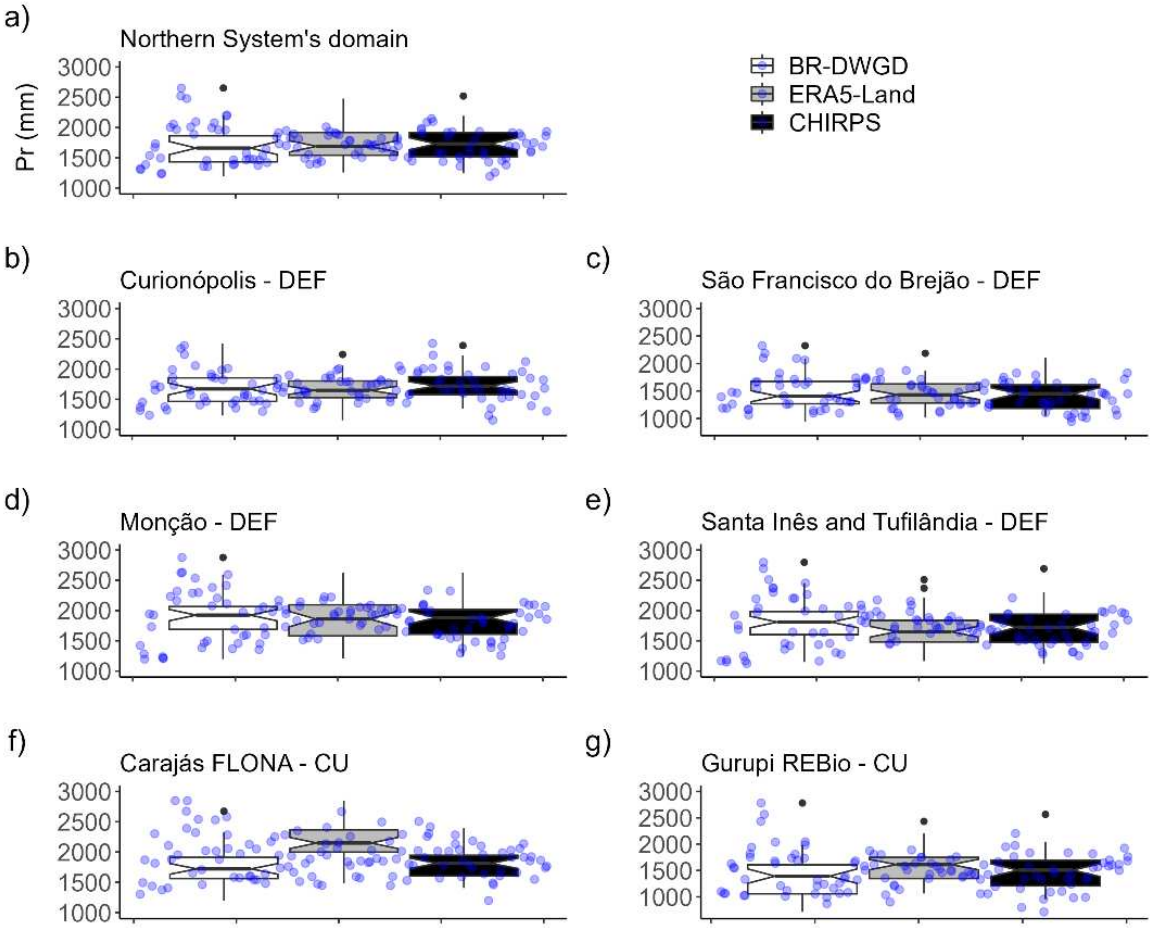

Own authorship

By downscaling the analyses to the specific sites, marked differences emerge in particular in Carajás FLONA and Gurupi REBio (Fig. 4f, g). Over these sites ERA5-Land

displays higher values of precipitation by about 2,300 mm and 1,600 mm, respectively. It must be noted that these areas are conservation unities with low deforestation. In opposite, good agreement among those datasets are delivered in deforested areas (Fig. 4a-d).

Turning to seasonal analyses in the Northern System's domain, it is demonstrated that the rainy (dry) season is concentrated from November to April (May to October) (Fig. 5a). Monthly averages show that the datasets fairly agree with each other, but higher variability for individual months is noted in ERA5-Land. This dataset also indicates greater monthly values, especially in February, when precipitation has already surpassed 600 mm/month over northern sites (Monção, Santa Inês and Tufilâdia) and Carajás FLONA. All datasets show greater inter-annual variability during the rainy season.

Fig. 5 Seasonality: Monthly precipitation variations of sites under study using 40-years (1981-2020) of data provided by BR-DWGD (white boxes), ERA5-Land (grey boxes) and CHIRPS (black boxes) datasets. The red dots represent the possible outliers

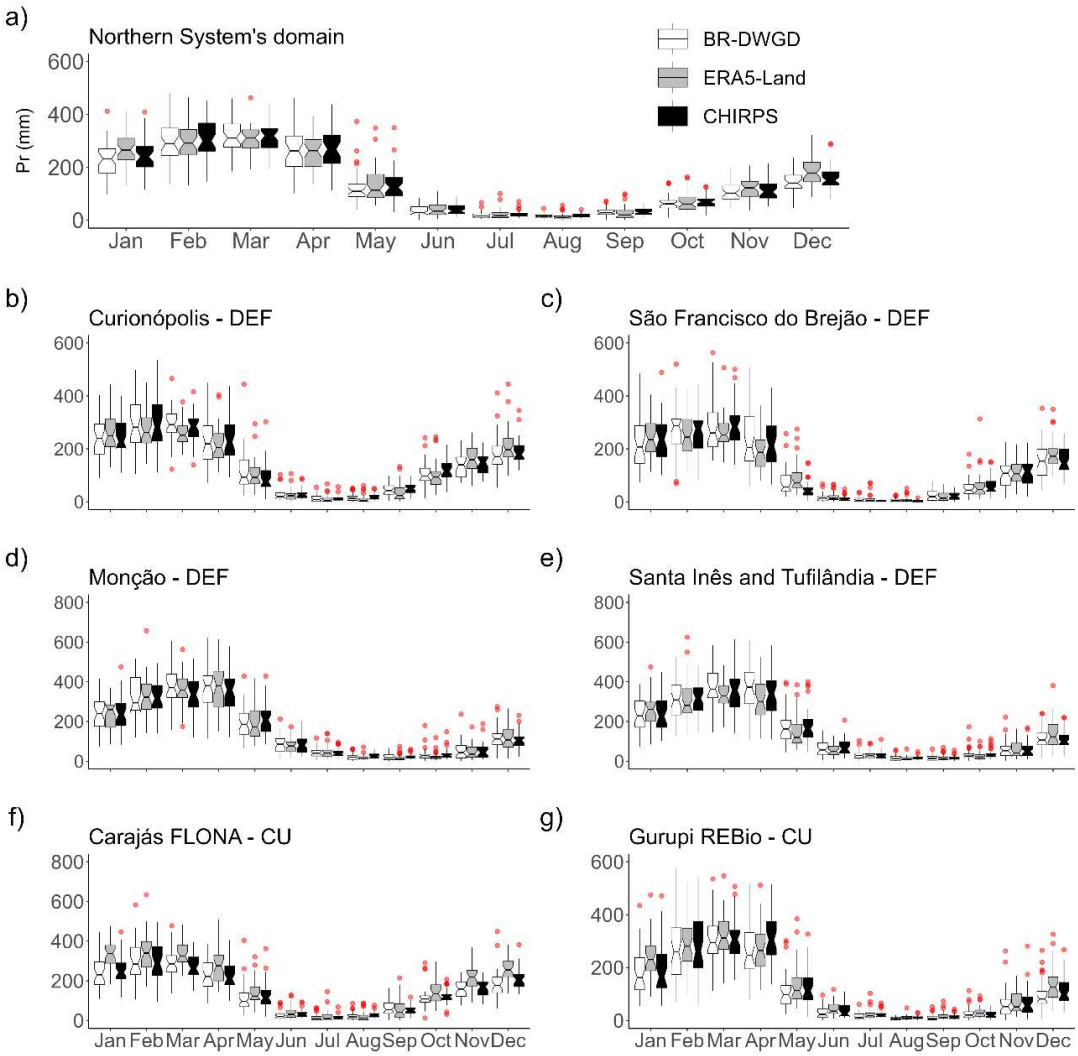

Own authorship

Further analyses for annual and seasonal precipitation, as displayed by point plot, boxplot, scatter plot, density chart and correlation coefficients among BR-DWGD, ERA5-Land and CHIRPS databases (Fig. 6a, b), show that most precipitation falls between 1,200 and 1,800 mm/year, with correlations with respect to BR-DWGD higher than 0.9. Interesting to note that based on power density (line chart in Fig. 6a), the CHIRPS distribution shows more values concentrated between 1,500 and 2,000 mm/year.

Fig. 6 Density charts and scatter plots of the annual data provided by BR-DWGD, ERA5-Land and CHIRPS databases for the Northern System's domain and the correlation between the datasets (correlation coefficients) **(a)** Point plots, boxplots, scatter plots and density charts of the seasonal data (dry season – pink and rainy season – blue) provided by BR-DWGD, ERA5-Land and CHIRPS databases for the Northern System's domain and the correlation between the datasets (correlation coefficients). The coefficients in grey express the correlation between the monthly data **(b)**

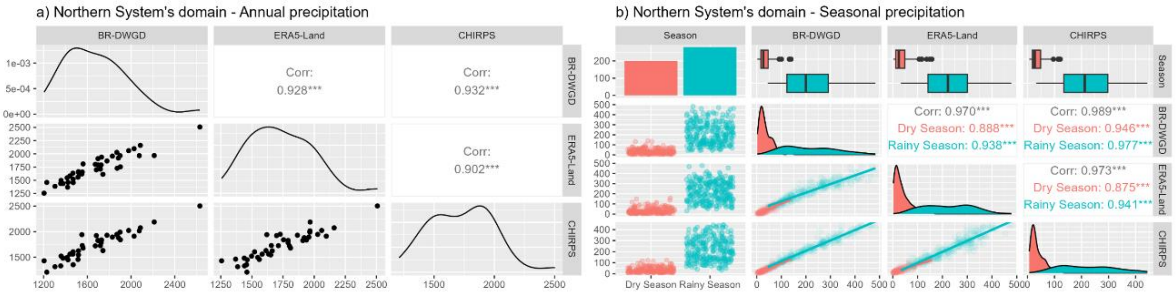

Own authorship

By verifying the seasonal pattern for the entire Northern System's domain, no substantial changes with respect to annual conditions arise, nevertheless, the correlation between BR-DWGD and ERA5-Land is reduced to about 0.8 in the dry season. Over the study region in the dry season, precipitation is within 100 mm, whereas during the rainy season the values vary from 10 to 500 mm, in which more spread amount is provided by ERA5-Land (Fig. 6b). Similar evaluation as conducted for the individual selected sites shows that correlations between BR-DWGD and the other datasets are lower with respect to annual calculation, ranging from 0.7 to 0.9 (Table 2). There is also a normal distribution in the rainy season in Curionópolis and Carajás FLONA, with peak by about 250 mm/month (Fig. S2 – Appendix). The other sites display a similar white noise distribution with precipitation being distributed under different values. Note that correlation coefficients are always higher in the dry season for sites in Pará and in the rainy season for sites in Maranhão, regardless of the dataset and land use and land cover.

Table 2 – Correlation coefficients between the monthly (black) and seasonal (dry season – orange and rainy season – blue) data provided by BR-DWGD, ERA5-Land and CHIRPS databases for the study sites.

Site	Correlation coefficients								
	BR-DWGD x ERA5-LAND			BR-DWGD x CHIRPS			ERA5-LAND x CHIRPS		
	Mon [a]	Dry [b]	Rainy [c]	Mon	Dry	Rainy	Mon	Dry	Rainy
Curionópolis	0.90	0.83	0.77	0.97	0.93	0.93	0.92	0.85	0.81
S.F.B.	0.91	0.67	0.83	0.96	0.89	0.93	0.93	0.71	0.86
Monção	0.93	0.80	0.87	0.97	0.92	0.95	0.93	0.81	0.89
S.I.T.	0.91	0.74	0.83	0.97	0.87	0.95	0.91	0.81	0.84
FLONA C.	0.90	0.86	0.77	0.95	0.92	0.88	0.93	0.88	0.81
REBio do Gurupi	0.92	0.72	0.86	0.97	0.83	0.94	0.92	0.79	0.85

S.F.B.: São Franciso do Brejão; S.I.T: Santa Inês e Tufilândia and FLONA C.: FLONA Carajás.

[a] Monthly, [b] Dry Season and [c] Rainy Season.

Own authorship

Regarding the performance of the datasets, CHIRPS provided stronger correlations with the standard precipitation dataset (BR-DWGD) always outperforming ERA5-Land either in annual or seasonal analyses, although the latter also exhibits good correlations.

3.3. Precipitation trends

Trends based on annual and monthly data are mostly not significant at 99 or 95% significance level by the Mann Kendall test (Table S1 – Appendix), as demonstrated by Cavalcante et. al (2019) and Arias et. al (2018) for Itacaiúnas and Tapajós River basins. Still, regarding annual data, BR-DWGD and CHIRPS display very similar trends, pointing out to precipitation increasing in Curionópolis and Flona Carajás (Pará), and a decreasing in Monção, Santa Inês and Tufilância (Maranhão) (Fig. 7a). Limberger et. al (2021) also observed the heterogeneity of precipitation trends at individual stations in Amazon basin, highlighting the occurrence of opposite trends in adjacent stations.

Fig. 7 Sen's slope estimative (S): Magnitude of trends detected using annual **(a)**, monthly **(b)**, and seasonal **(c)** data provided by BR-DWGD, ERA5-Land and CHIRPS datasets. The colors indicate the trend sign and the tone its strength: blue (red) color symbolizes the positive (negative) trends, and lighter (darker) tones symbolize weaker (stronger) trends. Overlapping dots denote statistically significant trends at study sites, identified through the Mann Kendall test with a confidence level of at least 95%.

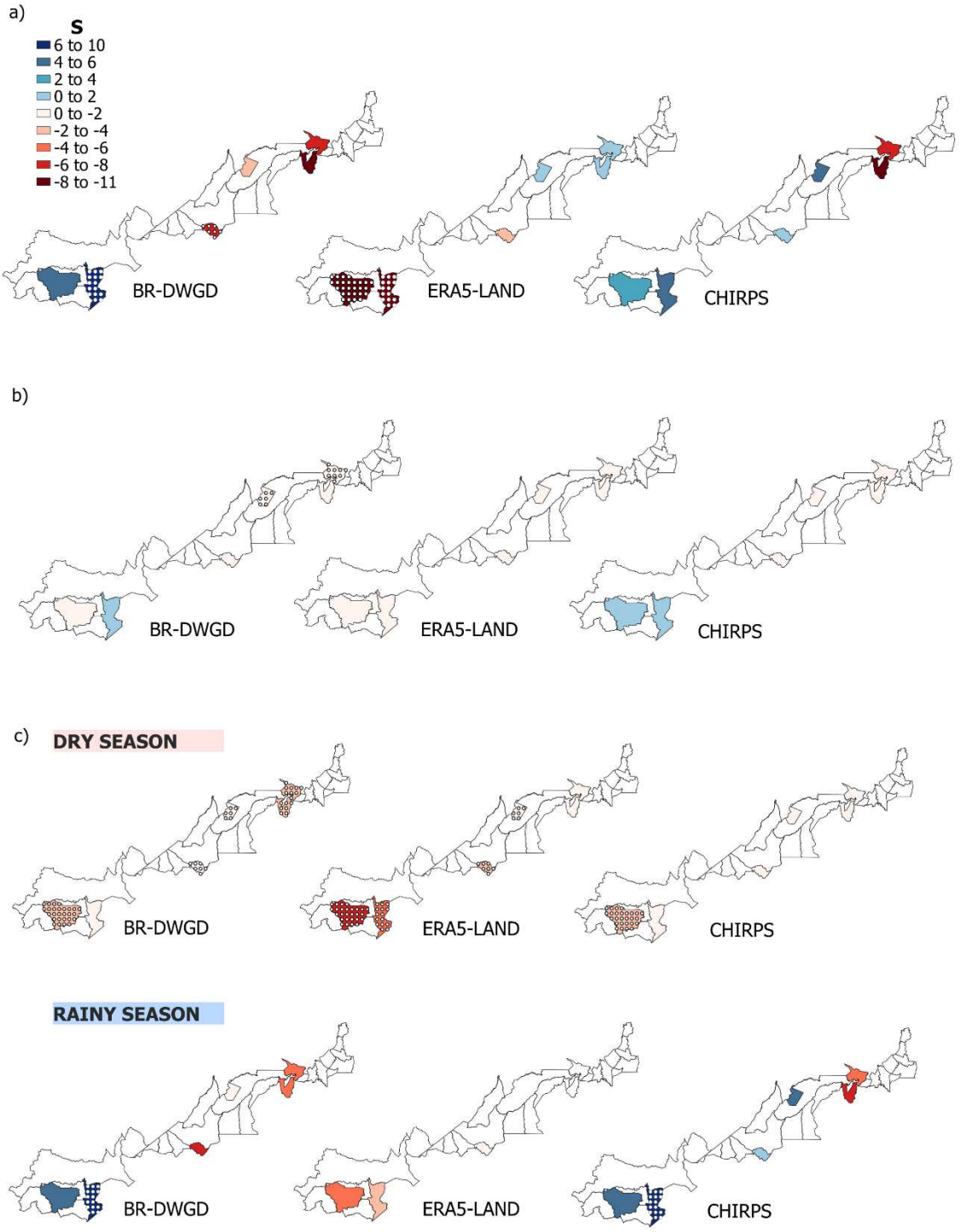

Own authorship

Despite the strong correlation between ERA5-Land and BR-DWGD, opposite trends for the same site are occasionally observed, especially in analyses carried out based on annual data. Such differences were mitigated in analyses based on monthly data, in which a general and slight downward trend in precipitation over the years is noted for all datasets (Fig. 7b). Trend analyses based on seasonal series revealed that the dry season is getting drier in the eastern Amazon (Table S2 – Appendix), insofar as the study region is concerned. This finding is in line with those of Mu et al. (2022), who identified reductions in rainfall trends during the dry season over previously deforested regions (10-15 years) in the Legal Amazon, opposing to increasing rainfall trends in recently deforested areas. Note yet that all datasets point out a strong and negative trend in Carajás FLONA, with respect to the studied sites. On the other hand, the rainy season is not getting rainier (mostly insignificant trends). According to CHIRPS and BR-DWGD data, some localities in Maranhão are getting drier in the rainy season as well, such as Tufilândia, Santa Inês and Monção (Fig. 7c). Haghtalab et. al (2020) also observed local changes in precipitation patterns, mentioning the increment of the number of dry days during both seasons in Tocantins.

Results present here contrast with those reported by Almeida et al. (2017), who found mostly non-significant trends in the Legal Amazon in analyses based on seasonal data of weather stations (1973–2013). On the other hand, it reinforces outcomes of de Souza et. al (2014), who projected drastic rainfall reductions during the dry season over south (Carajás-PA), and north sectors (São Luis-MA) of EFC Railroad. Furthermore, it should be noted that the trends based on the seasonal data from ERA5-Land, particularly for the rainy season, have opposite signs to those based on the standard dataset, except for São Francisco do Brejão.

3.4. Extreme precipitation indices assessment

Overall, indices based on CHIRPS and BR-DWGD data (Fig. 8a, c) exhibit a similar variation pattern over the years, reinforcing the stronger correlation between those datasets. The exception was mainly CDD and CWD, which varied considerably more for BR-DWGD. In fact, CHIRPS data only provide relevant variations for R10mm and Rx5day, while further indices remain fairly stable since 1985. ERA5-Land data delivered greater variations, except for R20mm (Fig. 8b). Regarding all datasets, indices which express the number of days with vigorous precipitation, such as R10mm and R20mm, display somewhat similar values. Note that R20mm shows persistent stability during the assessed period.

Fig. 8 Variations in the extension of the forest (green bars) and pasture (light green bars) classes of land use land cover across the Northern System's domain (1985-2020) with 1985 as the reference year, and the extreme precipitation indices (CDD – yellow line, CWD – grey line, R10mm – light blue line, R20mm – dark blue line, Rx1day – light pink line, Rx5day – brown line) obtained using the data provided by BR-DWGD **(a)** ERA5-Land **(b)** and CHIRPS **(c)**

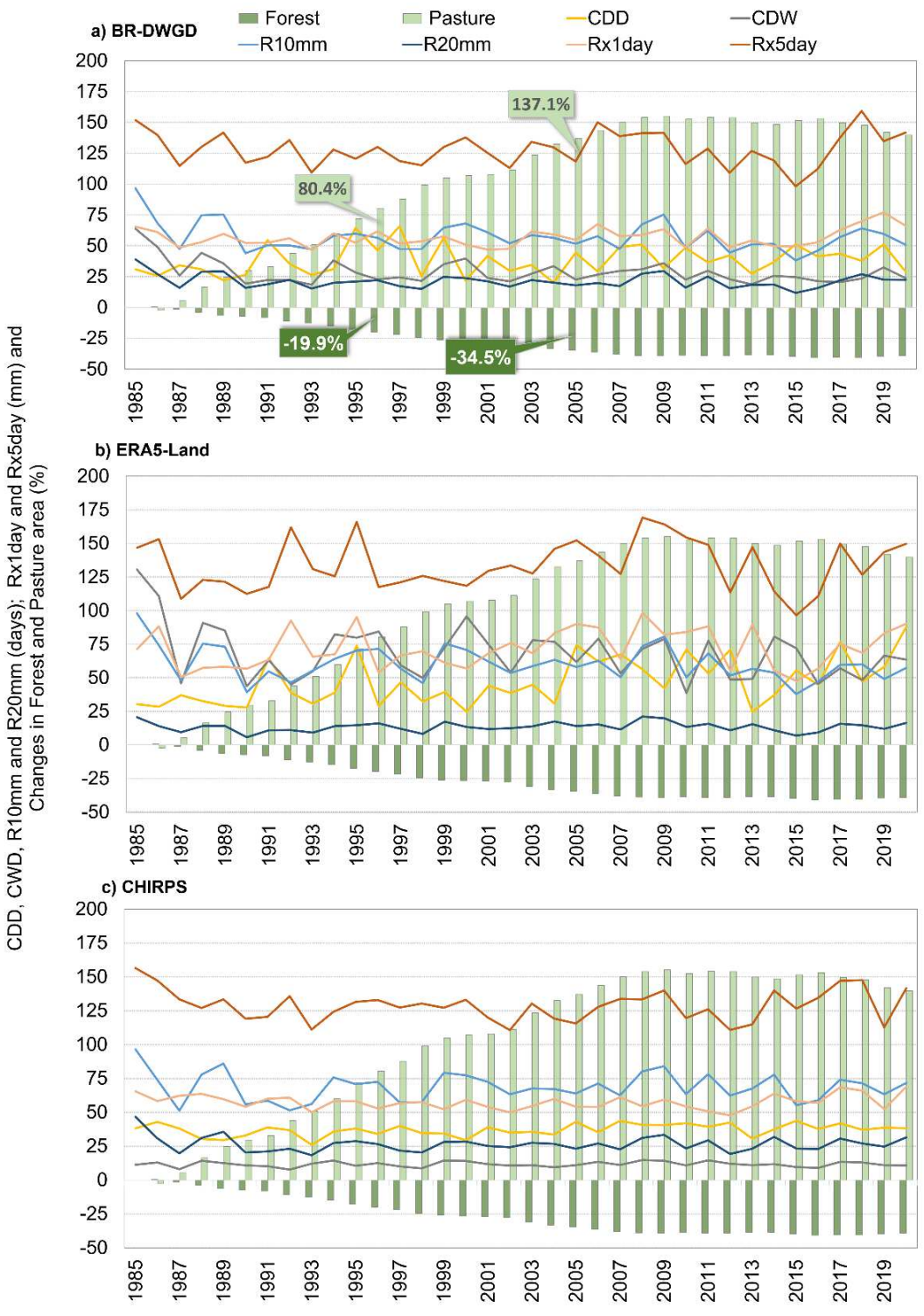

Own authorship

From now on, due to the similarity between CHIRPS and BR-DWGD data for brevity only indices based on BR-DWGD and ERA5-Land are evaluated. The spatial distribution of the indices shows a significant increase in CDD, mainly in the central region, indicating the maximum of about 2.3 and 3 months without precipitation (≥1mm) for BR-DWGD and ERA5-Land, respectively (Fig. 9). In addition, the maximum duration of precipitation (≥1mm) has been dramatically reduced, mainly in the southern region, where there is a greater extent of preserved sites (Fig. 10). There is a slight decrease in the number of days with precipitation higher than 10 mm and 20 mm (R10mm and R20mm) in the central region. ERA5-Lands results also pointed out a modest drop in precipitation in the south (Fig. 11, 12).

Fig. 9 Spatial distribution of the five-year averages of the Consecutive Dry Days (CDD – days) from 1981 to 2020 over the Northern System's domain. Lighter (darker) tones symbolize lower (higher) values

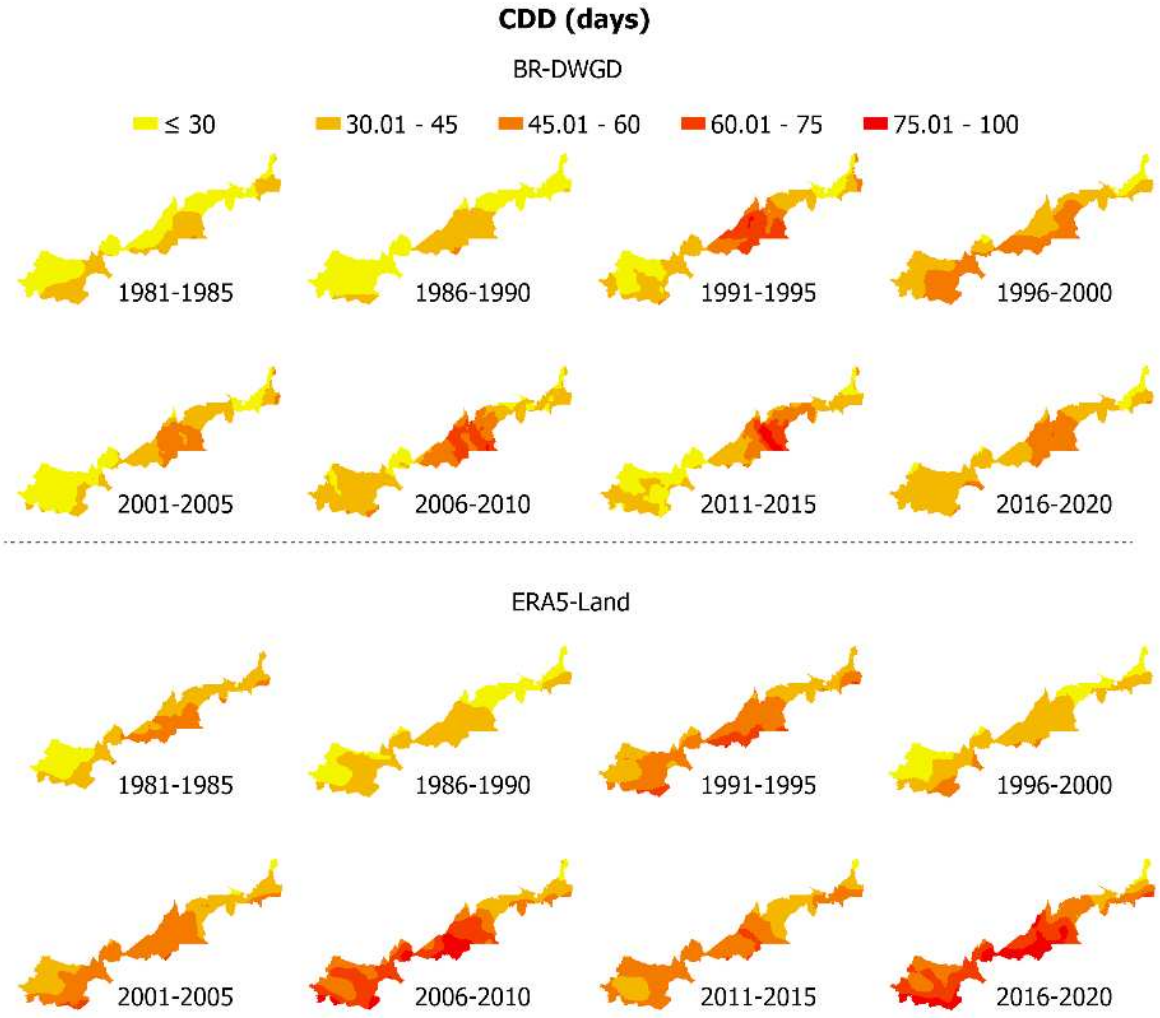

Own authorship

Fig. 10 Spatial distribution of the five-year averages of the Consecutive Wet Days (CWD – days) from 1981 to 2020 over the Northern System's domain. Lighter (darker) tones symbolize lower (higher) values

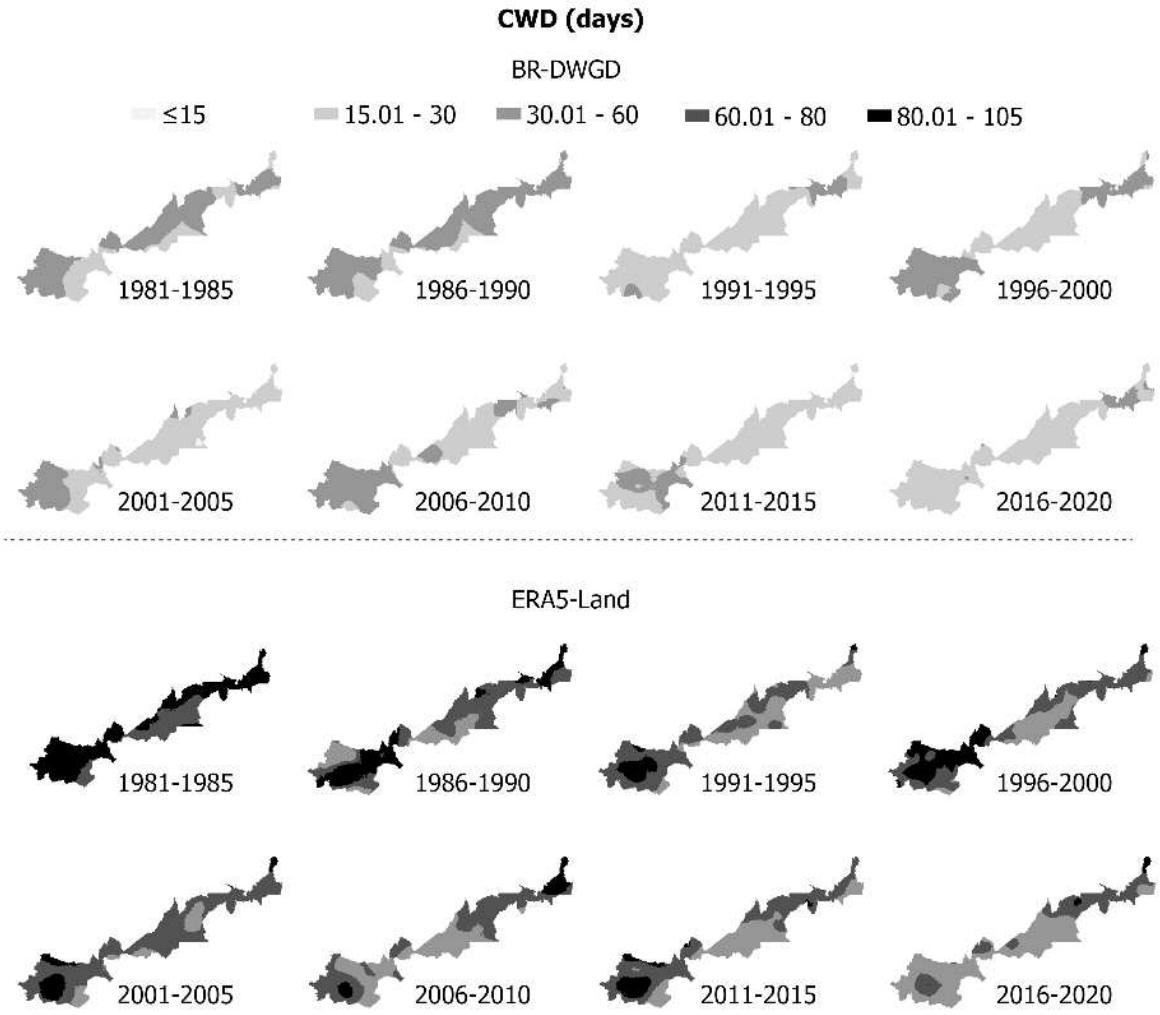

Own authorship

Fig. 11 Spatial distribution of the five-year averages of the Annual Count of Days when Daily Precipitation ≥10 mm (R10mm – days) from 1981 to 2020 over the Northern System's domain. Lighter (darker) tones symbolize lower (higher) values

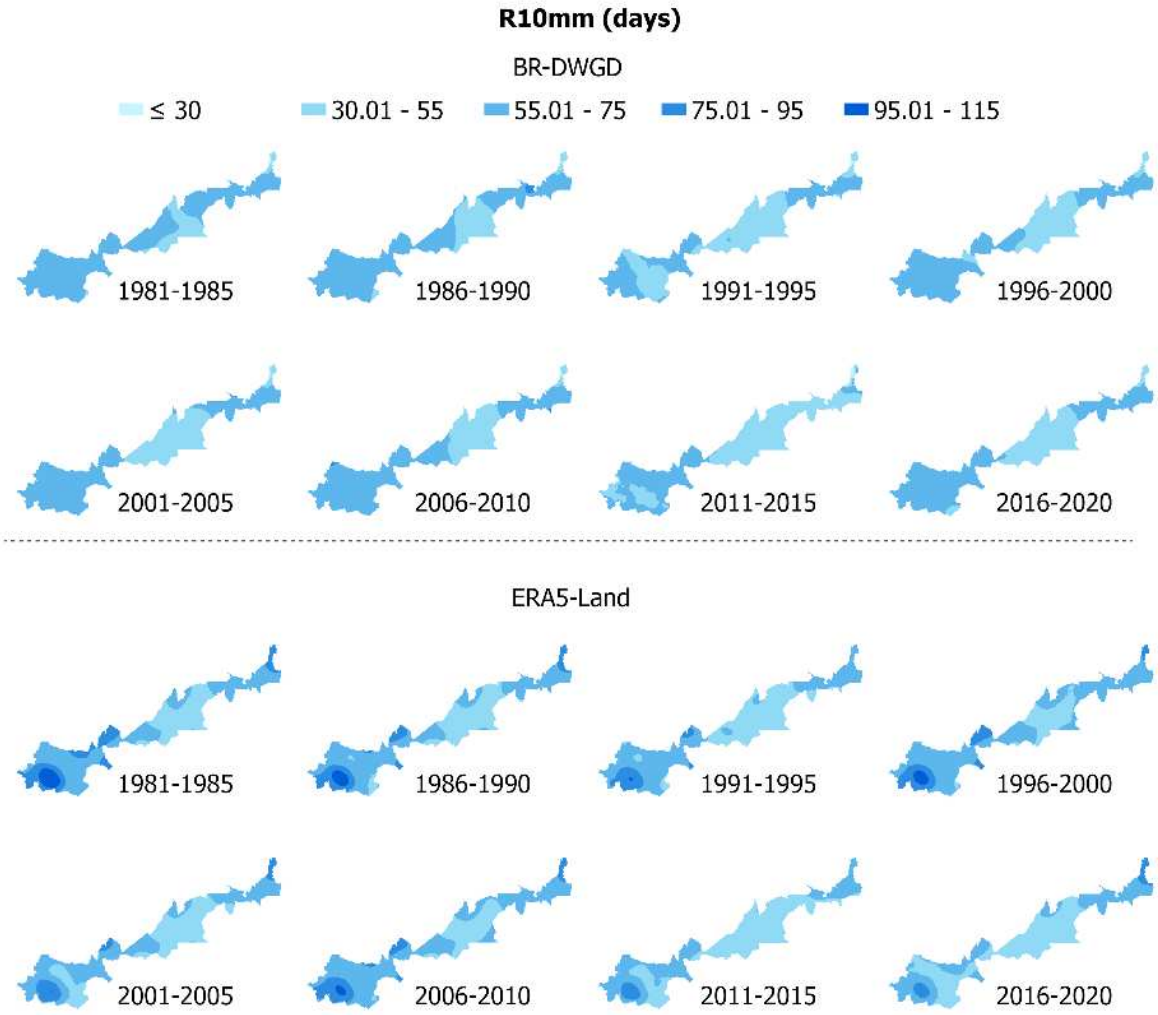

Own authorship

Fig. 12 Spatial distribution of the five-year averages of the Annual Count of Days when Daily Precipitation ≥20 mm (R20mm – days) from 1981 to 2020 over the Northern System's domain. Lighter (darker) tones symbolize lower (higher) values

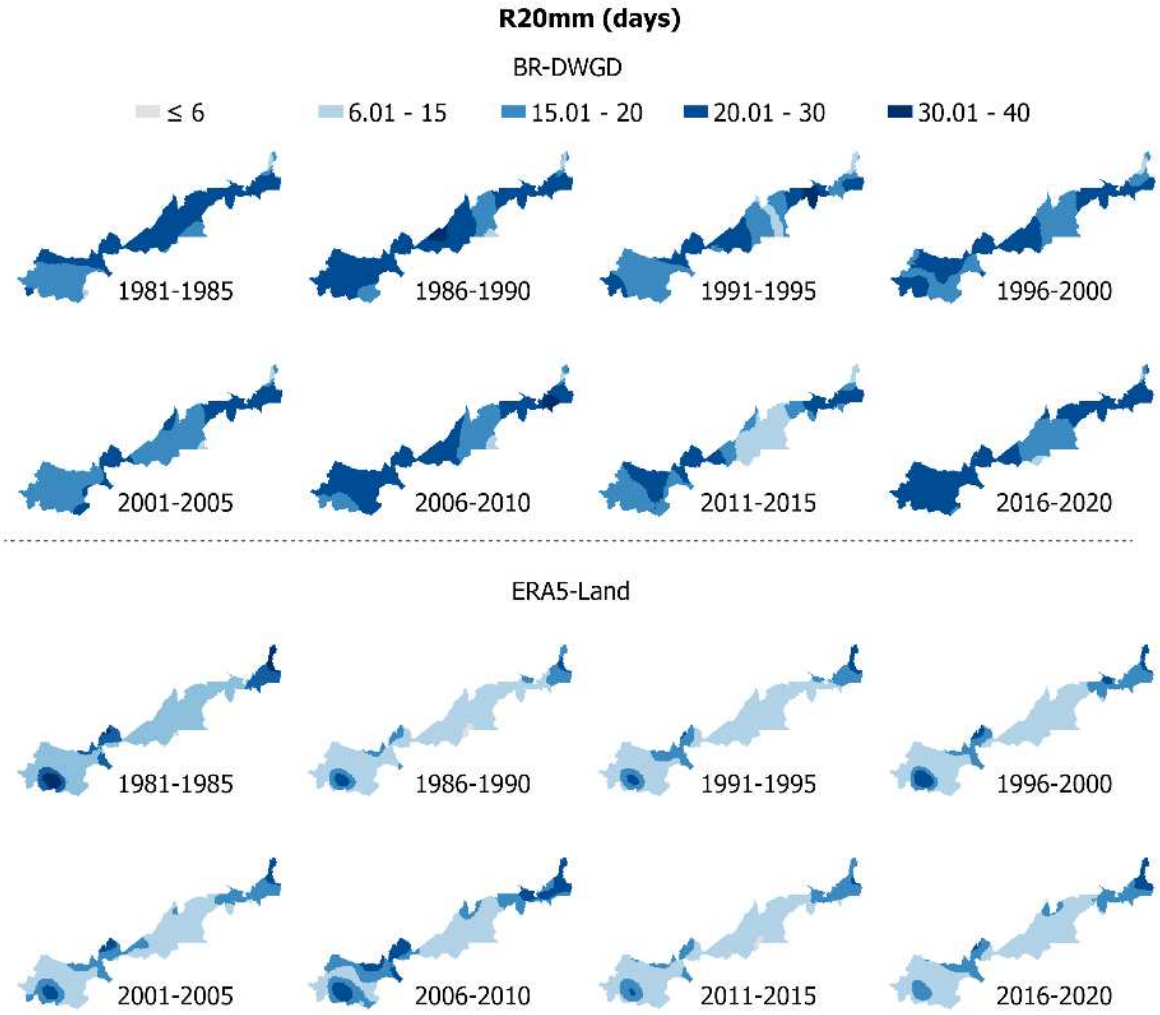

Own authorship

Although the indices assessment reveals a drier environment, a slight increase in the intensity of precipitation (Rx1day and Rx5day) for the Northern System's domain is noted, especially over the south sector with maximum about 75 mm one-day precipitation, and 130 mm five-day precipitation (Fig. 13, 14). It suggests that although the precipitation amount and persistence are decreasing, its intensity is likely increasing in some localities.

Fig. 13 Spatial distribution of the five-year averages of the Annual Maximum One-Day Precipitation (Rx1day – mm) from 1981 to 2020 over the Northern System's domain. Lighter (darker) tones symbolize lower (higher) values

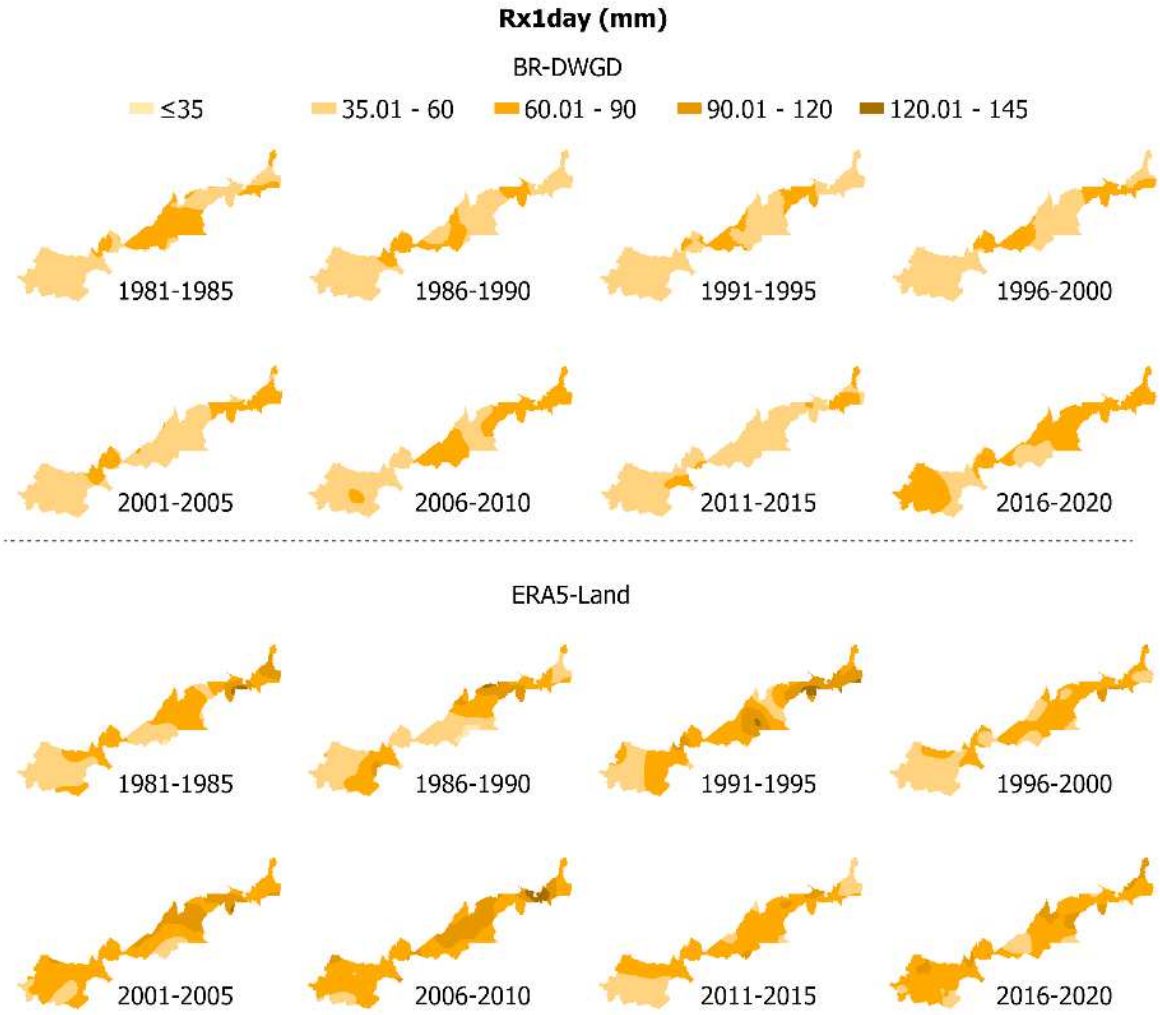

Own authorship

Fig. 14 Spatial distribution of the five-year averages of the Annual Maximum Consecutive Five-Day Precipitation (Rx5day – mm) from 1981 to 2020 over the Northern System's domain. Lighter (darker) tones symbolize lower (higher) values

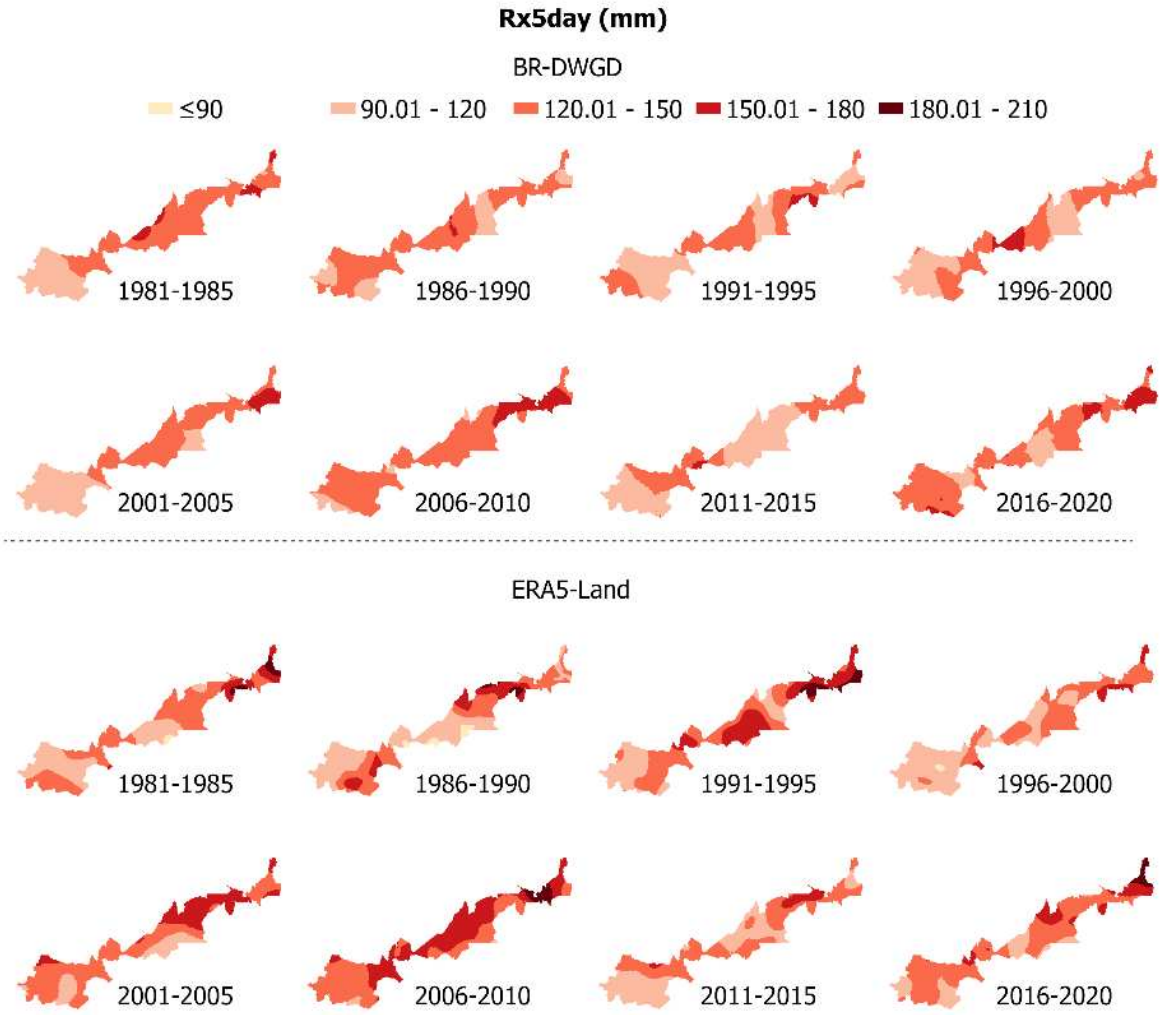

Own authorship

Regarding the trend analyses, significant results were found mainly for CDD, indicating the increasing of dry periods (Table 3). This result is in line with that of Haghtalab et. al (2020), which found an increasing in the number of dry days (NDD) for the eastern Amazon basin. Further significant trends based on the BR-DWG revealed the increment of one-day precipitation over the south sector (Curionópolis e Carajás FLONA), and the number of days when daily precipitation exceeds 20 mm over Curianópolis. Corroborating with seasonal trends, it can be argued that the wetter environment is intensifying in the rainy season, with enhanced precipitation over the southern sector of the study area. On the other hand, the precipitation is getting less intense and with lower magnitude over São Francisco do Brejão

(central sector). Again, analyses based on ERA5-Land indicate opposite trends, such as CWD and R10mm reduction over Curionópolis, and precipitation intensification over São Francisco do Brejão.

Table 3 – Trends in extreme precipitation indices: Sen's slope estimates and significance of the trends in extreme precipitation indices (1981-2020) grouped by dataset for the Northern System's domain and further study sites. Values in bold indicate significant trends at a significance level of at least 95% (Mann-Kendall test)

	Site	Sen's slope estimates (S)					
		cdd	cwd	R10mm	R20mm	Rx1day	Rx5day
BR-DWGD	Northern System's domain	**0.283***	-0.102	-0.044	0.012	0.141	0.034
	Curionópolis	0.043	0.246	0.231	**0.187***	**0.264***	0.542
	São Francisco do Brejão	0.234	0.017	-0.243	**-0.322****	-0.377	**-0.813***
	Monção	**0.360****	-0.074	-0.399	-0.135	0.169	0.057
	Santa Inês and Tufilândia	**0.530****	-0.123	-0.406	-0.171	0.092	-0.551
	Carajás FLONA	0.193	-0.105	-0.089	0.096	**0.374***	0.216
	Gurupi REBio	**0.686****	**-0.277***	-0.137	-0.022	0.381	-0.142
ERA5-Land	Northern System's domain	**0.715****	-0.474	-0.215	0.070	0.427	0.434
	Curionópolis	**0.978****	**-0.809****	**-0.293***	0.004	0.020	-0.047
	São Francisco do Brejão	**0.953****	-0.468	-0.187	0.000	**0.554***	0.828
	Monção	0.335	-0.139	0.042	0.141	-0.168	-0.165
	Santa Inês and Tufilândia	0.311	0.053	0.053	0.115	-0.887	-1.127
	Carajás FLONA	**0.813****	-0.691	**-0.610***	-0.071	0.308	-0.146
	Gurupi REBio	0.442	-0.354	-0.039	**0.148***	0.619	0.684

* Significant in Mann-Kendall trend test at 95% significance level.

** Significant in Mann-Kendall trend test at 99% significance level.

Own authorship

The breakpoints detection based on the precipitation data show that most of the shift in the central tendency of the time series of extreme precipitation indices over the Northern System's domain occurred between 1996-2005 (Table 4). Important to mention that the forest

formation occupies by about 80% of its original size (base year: 1985) in 1996, dropping to 65,5% in 2005. During the same period pasture extent grew from 80% to 137% of its original domain in 1985 (Fig. 8a).

Table 4 – Breakpoints (year of shift in the central tendency) in the time series (1981-2020) of extreme precipitation indices with significant trends grouped by dataset for the Northern System's domain and further study sites. Values in bold indicate significant breakpoints at a significance level of at least 95% (Petit test). Only breakpoints for time series with significant trends are displayed (check table 4)

	Site	**Breakpoint (year of shift)**					
		cdd	cwd	R10mm	R20mm	Rx1day	Rx5day
BR-DWGD	Northern System's domain	1990	-	-	-	-	-
	Curionópolis	-	-	-	**1998***	2005	-
	São Francisco do Brejão	-	-	-	**2000***	-	**2011***
	Monção	**1996****	-	-	-	-	-
	Santa Inês and Tufilândia	**1990***	-	-	-	-	-
	Carajás FLONA	-	-	-	-	2005	-
	Gurupi REBio	**2004**	2004	-	-	-	-
ERA5-Land	Northern System's domain	**2004****	-	-	-	-	-
	Curionópolis	**2004***	2006	2013	-	-	-
	São Francisco do Brejão	**2002***	-	-	-	**1990***	-
	Monção	-	-	-	-	-	-
	Santa Inês and Tufilândia	**-**	-	-	-	-	-
	Carajás FLONA	**2004****	-	2011	-	-	-
	Gurupi REBio	**-**	-	-	**1994***	-	-

* Significant in Mann-Kendall trend test at 95% significance level.

** Significant in Mann-Kendall trend test at 99% significance level.

Own authorship

4. DISCUSSION

4.1. Performance of the precipitation products

The greater match between BR-DWGD and CHIRPS data across all locations is possibly linked to the use of surface weather stations by both datasets and the use of physiographic indicators, such as elevation, by CHIRPS to estimate precipitation. On the other hand, the higher values shown by ERA5-Land on the conservation unities can be explained by the higher sensitivity of surface heat fluxes related to the forest, that are captured by the atmospheric model. In fact, overestimation by reanalysis precipitation products have been reported, reflecting issues in capturing the ground precipitation over some regions (WANG et al. 2020; REDA et al. 2021). However, in this study it was only notable on preserved sites.

Fessehaye et. al (2022) evaluating CHIRPS and ERA5-Land precipitation estimates over Eritrea, concluded that CHIRPS performs better over areas with convective rainfall, which is usually the case in the Amazon biome (TANG et al. 2016), although local orographic rainfall may occur during the dry season due to specific high-altitude plots in the Carajás FLONA and Curionópolis (BEHLING and HOOGHIEMSTRA 2001). Xu et. al (2022) also reported better performance of satellite-based precipitation products over model-based (ERA5-Land) for sub-regions of subtropical and tropical monsoon climates. On the other hand, Baker et. al (2021) stated that ERA5-Land tends to represent precipitation values relatively well over the Amazon, as it has also been found herein.

Thus, this study is in line with those that stated that satellite-based precipitation products perform better than those based on reanalysis (LEMMA et al. 2019; WANG et al. 2020; REDA et al. 2021; XU et al. 2022), which does not invalidate ERA5-Land as a great alternative to be used in locations with poor data availability, especially to study annual precipitation characteristics, due to its high correlations with the standard dataset. This discovery holds significance within the realm of climatology, as the evaluation of the ERA5-Land precipitation product has been relatively scarce up to this point (XU et al. 2022).

4.2. Effect of land use land cover on the rainfall pattern

Precipitation in the Amazon is recycled through constant vegetation evapotranspiration, primarily facilitated by the tall and deep-rooted trees. Tropical forests are composed by all sort of trees that account for the highly rough surface, which stimulates deep convection that transports the moisture high into the atmosphere. This eco-hydrological

mechanism supports cloud formation and, consequently, precipitation (Chambers and Artaxo 2017). At the local-scale, evaporating moisture promotes atmospheric cooling and moistening, whereas at larger-scales it regulates regional rainfall, preventing and ameliorating drought effects (Baker and Spracklen 2019). However, changes in land use land cover usually alter surface characteristics, such as roughness and reflectance, which potentially affect water and energy flows, therefore, impacting rainfall variability and its extremes (ALVES et al. 2017; HAGHTALAB et al. 2020).

Considering only BR-DWGD data, our local-scale study shows no consistent trend for deforested or preserved sites, but a general drying pattern, which is more intense over the northern sector of the study area (Maranhão), particularly during the dry season. In fact, climate simulations have long predicted that the impact of deforestation on precipitation in South America would occur mainly during the dry season (LEE et al. 2011), and have also demonstrated the association between high deforestation rates and a reduction in rainfall during this period of the year (ALVES et al. 2017). In addition, substantial positive trends in CDD can be related to a lengthening of the dry season within the Northern System's domain, which could be explained by a reduction in the residual dry season moisture flux, that triggers the late onset of the rainy season (COSTA and PIRES 2010; LEE et al. 2011).

Efforts have been made to detect the contribution of land use and land cover changes to climate change in the Amazon region (COSTA and PIRES 2010; HAGHTALAB et al. 2020; SIERRA et al. 2023). These previous studies primarily rely on defining the effect of deforestation on the regional climate. Large-scale and the age of deforestation exert a strong influence on climate responses, as it has been demonstrated that during dry season aged up to a decade deforested regions (often smaller deforestation extent) experience rising rainfall, whereas older deforestation (often larger deforestation) is related to rainfall reductions (MU and JONES 2022). Hence, the predominance of negative trends across the studied area during the dry season are in line with those results presented by Mu and Jones (2022). The occurrence of most breakpoints in the time series, during 1996-2005 reported herein, is potentially linked to the intense and old-aged deforestation in the Northern System's domain and its vicinity.

It is interesting to notice that Curionópolis in Pará, the second most deforested municipality since 1985, exhibits positive and significative rainfall trend during rainy season and negative trend during dry season, but the latest is non-significant. This site borders a set of juxtaposed federal conservation units, including Carajás FLONA (Fig. S3 – Appendix). In this instance, particularly, we argue that the proximity of Curionópolis to a significant, intact forest remnant may induce a convection mechanism, facilitating the transport of moisture-laden air to

the deforested area, thereby increasing both the quantity and intensity of rainfall. Alves et. al (2017) by performing climate simulations observed an increase in precipitation over deforested areas, concluded that differences in physical properties between forested and deforested areas, result in a pressure gradient responsible for transporting moisture from forests to deforested sites ("vegetation breeze"). In fact, enhanced rainfall over patches of forest loss have been reported, especially few kilometers close to forest edges (BAKER and SPRACKLEN 2019), which is the case here.

Conversely, rainfall trends based on annual, monthly, and seasonal data over deforested sites in Maranhão (northern and central sectors of the Northern System's domain) are in general statistically significant and negative. Drying trends have constantly been appointed in the region and nearby, especially during the dry season (SANTOS et al. 2020; LUCAS et al. 2021; MU and JONES 2022). Due to the progressive and accelerated deforestation process in Maranhão, where only about 25% of the original forest cover persists (CELENTANO et al. 2017), negative rainfall trends may be attributed to the extensive deforestation, which elevates surface albedo and sensible heat flux, diminishing evapotranspiration and moisture recycling. This consequently disrupts the hydrological and energy balances, which adversely affects rainfall (ALMEIDA et al. 2017; BAKER and SPRACKLEN 2019).

Despite being a conservation unity, Gurupi REBio in Maranhão is surrounded by deforestation (Fig. S3 – Appendix) and also displays significant negative trends, based on monthly and seasonal (dry) data. In this context, we suggest that highly deforested vicinity influences the local climate. Khanna et al. (2017) pointed out a shift from a thermodynamically to a dynamically driven convective regime due to large-scale deforestation in the southwestern Brazilian Amazon. This mechanism induces a convection suppression downwind and an increasing upwind. Therefore, it is possible that a larger-scale dynamic mechanism suppresses convections over Gurupi REBio, driving the air moisture elsewhere.

Besides local change in land use, topography, climate and vegetation typology (biome) can influence the atmospheric response. The EFC region is dominated by large variability in altitude, and lies over a biome transition zone, which indicates that the rainfall pattern is affected by both, the Cerrado (savannah-like) and Amazon deforestation (COSTA and PIRES 2010). Additionally, O'Connor et al. (2021) have recently disclosed a strong spatial gradient from west (~40%) to east (~10%) in the forest's contribution to precipitation in the Amazon Arc of deforestation. Their findings demonstrate that non-forest elements (ocean evaporation and small-vegetation evapotranspiration) play a substantial role in generating precipitation as

compared to forests, particularly in Maranhão, and to some extent in Pará. Therefore, questions remain due to the important influence of El Niño-Southern Oscillation (ENSO), Sea Surface Temperatures (SSTs) and the Intertropical Convergence Zone (ITCZ) – one of the major rainfall generating systems in the Amazon Basin (ALMEIDA et al. 2017) – in the precipitation of the eastern Amazon (HAGHTALAB et al. 2020).

Regarding statistical analysis, it is important to emphasize that significant trends are tightly related to the length of the time series, and in the case herein 40 years, it is perhaps short to indicate 95% or above significance level. In fact, the current study provides a perspective on the impacts of rampant regional deforestation, which in the last three decades is inducing a dry climate intensified by the increasing number of dry spells.

Changes in land use land cover influence the rainfall pattern and, in turn, the spatio-temporal changes in precipitation. This affects the development of the plants and species composition. Overall, the responses of vegetal species of tropical forests to climate change are influenced mainly by the water availability and temperature. However, questions regarding effects of CO_2-fertilization and the limits of plant acclimatization are still to be better clarified (OMETTO et al. 2022). Such responses, especially regarding seedlings and newly recruited trees, should be deeply investigated in this particular region, where many restauration and reforestation projects are being carried out.

5. CONCLUSIONS AND RECOMMENDATIONS

Based on variability and trend analyzes carried out with 40 years-data, it is indicated that the precipitation pattern across the Northern System's domain has been changing. The region is becoming drier, with a significant reduction in rainfall, especially during the dry season. Uninterrupted dry periods have been prolonged, especially in the northern sector of the study area (Monção, Santa Inês, Tufilândia and Gurupi REBio). Apparently, the rainy season is not getting rainier, even though study sites in the state of Pará (higher altitudes and closer to more federal conservation unities) show increasing trends in the amount and intensity of precipitation.

Plants can suffer physiological stress in this environment, due to reduced rainfall and prolonged dry periods, which affects their growth, mortality and regeneration. For this reason, we encourage research that evaluates plant responses to this new climatic condition, especially those used in restoration projects. On the other hand, the increase in the intensity of rainfall in the southern sector is also worrying. Land reclamation projects in open pit mines can be

seriously hampered by changes in the precipitation pattern, due to low water availability and hydroseeding liquid leaching during the dry and rainy seasons, respectively. In light of these circumstances, we have a firm conviction that the implementation of well-managed irrigation systems at the end of the rainy season poses a practical alternative to address these difficulties, effectively reducing financial setbacks associated with corrective actions.

Changes in land use and land cover contribute to shifts in precipitation patterns, with varying mechanisms and degrees of impact across the study area. Despite being a conservation unit, the local precipitation regime over the Gurupi REBio also tends to be much drier, suggesting that possible local effects of fragmented conservation on the climate are outweighed by the effects of surrounding areas. Possibly, the "vegetation breeze" has been occurring, generating positive precipitation trends in Curionópolis, where native vegetation was about 59% deforested with respect to its area in 1985.

Differences between trends based on annual, monthly, and seasonal data were observed. Thus, it is recommended to use seasonal data for a more meticulous study of precipitation pattern, which has great seasonal variability. We also encourage the use of satellite-based data (CHIRPS) for future studies in the region, due to better correlations with the standard database and less opposite trends. The model-based ERA5-Land also provides satisfactory results for the dry season. However, it has been found that ERA5-Land delivers drawbacks to show the spatial distribution of precipitation extremes.

REFERENCES

ALMEIDA, C. T. et al. Spatiotemporal rainfall and temperature trends throughout the Brazilian Legal Amazon, 1973-2013. **International Journal of Climatology**, v. 37, n. 4, p. 2013–2026, mar. 2017.

ALVARES, C. A. et al. Köppen's climate classification map for Brazil. **Meteorologische Zeitschrift**, v. 22, n. 6, p. 711–728, 2013.

ALVES, L. M. et al. Sensitivity of Amazon Regional Climate to Deforestation. **American Journal of Climate Change**, v. 06, n. 01, p. 75–98, 2017.

ARIAS, M. E. et al. Decoupling the effects of deforestation and climate variability in the Tapajós river basin in the Brazilian Amazon. **Hydrological Processes**, v. 32, n. 11, p. 1648–1663, 30 maio 2018.

ARIAS, P. A. et al. Technical Summary. Em: MASSON-DELMOTTE, V. , et al. (Eds.). **Climate Change 2021 – The Physical Science Basis. Contribution of Working Group I to the Sixth Assessment Report of the Intergovernmental Panel on Climate Change**.

Cambridge, United Kingdom and New York, NY, USA: Cambridge University Press, 2023. p. 35–144.

AVILA-DIAZ, A. et al. Climatological aspects and changes in temperature and precipitation extremes in Viçosa-Minas Gerais. **Anais da Academia Brasileira de Ciências**, v. 92, n. 2, 2020.

BAKER, J. C. A. et al. An Assessment of Land–Atmosphere Interactions over South America Using Satellites, Reanalysis, and Two Global Climate Models. **Journal of Hydrometeorology**, v. 22, n. 4, p. 905–922, abr. 2021.

BAKER, J. C. A.; SPRACKLEN, D. V. Climate Benefits of Intact Amazon Forests and the Biophysical Consequences of Disturbance. **Frontiers in Forests and Global Change**, v. 2, 30 ago. 2019.

BEHLING, H.; HOOGHIEMSTRA, H. Neotropical Savanna Environments in Space and Time. Em: **Interhemispheric Climate Linkages**. [s.l.] Elsevier, 2001. p. 307–323.

BOCHOW, N.; BOERS, N. The South American monsoon approaches a critical transition in response to deforestation. **Science Advances**, v. 9, n. 40, 6 out. 2023.

CAVALCANTE, R. B. L. et al. Opposite Effects of Climate and Land Use Changes on the Annual Water Balance in the Amazon Arc of Deforestation. **Water Resources Research**, v. 55, n. 4, p. 3092–3106, 15 abr. 2019.

CELENTANO, D. et al. Towards zero deforestation and forest restoration in the Amazon region of Maranhão state, Brazil. **Land Use Policy**, v. 68, p. 692–698, nov. 2017.

CHAMBERS, J. Q.; ARTAXO, P. Deforestation size influences rainfall. **Nature Climate Change**, v. 7, n. 3, p. 175–176, 20 mar. 2017.

COSTA, M. H.; PIRES, G. F. Effects of Amazon and Central Brazil deforestation scenarios on the duration of the dry season in the arc of deforestation. **International Journal of Climatology**, v. 30, n. 13, p. 1970–1979, 15 nov. 2010.

CRISTO, L. DE A.; SANTOS, M. A.; MATLABA, V. J. Socioeconomic and Environmental Vulnerability Index in the Brazilian Amazon: The Case of the Carajás Railroad. **The Extractive Industries and Society**, v. 11, p. 101128, set. 2022.

DA CRUZ, D. C. et al. An overview of forest loss and restoration in the Brazilian Amazon. **New Forests**, v. 52, n. 1, p. 1–16, 3 jan. 2021.

DA SILVA, J. M. C.; RYLANDS, A. B. .; DA FONSECA, G. A. B. . The Fate of the Amazonian Areas of Endemism. **Conservation Biology**, v. 19, n. 3, p. 689–694, jun. 2005.

DE SOUZA, E. B. et al. Dynamical Donwscaling for Railroad Areas in Eastern Amazon and Southeastern Brazil: Current Climate and Near-Future Projections. **Atmospheric and Climate Sciences**, v. 04, n. 02, p. 155–163, 2014.

FERNANDES, T. et al. Detecção e análise de focos de calor no município de Parauapebas-PA, Brasil por meio da aplicação de geotecnologia. **Enciclopédia biosfera**, v. 15, n. 28, p. 398, 2018.

FESSEHAYE, M.; FRANKE, J.; BRÖNNIMANN, S. Evaluation of satellite-based (CHIRPS and GPM) and reanalysis (ERA5-Land) precipitation estimates over Eritrea. **Meteorologische Zeitschrift**, v. 31, n. 5, p. 401–413, 8 dez. 2022.

FUNK, C. et al. The climate hazards infrared precipitation with stations—a new environmental record for monitoring extremes. **Scientific Data**, v. 2, n. 1, p. 150066, 8 dez. 2015.

GATTI, L. V. et al. Amazonia as a carbon source linked to deforestation and climate change. **Nature**, v. 595, n. 7867, p. 388–393, 2021.

GIULIETTI, A. M. et al. Edaphic Endemism in the Amazon: Vascular Plants of the canga of Carajás, Brazil. **The Botanical Review**, v. 85, n. 4, p. 357–383, 8 dez. 2019.

HAGHTALAB, N. et al. Evaluating spatial patterns in precipitation trends across the Amazon basin driven by land cover and global scale forcings. **Theoretical and Applied Climatology**, v. 140, n. 1–2, p. 411–427, 17 abr. 2020.

HASE UETA, M. et al. Food sustainability in a context of inequalities: meat consumption changes in Brazil (2008–2017). **Environment, Development and Sustainability**, 31 jan. 2023.

HIJMANS, R. **_raster: Geographic Data Analysis and Modeling_. R package version 3.6-3, <https://CRAN.R-project.org/package=raster>.project.org/package=raster**, 2022.

IPCC. **Climate Change 2021: The Physical Science Basis. Contribution of Working Group I to the Sixth Assessment Report of the Intergovernmental Panel on Climate Change**. Cambridge, United Kingdom and New York, NY, USA: Cambridge University Press, 2021.

KENDALL, M. G. **Rank Correlation Methods**. 4. ed. London: Charles Griffin, 1975.

LEE, J.-E. et al. Land use change exacerbates tropical South American drought by sea surface temperature variability. **Geophysical Research Letters**, v. 38, n. 19, p. n/a-n/a, out. 2011.

LEMMA, E.; UPADHYAYA, S.; RAMSANKARAN, R. Investigating the performance of satellite and reanalysis rainfall products at monthly timescales across different rainfall regimes of Ethiopia. **International Journal of Remote Sensing**, v. 40, n. 10, p. 4019–4042, 19 maio 2019.

LIMBERGER, L. et al. Streamflow and precipitation trends in the Brazilian Amazon basin and their association with Pacific decadal oscillation and deforestation. **Theoretical and Applied Climatology**, v. 146, n. 1–2, p. 511–526, 17 out. 2021.

LUCAS, E. W. M. et al. Trends in climate extreme indices assessed in the Xingu river basin - Brazilian Amazon. **Weather and Climate Extremes**, v. 31, p. 100306, mar. 2021.

MAGALHÃES, M. P. et al. A cultura tropical. Em: MARCOS PEREIRA MAGALHÃES (Ed.). **Amazônia Antropogênica**. Museu Emílio Goeldi ed. Belém: [s.n.]. p. 429.

MANN, H. B. Nonparametric Tests Against Trend. **Econometrica**, v. 13, n. 3, p. 245, jul. 1945.

MAPBIOMAS. **Projeto Mapbiomas - Coleção 7.0 da Série Anual de Mapas da Cobertura e Uso do Solo do Brasil, acessado em 26/03/2023 através do link: https://mapbiomas.org/estatisticas**, 2022.

MARENGO, J. A. et al. Changes in Climate and Land Use Over the Amazon Region: Current and Future Variability and Trends. **Frontiers in Earth Science**, v. 6, 21 dez. 2018.

MARTÍNEZ, M. D. et al. Time trends of daily maximum and minimum temperatures in Catalonia (ne Spain) for the period 1975-2004. **International Journal of Climatology**, 2009.

MATLABA, V. J. et al. Socioeconomic dynamics of a mining town in Amazon: a case study from Canaã dos Carajás, Brazil. **Mineral Economics**, v. 32, n. 1, p. 75–90, 23 abr. 2019.

MCLEOD, A. **_Kendall: Kendall Rank Correlation and Mann-Kendall Trend Test_. R package version 2.2.1, <https://CRAN.R-project.org/package=Kendall>.** 2022.

MU, Y.; JONES, C. An observational analysis of precipitation and deforestation age in the Brazilian Legal Amazon. **Atmospheric Research**, v. 271, p. 106122, jun. 2022.

MUÑOZ-SABATER, J. et al. ERA5-Land: a state-of-the-art global reanalysis dataset for land applications. **Earth System Science Data**, v. 13, n. 9, p. 4349–4383, 7 set. 2021.

O'CONNOR, J. C. et al. Atmospheric moisture contribution to the growing season in the Amazon arc of deforestation. **Environmental Research Letters**, v. 16, n. 8, p. 084026, 1 ago. 2021.

OMETTO, J. P. , et al. Tropical Forests. Em: PÖRTNER, H.-O. et al. (Eds.). **Climate Change 2022: Impacts, Adaptation and Vulnerability. Contribution of Working Group II to the Sixth Assessment Report of the Intergovernmental Panel on Climate Change**. Cambridge, UK and New York, NY, USA,: Cambridge University Press, 2022. p. 2369–2410.

PAIVA, P. F. P. R. et al. Deforestation in protect areas in the Amazon: a threat to biodiversity. **Biodiversity and Conservation**, v. 29, n. 1, p. 19–38, 16 jan. 2020.

PETTITT, A. N. A Non-Parametric Approach to the Change-Point Problem. **Applied Statistics**, v. 28, n. 2, p. 126, 1979.

PIERCE, D. **_ncdf4: Interface to Unidata netCDF (Version 4 or Earlier) Format Data Files_. R package version 1.20, <https://CRAN.R-project.org/package=ncdf4>**, 2022.

POHLERT, T. **_trend: Non-Parametric Trend Tests and Change-Point Detection_. R package version 1.1.4, <https://CRAN.R-project.org/package=trend>**, 2020.

R CORE TEAM. **R: A language and environment for statistical computing**. **R Foundation for Statistical Computing**Vienna, Austria. R Foundation for Statistical Computing, 2022. Disponível em: <Available from: http://www.R-project.org/>. Acesso em: 7 ago. 2023

REDA, K. W. et al. Evaluation of Global Gridded Precipitation and Temperature Datasets against Gauged Observations over the Upper Tekeze River Basin, Ethiopia. **Journal of Meteorological Research**, v. 35, n. 4, p. 673–689, 11 ago. 2021.

SANT'ANA JÚNIOR, H. A. DE; ALVES, E. DE J. P. MINING-RAILROAD-PORT: "AT THE END OF THE LINE", A CITY IN QUESTION. **Vibrant: Virtual Brazilian Anthropology**, v. 14, n. 2, 7 dez. 2017.

SANTOS, J. R. N. et al. TENDÊNCIAS DE EXTREMOS CLIMÁTICOS NA REGIÃO DE TRANSIÇÃO AMAZÔNIA-CERRADO NO ESTADO DO MARANHÃO. **Revista Brasileira de Climatologia**, v. 26, 14 fev. 2020.

SCHAEFER, C. E. G. R. et al. Soils from Brazilian Amazonia. Em: **The Soils of Brazil**. [s.l: s.n.]. p. 85–128.

SEN, P. K. Estimates of the regression coefficient based on Kendall's Tau. **Journal of the American Statistical Association,** v. 63, n. 324, p. 1379–1389, 1968.

SIERRA, J. P. et al. Impacts of land-surface heterogeneities and Amazonian deforestation on the wet season onset in southern Amazon. **Climate Dynamics**, 26 maio 2023.

SILVA JUNIOR, C. et al. Spatiotemporal Rainfall Trends in the Brazilian Legal Amazon between the Years 1998 and 2015. **Water**, v. 10, n. 9, p. 1220, 10 set. 2018.

TANG, S. et al. Large-scale vertical velocity, diabatic heating and drying profiles associated with seasonal and diurnal variations of convective systems observed in the GoAmazon2014/5 experiment. **Atmospheric Chemistry and Physics**, v. 16, n. 22, p. 14249–14264, 16 nov. 2016.

TORRES, M. **Painel científico para a Amazônia participa da COP 27**.

WANG, N. et al. Evaluating satellite-based and reanalysis precipitation datasets with gauge-observed data and hydrological modeling in the Xihe River Basin, China. **Atmospheric Research**, v. 234, p. 104746, abr. 2020.

WIJNGAARD, J. B.; KLEIN TANK, A. M. G.; KÖNNEN, G. P. Homogeneity of 20th century European daily temperature and precipitation series. **International Journal of Climatology**, v. 23, n. 6, p. 679–692, maio 2003.

XAVIER, A. C. et al. New improved Brazilian daily weather gridded data (1961–2020). **International Journal of Climatology**, v. 42, n. 16, p. 8390–8404, 30 dez. 2022.

XU, J. et al. Do ERA5 and ERA5-land precipitation estimates outperform satellite-based precipitation products? A comprehensive comparison between state-of-the-art model-based

and satellite-based precipitation products over mainland China. **Journal of Hydrology**, v. 605, p. 127353, fev. 2022.

ZANDLER, H.; SENFTL, T.; VANSELOW, K. A. Reanalysis datasets outperform other gridded climate products in vegetation change analysis in peripheral conservation areas of Central Asia. **Scientific Reports**, v. 10, n. 1, p. 22446, 31 dez. 2020.

APPENDIX

Fig. S1 Georeferenced points used to extract the rainfall information from netCDF files comprising BR-DWGD, ERA5-Land and CHIRPS data: Mid-points of cells of a regular-gridded square box (0.1°) over the study area (a), within the Northern System's domain (b), and within further study sites: Monção (pink), Santa Inês and Tufilândia (orange), Gurupi REBio (blue), São Francisco do Brejão (brown), Cuionópolis (red) and Carajás FLONA (green) (c)

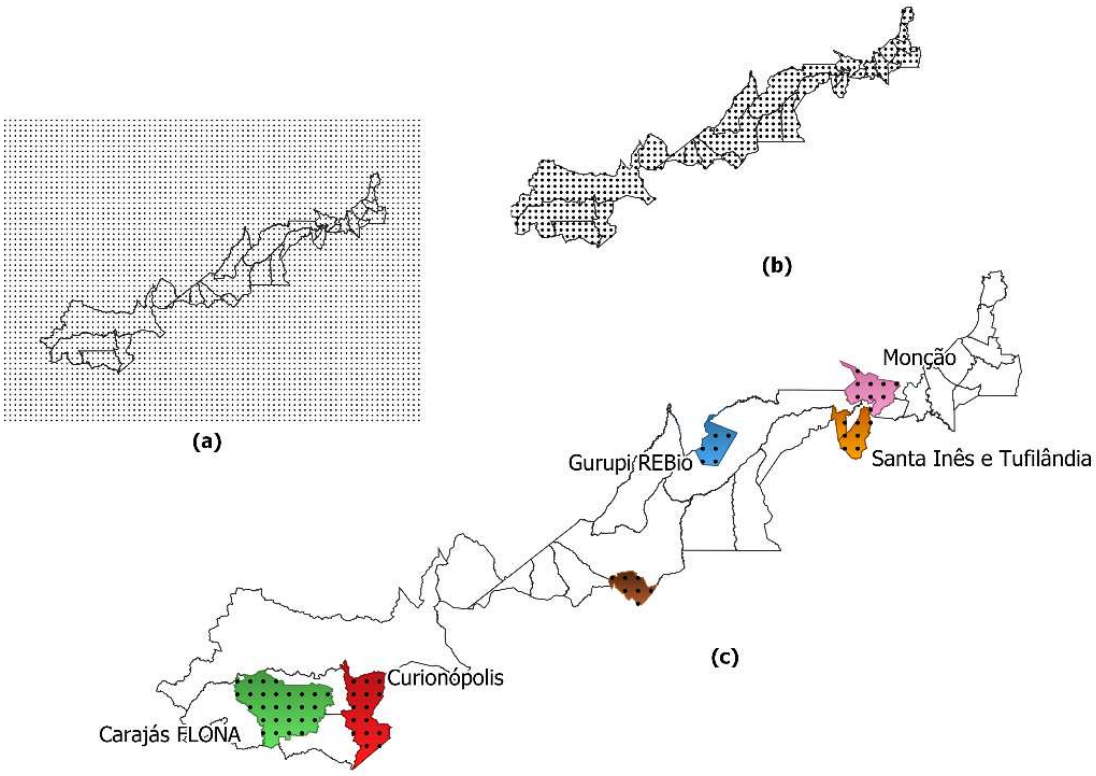

Own authorship

Fig. S2 Density of frequency distribution of seasonal precipitation data (dry season – orange and rainy season – blue) provided by BR-DWGD, ERA5-Land and CHIRPS datasets for the Northern System's domain **(a)**; Curionópolis **(b)**; São Francisco do Brejão **(c)**; Monção **(d)**; Santa Inês and Tufilândia **(e)**; FLONA Carajás **(f)** and REBio Gurupi **(g)**.

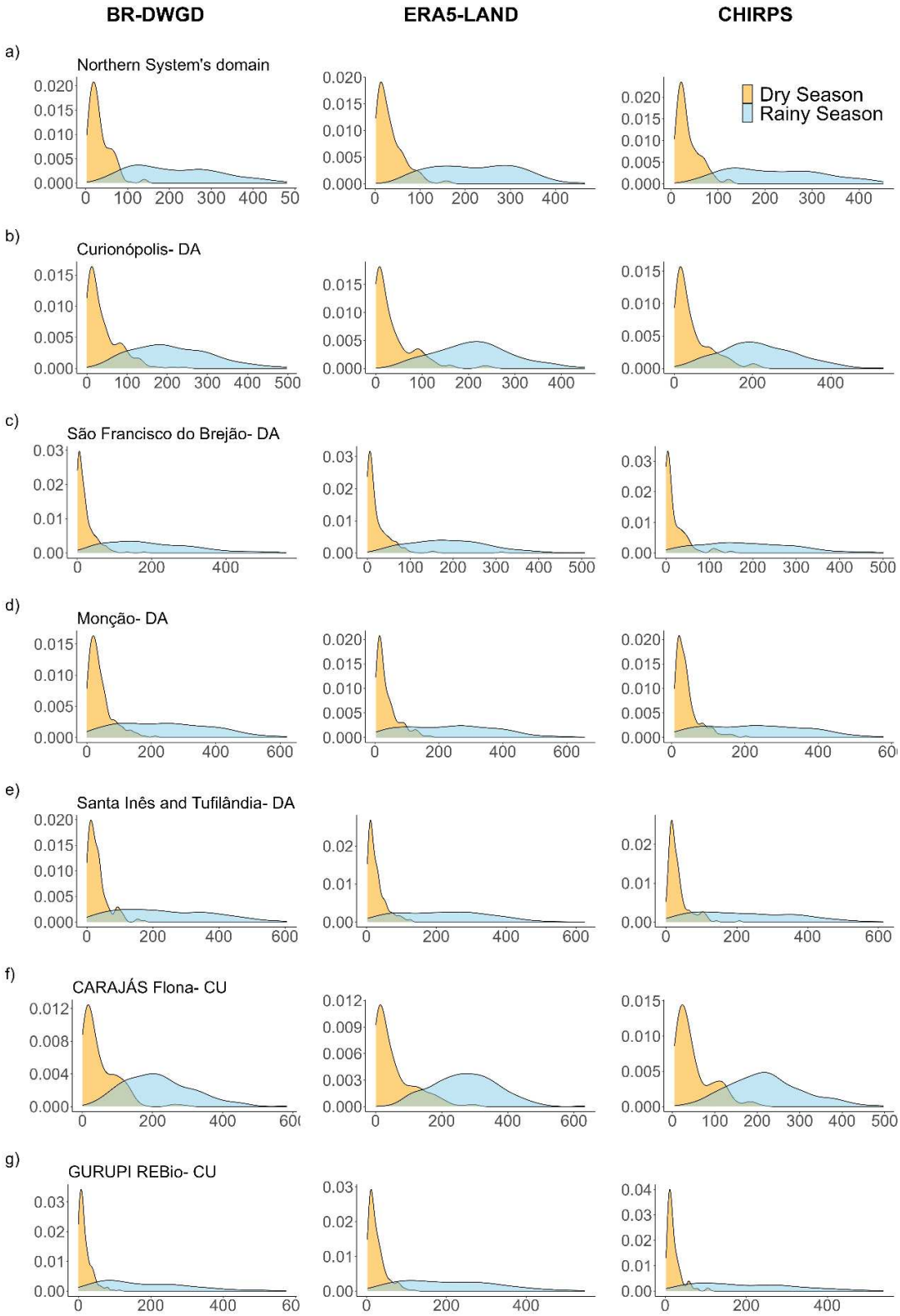

Own authorship

Table S1 – Precipitation annual and monthly trends: Sen's slope estimates and significance of annual and monthly trends (1981-2020) grouped by dataset for the Northern System's domain and further study sites. Values in blue (orange) indicate positive (negative) trends.

	Site	Sen's slope estimates (S)	
		Annual data	Monthly data
OBS-BR	Northern System's domain	1.10	-0.02
	Curionópolis	8.62*	0.02
	São Francisco do Brejão	-7.55*	-0.03
	Monção	-7.19	-0.05*
	Santa Inês e Tufilândia	-8.57	-0.04
	FLONA Carajás	4.07	-0.01
	REBio do Gurupi	-2.38	-0.03*
ERA5-Land	Northern System's domain	-3.19	-0.04
	Curionópolis	-8.06*	-0.04
	São Francisco do Brejão	-2.87	-0.03
	Monção	1.47	-0.01
	Santa Inês e Tufilândia	0.54	-0.01
	FLONA Carajás	-10.81*	-0.07
	REBio do Gurupi	0.74	-0.01
CHIRPS	Northern System's domain	2.69	-0.01
	Curionópolis	5.42	0.01
	São Francisco do Brejão	0.99	-0.01
	Monção	-6.91	-0.04
	Santa Inês e Tufilândia	-9.76	-0.03
	FLONA Carajás	3.82	0.00
	REBio do Gurupi	4.02	-0.01

* Significant in Mann-Kendall trend test at 95% significance level.

Table S2 – Precipitation seasonal trends: Sen's slope estimates and significance of seasonal trends (1981-2020) grouped by dataset for the Northern System's domain and further study sites. Values in blue (orange) indicate positive (negative) trends.

Site	Sen's slope estimates (S)					
	BR-DWGD		ERA5-Land		CHIRPS	
	Dry S.[a]	Rainy S.[b]	Dry S.[a]	Rainy S.[b]	Dry S.[a]	Rainy S.[b]
Northern System's domain	-1.60**	1.97	-3.36**	-0.26	-1.42	3.13
Curionópolis	-1.11	9.21**	-4.21**	-2.98	-1.62	7.93*
São Francisco do Brejão	-1.78**	-7.01	-2.73**	-0.34	-1.24	0.73
Monção	-3.25**	-4.29	-0.63	3.49	-1.61	-5.22
Santa Inês and Tufilândia	-2.48**	-5.40	-1.03	1.10	-1.28	-7.32
Carajás FLONA	-2.43*	5.65	-6.87**	-4.75	-2.50**	5.75
Gurupi REBio	-1.93**	-0.89	-1.66*	2.19	-0.90	5.14

a Dry Season and b Rainy Season.

* Significant in Mann-Kendall trend test at 95% significance level.

** Significant in Mann-Kendall trend test at 99% significance level.

Fig. S3 Curianópolis (light blue) borders a set of juxtaposed federal conservation units that includes Carajás FLONA (red) **(a)** and Gurupi REBio (yellow) is surrounded by deforestation and forest patches **(b)**.

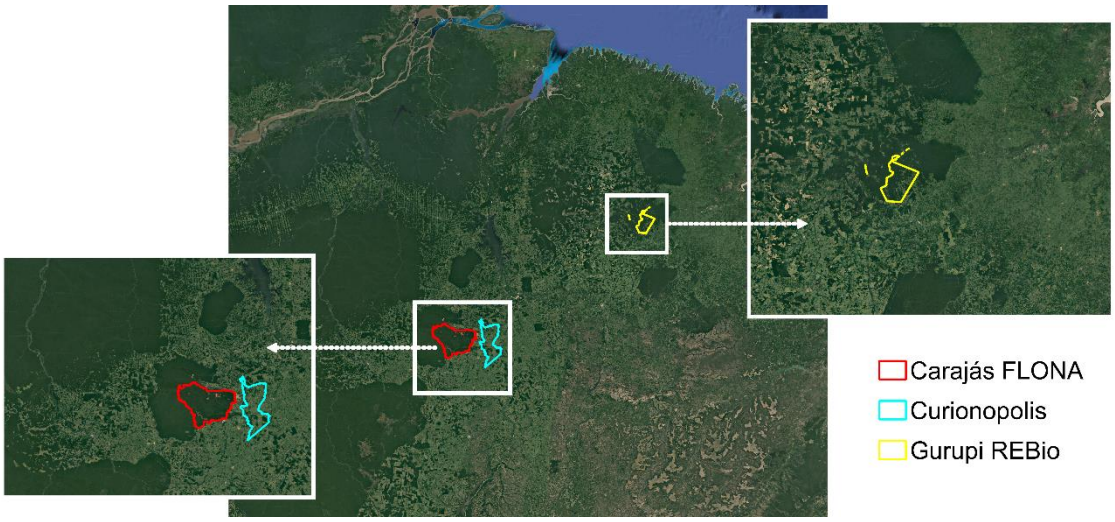

Own authorship

CHAPTER 2 – COMBINED EFFECT OF WATER STRESS AND INCREASED CARBON DIOXIDE ON LAND COVER ESTABLISHMENT AND DEVELOPMENT AT MINING SITES

Maísa Quintiliano Alves[1], Flávio Barbosa Justino[2], Francisco Cássio Gomes Alvino[3], Rafael Gomes Viana[4], Carlos Augusto Brasileiro de Alencar[5], Paulo Roberto Cecon[6], Rafael Ferreira da Costa[7], Fernando França da Cunha[8], Rubens Alves de Oliveira[9] and Renan Rodrigues Coelho[10]

ABSTRACT

In light of the escalating atmospheric CO_2 levels and the growing occurrence of drought events in the Eastern Amazon, this study investigates the impact of water deficit on photosynthesis and plant growth of fast-growing C_3 and C_4 herbaceous species (Pigeon pea – C_3, Jack bean – C_3, and Sudan grass – C_4), commonly utilized in the land reclamation of mining areas, under elevated atmospheric CO_2 concentrations. The experiment was conducted in the Amazon biome, employing nine open-top chambers. Three treatments were applied: (i) current atmospheric CO_2 concentration without irrigation; (ii) elevated CO_2 without irrigation; and (iii) elevated CO_2 with irrigation. Air temperature and humidity within the chambers were monitored, along with plant dry matter, growth, and physiological attributes. The outcomes revealed no evidence that the evaluated species are deeply affected by the increase in atmospheric CO_2 and intense drought events— at least regarding height growth and biomass production. Nonetheless, they were potentially impacted by the extreme heat. Ultimately, a notable reduction in the emergence of Pigeon pea individuals was observed, which declined by half in resource-rich environments (elevated atmospheric CO_2 and irrigation). This is likely a consequence of interspecific competition within the chambers and may indicate a shift in the composition of developing vegetation.

Keywords: Climate-change; Pigeon-pea; Jack-bean; Sudan-grass; The-Amazon; Water-deficit

Authors affiliation:

1-3, 5, 8, 9 Universidade Federal de Viçosa, Agricultural Engineering Department, Viçosa, Brazil.

4 Universidade Federal Rural da Amazônia, Agronomy Department, Belém, Brazil.

6 Universidade Federal de Viçosa, Statistics Departament, Viçosa, Brazil.

7 Universidade Federal Rural da Amazônia, Agronomy Department, Parauapebas, Brazil.

10 Vale S.A., Carajás Industrial Complex, Parauapebas, Brazil.

1. INTRODUCTION

During the pre-industrial period, the atmospheric concentration of CO_2 stood at approximately 280 ppm (FAN et al., 2020). From 1850 to 2019, human activities released circa 2400 $GtCO_2$ into the atmosphere, increasing the concentration to 410 ppm. In the worst-case emissions scenario driven by socioeconomic features (SSP5-8.5), atmospheric CO_2 concentration is expected to reach 700 ppm before 2070. As a transient climate response, the temperature has risen attendant to CO_2 levels, nearly 1.65°C per 1000 PgC, warming thus the global surface in 1.09°C (relative to 1850–1900) (ARIAS et al., 2023).

Due to climate change, general downward trends in precipitation and rising air temperatures have been recently observed in South America, accompanied by a heightened frequency of extreme events in the Amazon (ARIAS et al., 2023; BOCHOW & BOERS, 2023; LUCAS et al., 2021). In the eastern Amazon, particularly, the dry season is generally getting drier, with the increase of consecutive dry days (LUCAS et al., 2021; MU & JONES, 2022; SANTOS et al., 2020). Additionally, the wet season is also getting wetter in certain areas, accompanied eventually by more intense rainfall. Changes in the water cycle are likely to result in greater variability in soil moisture. Some regions in the eastern Amazon are foreseen to experience agricultural and ecological droughts, impacting local vegetation (ARIAS et al., 2023).

Given the Amazon global importance, several ongoing projects and the novel proposal for a bold large-scale restoration, the "Arc of restoration" (DA CRUZ et al., 2021; TORRES, 2022) have attracted worldwide attention. In this context, it is imperative to incorporate future predominant climate conditions into restoration programs planning (SAGE et al., 2008). Potential impacts of climate change on tropical forest biomes must be considered in the early designing step of restoration projects, but such impacts are still uncertain. It is pressing, thus, to understand how plants used in restoration physio- and morphologically respond to rising CO_2 and temperature, likely accompanied by water deficit. There is a consensus that plants can adapt (i.e., acclimate/downregulate) to moderate temperature increases in tropical biomes, but inconsistencies regarding how well they can acclimate and whether their grow rate increases as a result of the CO_2 fertilization effect are pointed out (OMETTO et al., 2022).

The assessment of plants' response to climate change can span various scales. In general, results of field experiments point out the greater sensitivity of C_3 species to elevated CO_2 levels compared to C_4, manifesting greater photosynthetic rates (TAIZ et al., 2017). Furthermore, the maintenance or increase of photosynthesis rates and carbon uptake are

reported in water-stressed environments due to stomatal regulation, contributing to improved WUE in C_4, as expected (ALLEN et al., 2011; ZISKA & BUNCE, 2006), but also in C_3 plants, especially those under severe drought (ZHANG et al., 2018). Multiple documented effects of global warming on individual plants include amplified plant growth, increased seed germination and emergence in herbaceous plants, heightened root growth, and greater tiller and leaf formation in both herbaceous and woody C_3, as well as some C_4 species (ZISKA & BUNCE, 2006). In an exosystemic standpoint, tropical forests may experience temporary physiological benefits in response to higher temperatures and shifts in precipitation patterns. Nevertheless, the declining resilience of these forests to such stressors has led to a reduction in the provision of essential ecosystem services (MAGALHÃES et al., 2021; OMETTO et al., 2022).

In the eastern of the Amazon tropical forest, mining stands as a significant activity (MAGALHÃES et al., 2021). Within this region, the S11D project, one of the world's largest iron ore exploration endeavors, is situated (MATLABA et al., 2019). As a result, there is a substantial demand for land reclamation in challenging areas, such as the slopes of open pits, typically achieved through hydroseeding with a diverse mix of native and non-native species seeds (RAMOS et al., 2022). While the use of native species must be prioritized according to Brazilian legislation, the inclusion of non-native species may be allowed with well-based justification (GASTAUER et al., 2019). Non-native, fast-growing N-fixing legumes and grass species are often essential for accelerating vegetation development and ensuring soil coverage in this environment (RAMOS et al., 2022).

Considering the increase in atmospheric CO_2 and drought spells in easter Amazon, this study aims to evaluate how water deficit affects photosynthesis and plant growth of fast-growing species used in land reclamation of mining areas under high atmospheric concentrations of CO_2. The purpose is to improve the understanding of plants' response to climate change and provide important insights for future restoration and reforestation programs.

2. MATERIALS AND METHODS

2.1. Characterization of the study area

2.1.1. Location and climate

The experiment was carried out spanning from July 27, 2022, to November 21, 2022, within a 225 m² area (15x15 m) situated at the seedling nursery of Vale S.A., within the Carajás Mining Complex and FLONA Carajás in the state of Pará, Brazil (50º04'49.88" W and 6º02'59.88" S) (Fig.1).

Figure 1 – Experimental area location in the seedling nursery of VALE S.A. within the Carajás Mining Complex in the state of Pará, Brazil

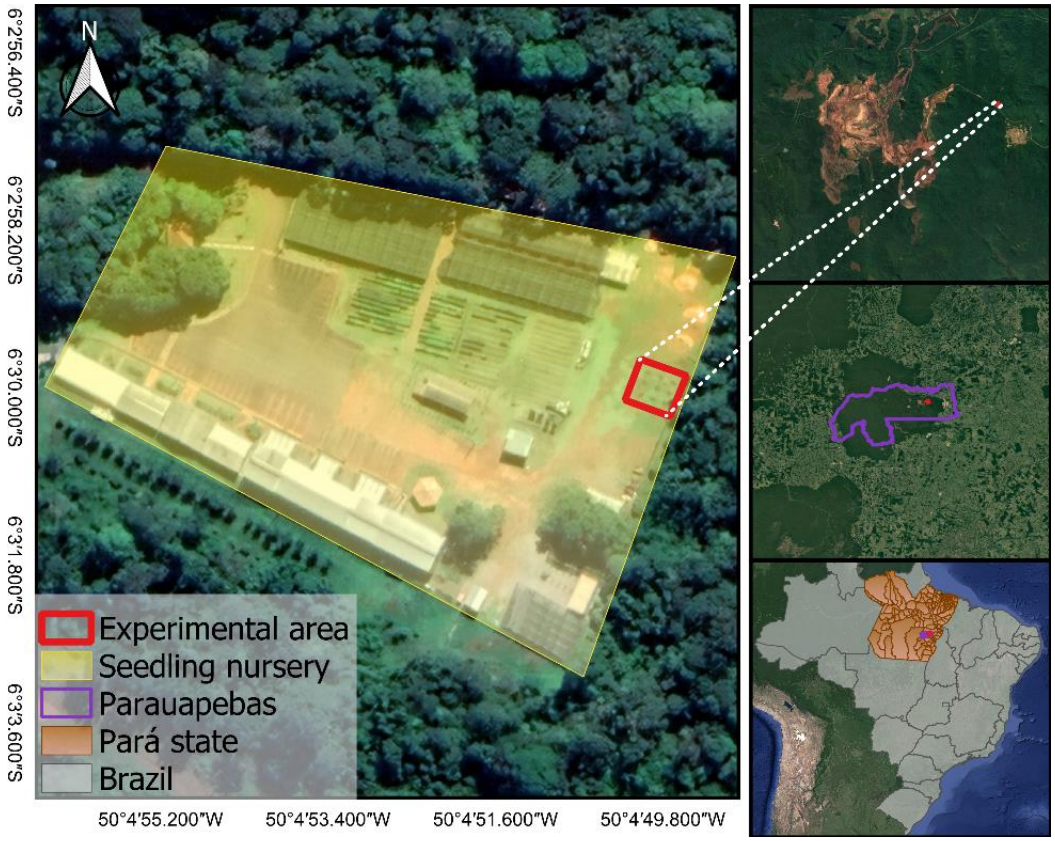

Own authorship

The local climate is Aw-Köppen, hot-humid tropical with a dry winter, markedly seasonal. The wet period occurs from November to May, while the dry period extends from June to October, with monthly precipitation dropping below 60 mm in the most critical month. The annual average air temperature is 26ºC, with maximum and minimum temperatures around 32 and 22ºC, respectively. The annual average maximum relative humidity is 78%, and the minimum is 32% (FERNANDES et al., 2018).

2.2. Open top chambers

To shelter the plants and enable the enrichment of the atmosphere with CO_2, nine open-top chambers were developed based on the proposal by Silva et al. (2020). Similar to the

authors, instead of constructing a solid structure, modules were added on top of each other as demanded by plant growth. Thus, the chambers were assembled with hexagonal modules, equipped with two side doors for ease of measurements and collection. The upper module of the chambers featured an opening at the top of approximately 0.56 m², allowing gas exchange between the internal and external environments. However, a bell was attached to the structure, covering this opening, with the aim of preventing rainwater entry and, consequently, facilitating control over soil water deficit. Segments of iron pipes (12.5mm) employed at the edges of the modules, windows, and bell provided stability to the structures, which were enveloped with transparent plastic film (Fig. S1). The chambers were installed 2 m apart from each other, forming a configuration of three rows and three columns.

2.3. Soil, seed sowing and species

For soil characterization, we collected single soil samples (0-20 cm) at three points within the experimental site and homogenized them to create a composite sample. Then, we determined physical and chemical soil attributes following the methods outlined in the Soil Analysis Method (TEIXEIRA et al., 2017). The soil used for plant establishment was a very clayey soil with low fertility of an anthropized area in Vale's seed nursery (Table 1). Considering the texture, the gravimetric moisture at field capacity (30 kPa) is 0.29 g g^{-1} or 29.50%.

Table 1 – Soil properties in the study area: Chemical and hydrophysical characteristics

Coarse sand	**Fine sand**	**Silt**	**Clay**	**Φs**	**Bd**	**Pd**
(%)					**(g cm^{-3})**	
8.80	1.90	9.10	80.20	41	1.78	3.03
Soil water retention curve						
Tension (kPa)	10	30	100	300	800	1.500
Moisture (g g^{-1})	0.30	0.29	0.27	0.26	0.24	0.23
Ca^{2+}	**Mg^{2+}**	**Al^{3+}**	**H+Al**	**SB**	**CEC**	**CTC**
($cmol_c$ dm^{-3})						
0.67	0.02	0.00	5.3	0.71	0.71	6.01
P	**K**	**V**	**m**	**SOM**	**P-rem**	
(mg dm^{-3})		**(%)**		**(dag kg^{-1})**	**(mg L^{-1})**	
0.1	7	11.8	0.0	3.90	10.5	

Φs: Soil porosity; Bd: Bulk density; Pd: Particle density; Ca^{2+}: Calcium content; Mg^{2+}: Magnesium content; Al^{3+}: Aluminum content; H+Al: Potential acidity; SB: Sum of bases; CEC: cation exchange capacity; CTC: cation total capacity; P: Phosphorus content; K: Potassium content; V: base saturation; m: Aluminum saturation; SOM: Soil organic matter and P-rem: Remaining phosphorous.
Own authorship

The seedling process was conducted using a seed mix comprising both native and non-native species, commonly employed through hydroseeding in reclamation projects for terrains with challenging topography and difficult access (RAMOS et al., 2022). The list of utilized species is provided in the appendix (Table S1). The preparation of the chamber soils in this process involved manual scarification using a garden scarifier. During seeding, a mixture of sifted soil, organic fertilizer derived from crushed plant residues, and the seed mix in a ratio of 0.43:1 (non-native: native) was broadcasted onto the chambers' soil.

Although various species thrived within the chambers, on the first measurement day (49th Day After Sowing – DAS) only three were selected for in-depth study according to the following criteria: (i) being an opportunistic specie (resilient and fast-growing); (ii) being present in all chambers; (iii) demonstrating numerical superiority of individuals within the chambers; and (iv) having its initial development observed in real-world conditions on the revegetated slopes of the mining area. The species that met all the criteria were Pigeon pea (Cajanus cajan), Jack bean (Canavalia ensiformes), and Sudan grass (Sorghum sudanense). The first two are dicotyledonous legumes (Leguminosae) with a short life cycle (3 to 4 years and annual, respectively) and a C_3 photosynthetic pathway. Sudan Grass is an annual monocotyledonous grass (Poacea) with a C_4 photosynthetic pathway.

2.4. Experiment design and growing conditions

The experiment was arranged in a split-plot design, with treatments serving as the main plot (three levels, detailed below) and species comprising the subplot, also with three levels (Pigeon Pea, Jack Bean, and Sudan Grass) in CRD (Completely Randomized Design), each replicated three times. Each replication represents the average of measurements taken from four plants. A total of nine open-top chambers (three for each treatment) were utilized to sustain plant growth and control CO_2 concentration. The treatments included: (i) current atmospheric CO_2 concentration without irrigation – C400DH; (ii) elevated CO_2 without irrigation – C700DH; and (iii) elevated CO_2 with irrigation – C700IR. The data were analyzed using analysis of variance, and means were compared using the Tukey test at a 5% significance level. Regardless of the significance of higher-order interactions, they were unfolded due to the study's interest. Statistical analyses were performed in SAEG environment, version 9.1. Additionally, it is important to mention that the treatment involving current atmospheric CO_2 concentration and irrigation was intentionally not performed as it did not align with the objectives of our study.

The differentiation of the treatments in this study occurred on the 50th DAS. In the first 49 days, all chambers were irrigated and did not increment the current atmospheric CO_2 concentration of 400 ppm. Irrigation was carried out through 16 mm drip tapes spaced at 0.70 m, equipped with self-compensating drippers (Rivulis– D5000 PC) spaced at 0.30 m with an average flow rate of 1.9 L h^{-1}. Each chamber, therefore, had five intersecting tapes, totaling 12 drippers. The water distribution uniformity of the irrigation system, measured by the Christiansen Uniformity Coefficient, was determined to be 95.8%. This value was taken as the irrigation system efficiency, given the absence of leaks (conveyance efficiency = 100%) and the localized irrigation method (application efficiency = 100%).

Irrigation was applied uniformly across all chambers until the 49th DAS to facilitate leaf emergence and promote the establishment of plants. For the initial 12 days, a 2-day irrigation interval was adhered to. Subsequently, from the 13th DAS onward, the irrigation interval was extended to 3 days. Starting at the 50th DAS, exclusive irrigation was maintained solely for the three chambers subjected to the C700IR treatment, with a consistent 3-day irrigation interval (Fig. 2a). However, throughout the entire experiment, precipitation volumes were replenished in all chambers one day after rainfall events in an attempt to simulate the local rainfall regime. In those instances, there was a 3-day interval between rainfall and the subsequent irrigation event. In contrast to irrigated plants, which rarely faced water deficit, plants under non-irrigated treatments from the 50th DAS experienced water stress for a significant portion of the experiment. At times, this stress was characterized by severe water deficit, with soil water tension nearing the Permanent Wilting Point (PWP) (Fig. 2b).

Fig.2. Water balance in chambers under C700IR treatment **(a)** and under C400DH and C700DH treatments **(b)**

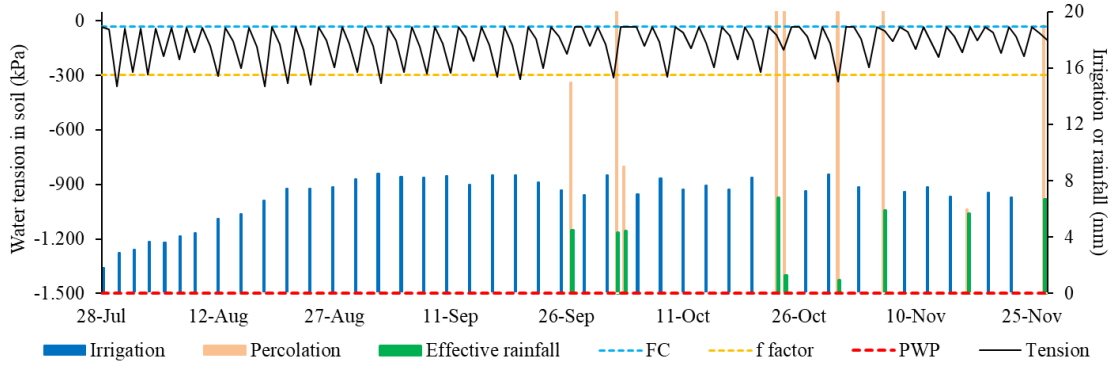

(a)

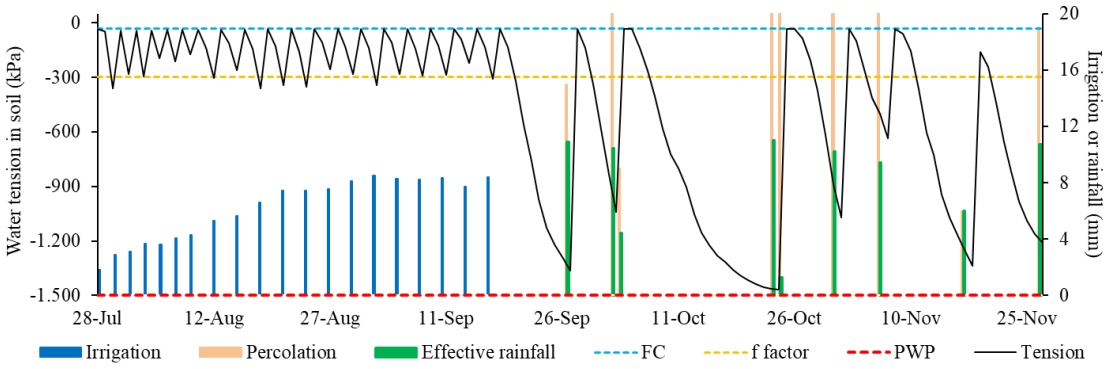

(b)

Own authorship

With respect to CO_2 increment, CO_2 was injected into six chambers to increase CO_2 levels using a system consisting of a 25 kg compressed gas cylinder, an automatic digital CO_2 level controller (Pro-Leaf – PPM-B1), an air compressor (Fiac – 40 psi 1/4 hp dual voltage), and a high-speed single-phase axial fan (Ventisilva–E 30 M4). These components were connected in that order by a flexible PVC hose with textile fiber reinforcement. The CO_2 injection began on the 50th DAS when the controller was set to maintain a CO_2 concentration of 700 ppm in the internal environment of the chambers under C700IR and C700DH conditions. Consequently, a solenoid valve was automatically activated whenever the concentration dropped, releasing gas from the cylinder into the rest of the injection system. The sensor, featuring a photocell that regulates its operation based on light incidence, ensured that gas was released only during daylight hours.

2.5. Climatic data

From the 49th DAS onward, the average temperature and air humidity inside the chambers were automatically recorded every 15 minutes using Data Loggers equipped with external temperature and humidity sensors (Elitech – RC-61). The data were aggregated to obtain hourly values. The meteorological data were obtained using an automatic weather station near the experimental site (7° 6'36.00"S and 49°55'48.00"O), including precipitation volumes to be replenished through irrigation within the chambers.

2.6. Growth variables and dry matter

After the 49th, 57th, 81st, 92nd, and 116th DAS, height (H) measurements were taken with a graduated tape from the soil surface to the apical bud. Diameter (Φ) measurements were taken on the plant stem 1 cm above the ground with a caliper. On the 123rd DAS, stems and leaves were separated, placed in paper bags, and dried in a forced-air circulation oven (65 ºC) until reaching a constant mass. Finally, the plant material was weighed using a balance with an accuracy of 0.01 g.

2.7. Physiological variables

For Jack Bean and Sudan Grass, physiological variables were obtained using an Infrared Gas Analyzer (IRGA - LI-COR–LI6400XT) at PAR of 1,000 μmol of photons $m^{-2}s^{-1}$ in a single campaign, which occurred at the 57th DAS, between 9:00 and 10:00 in the morning, under favorable environmental conditions. The CO_2 levels exhibited variations among the chambers in response to the specific treatments applied (400 or 700 ppm). The physiological variables obtained included Net Photosynthesis (A), Stomatal Conductance (gs), Substomatal CO_2 concentration (Ci), Transpiration (E), Vapor Pressure Deficit (VpdL) and Leaf Temperature (Tl). Further variables were calculated, including the ratio of Ci to atmospheric CO_2 concentration (Ci/Ca) and Water Use Efficiency (WUE), the last one comprises the ratio A/E. Given constraints in equipment availability and favorable environmental conditions, no physiological variable was measured for Pigeon Pea.

3. RESULTS

3.1. Air temperature and humidity

The open-top chambers were developed to accommodate developing vegetation and promote the formation of a microclimate considering future climate scenarios, which predict an increase in CO_2 concentration and rising air temperatures. The hourly averages of air temperature and humidity data inside the chambers were found to be high. The highest maximum temperature and average humidity values occurred at 14:00, reaching 46.2°C and 73.5% (C400DH – Fig. 3a); 47.0 and 83.6% (C700DH – Fig. 3b); and 48.5 °C and 75.6% (C700IR – Fig. 3c).

Fig.3. Average of hourly data for mean humidity and mean, minimum, and maximum temperatures throughout the experiment inside the chambers under current atmospheric CO_2 concentration without irrigation – C400DH (a), elevated CO_2 without irrigation – C700DH (b) and elevated CO_2 with irrigation – C700IR (c) treatments

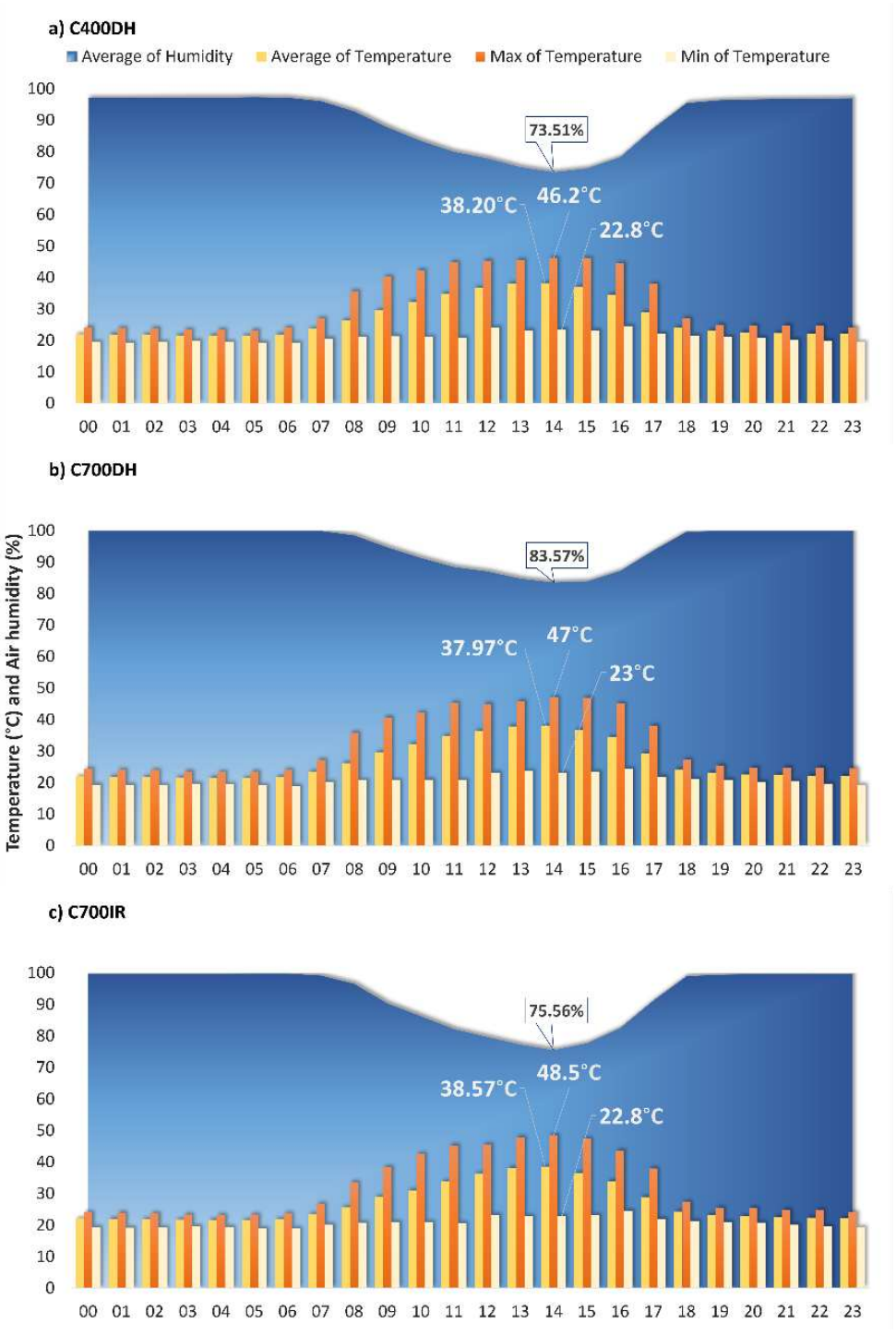

Own authorship

The average temperatures in the chambers do not seem to differ significantly between chambers' conditions; however, the maximum temperatures during the hottest time exhibit a variation of over 2 °C between C700IR (48.5 °C) and C400DH (46.2 °C). For C700DH, the

maximum temperature reached 47.0 °C. Those values markedly exceed the typical maximum temperature outside the chambers, which is ~32°C, according to literature (FERNANDES et al., 2018).

Regarding air humidity, the average values observed within the chambers align with findings reported by Fernandes et al (2018), who documented humidity ranging from 62% to 82.2%. Chambers subjected to the C400DH and C700IR treatments indicate similar humidity levels, whereas those associated with the C700DH treatment exhibit higher values.

3.2. Physiological variables

Significant differences were identified among treatments for most physiological variables, with exceptions for Ci/Ca and WUE. Additionally, within the same treatment, the response of the species significantly differed regarding all physiological attributes, except for Net Photosynthesis. The means comparison through Tukey test at 5% probability is presented in Table 2. The summary of the Analysis of Variance (ANOVA) for physiological data can be found in the appendix (Table S2 – Appendix).

Table 2 – Mean Net Photosynthesis (A), Stomatal Conductance (gs), CO_2 Concentration in the Sub-stomatal Chamber (Ci), Transpiration (E), Vapor Pressure Deficit (VpdL), Leaf Temperature (T_l), the ratio between Ci and atmospheric CO_2 concentration (Ci/Ca), and Water Use Efficiency (WUE) values for respective treatment (TR) and species (SP) combinations

TR	**A** (μmol $m^{-2}s^{-1}$)		**gs** (mol H_2O $m^{-2}s^{-1}$)		**Ci** (μmol mol^{-1})		**E** (mol H_2O $m^{-2}s^{-1}$)	
	Jack b.	**Sudan g.**	**Jack b.**	**Sudan g.**	**Jack b.**	**Sudan g.**	**Jack b.**	**Sudan g.**
C400DH	19,42 **aB**	19,33 **aB**	0,795 **aAB**	0,116 **bA**	334,4 **aB**	95,1 **bA**	10,32 **aB**	3,21 **bB**
C700DH	25,41 **aB**	19,22 **aB**	0,637 **aB**	0,084 **bA**	458,8 **aA**	129,7 **bA**	11,79 **aB**	3,60 **bB**
C700IR	34,75 **aA**	35,36 **aA**	0,845 **aA**	0,164 **bA**	483,5 **aA**	192,7**bA**	15,34 **aA**	6,45 **aA**
TR	**VpdL** (kPa)		**T_l** (ºC)		**Ci/Ca**		**WUE**	
	Jack b.	**Sudan g.**	**Jack b.**	**Sudan g.**	**Jack b.**	**Sudan g.**	**Jack b.**	**Sudan g.**
C400DH	1,288 **bB**	2,599 **aB**	26,70 **bB**	30,51 **aB**	0,870 **aA**	0,246 **bA**	1,880 **bA**	6,114 **aA**
C700DH	2,233 **bA**	4,059 **aA**	31,58 **bA**	36,10 **aA**	0,794 **aA**	0,222 **bA**	2,315 **bA**	5,875 **aA**
C700IR	1,795 **bAB**	3,627 **aA**	30,36 **bA**	35,04 **aA**	0,847 **aA**	0,336 **bA**	2,268 **bA**	5,525 **aA**

[1] C400DH: current atmospheric CO_2 concentration without irrigation; C700DH: elevated CO_2 without irrigation; C700IR: elevated CO_2 with irrigation; Jack b.: Jack bean and Sudan g.: Sudan grass.
[2] The means followed by at least one same uppercase letter in the column and lowercase letter in the row for each variable do not differ from each other at a 5% probability level according to the Tukey test.
Own authorship

Figure 4 helps with results visualization. The elevated photosynthetic rate observed in both species, Jack bean (C_3) and Sudan grass (C_4), under the treatment involving elevated CO_2

and irrigation (C700IR) is noteworthy. However, it is important to highlight that the increment in CO_2 levels, when coupled with water deficit (C700DH), does not lead to a significant increase in the photosynthetic rate. In this scenario, the photosynthetic rate remains statistically equivalent to that of plants grown under current CO_2 concentrations and water deficit conditions (C400DH). It is worth mentioning that a marginal positive trend is observed for the Jack bean under the C700DH treatment (Fig. 4a).

Fig.4. Mean values of Net Photosynthesis – A (a), Stomatal Conductance – gs (b), CO_2 Concentration in the Sub-stomatal Chamber – Ci (c), the ratio between Ci and atmospheric CO_2 concentration – Ci/Ca (d), Vapor Pressure Deficit – VpdL (e), Leaf Temperature – Tl (f), Transpiration – E (g) and Water Use Efficiency – WUE (h) for respective treatment (TR) and species (SP) combinations. The significance of the differences between means is presented in Table 2. Note that physiological attributes were exclusively assessed in Jack Bean and Sudan Grass.

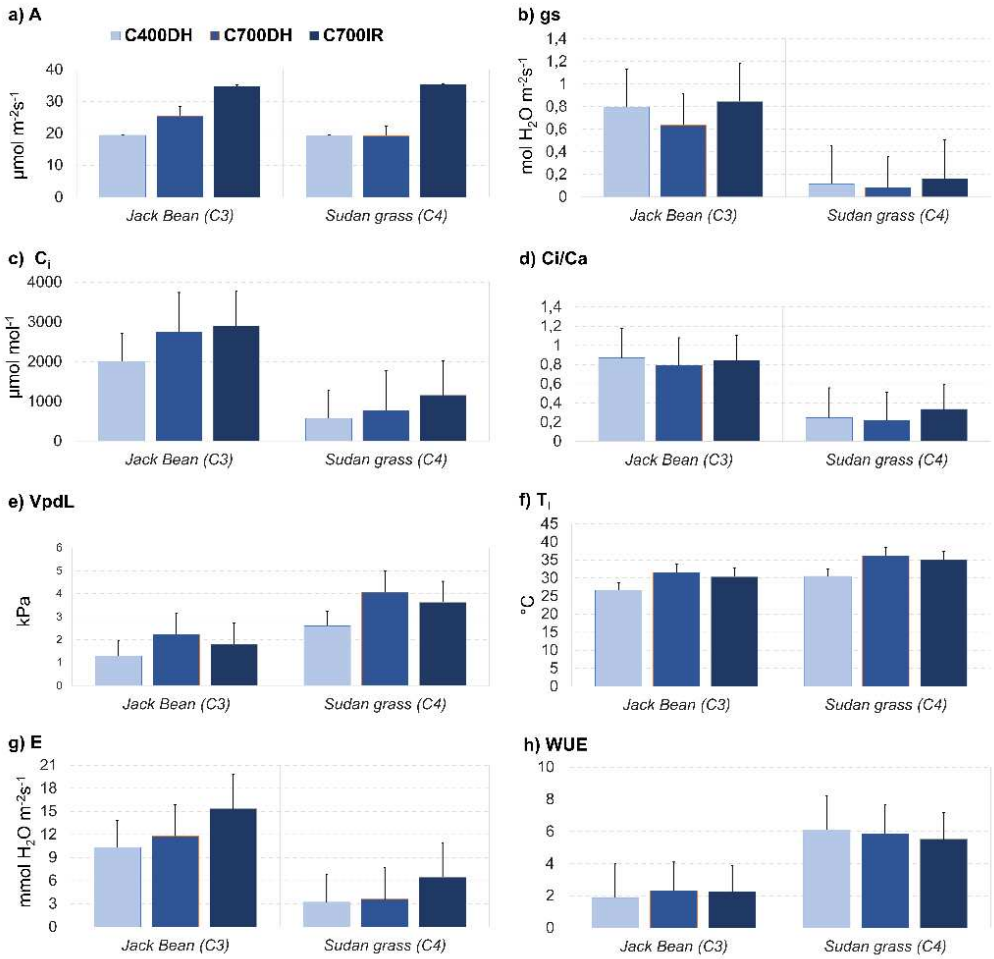

Own authorship

In terms of stomatal conductance, the mean values for Sudan grass were considerably lower than those for Jack bean, with values below 0.2 mol H_2O $m^{-2}s^{-1}$ (Fig. 4b). Furthermore,

the treatments did not show any significant effect on the C_4 species in this regard. However, Jack bean exhibited lower stomatal opening in the C700DH treatment.

As expected, the CO_2 concentration in the sub-stomatal chambers of Jack bean was markedly higher in treatments with increased gas (Fig. 4c). For Sudan grass, the treatments did not show significant differences. It is observed that water stress under elevated CO_2 does not interfere with gas concentration in the leaf mesophyll in any species, even though the C_3 plant has reduced stomatal opening frequency.

Regarding transpiration, plants in the C700IR treatment exhibited higher averages, most likely due to greater water availability for their metabolic functions (Fig. 4g). Vapor pressure deficit in the leaf does not seem to have been a determining factor for higher transpiration rates in plants from this treatment, as there are no significant differences between the means of the variable in the C700IR and C700DH treatments, contrary to what is observed for transpiration (Fig. 4e).

Plants under the C700IR and C700DH treatments had higher leaf temperature, possibly due to a more intense increase in air temperature inside the CO_2-enriched chambers (Fig. 4f).

The treatments did not significantly impact water use efficiency, as despite the higher net photosynthetic rate in the C700IR treatment, transpiration and conductance (in Jack bean) also exhibited the same behavior (Fig. 4h).

3.3. Morphology

The spontaneous heterogeneous distribution of plant species within the chambers occurred due to the broadcast seeding method. Throughout the experiment, the seeded plants, which exhibit different growth cycles and photosynthetic patterns, completely covered the chamber soil. The germination of grasses such as Sudan grass was quickly observed. Although species from this group apparently reached the tallest heights overall (Fig.5a), significant differences regarding plant's height and diameter were not observed between the treatments and species (Table 3) – the summary of the Analysis of Variance (ANOVA) for morphological data can be found in the appendix (Table S3 – Appendix).Yet, it is interesting to note that the development in height and thickness of Pigeon Pea (C_3) tends to be harmed by irrigation, whereas the other species can be adversely affected by water deficiency (Fig. 5a,b).

Table 3 – Mean final Height (Hf) and Diameter (Φf) values for respective treatment (TR) and species (SP) combinations

TR	**Hf** (cm)			**Φf** (cm)		
	Pigeon p.	**Jack b.**	**Sudan g.**	**Pigeon p.**	**Jack b.**	**Sudan g.**
C400DH	152.8333 **Aa**	131.6667 **Aa**	160.25 **Aa**	0.6617 **Aa**	0.5658 **Aa**	0.6467 **Aa**
C700DH	143.25 **Aa**	104.8333 **Aa**	148.5 **Aa**	0.6533 **Aa**	0.4783 **Aa**	0.6908 **Aa**
C700IR	94.25 **Aa**	145.5 **Aa**	180.5 **Aa**	0.48 **Aa**	0.5983 **Aa**	0.555 **Aa**

[1] C400DH: current atmospheric CO_2 concentration without irrigation; C700DH: elevated CO_2 without irrigation; C700IR: elevated CO2 with irrigation; Pigeon p.: Pigeon pea; Jack b.: Jack bean and Sudan g.: Sudan grass.
[2] The means followed by at least one same uppercase letter in the column and lowercase letter in the row for each variable do not differ from each other at a 5% probability level according to the Tukey test.
Own authorship

Fig.5. Mean values of final height (Hf) and final diameter (Φf) for respective treatment (TR) and species (SP) combinations.

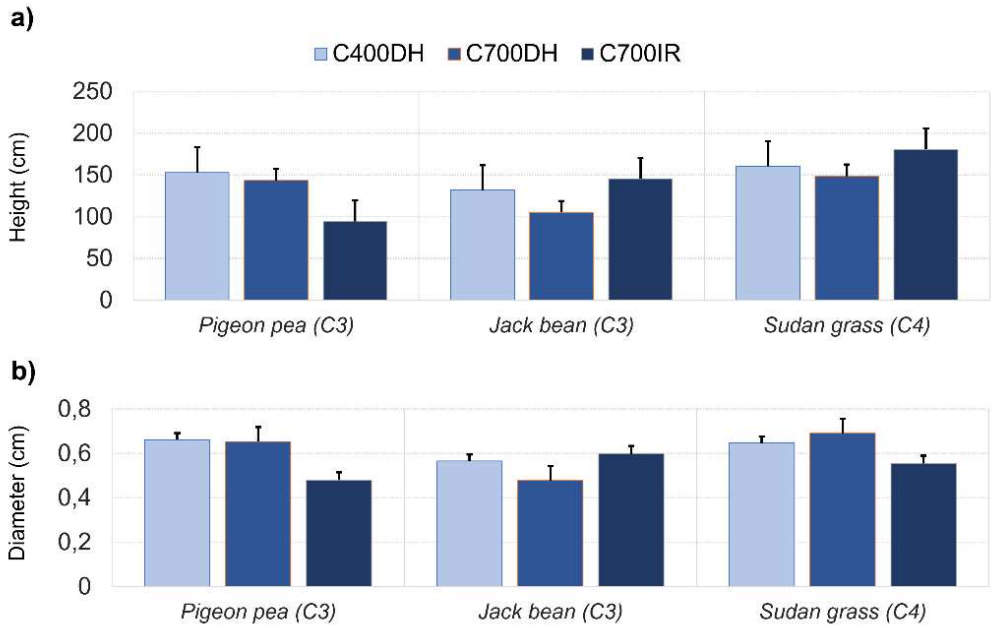

Own authorship

Although the differences are not statistically significant, some points can be highlighted regarding the development of species over time. Jack Bean (C_3) and Sudan grass (C_4) under the C700DH treatment showed the least height growth during the evaluations. While treatments C700IR and C400DH exhibited similar effects over time, a divergence in averages occurred in the final measurement, with plants from these species reaching greater height under the C700IR treatment at the end of the experiment. Conversely, for Pigeon pea, plants under this treatment showed the poorest performance in this aspect (Fig. 6a, b, c).

The same pattern was observed for the stem thickness growth among the applied treatments, except for Sudan grass (Fig. 6d, e, f). The occurrence of etiolation was observed in the basal part of several individuals of this specie (Fig. S2 – Appendix). Due to this behavior, which was noticed belatedly, at a certain point, the new diameter measurements became smaller than the previous ones, suggesting a narrowing of the stem, which did not actually occur.

Fig.6. Mean height and stem diameter values on the 49th, 57th, 81st, 92nd, and 116th days after sowing (DAS) in Pigeon Pea plants (a, d), Jack Bean Plants (b, e), and Sudan Grass (c, f) under C400DH, C700DH, and C700IR treatments

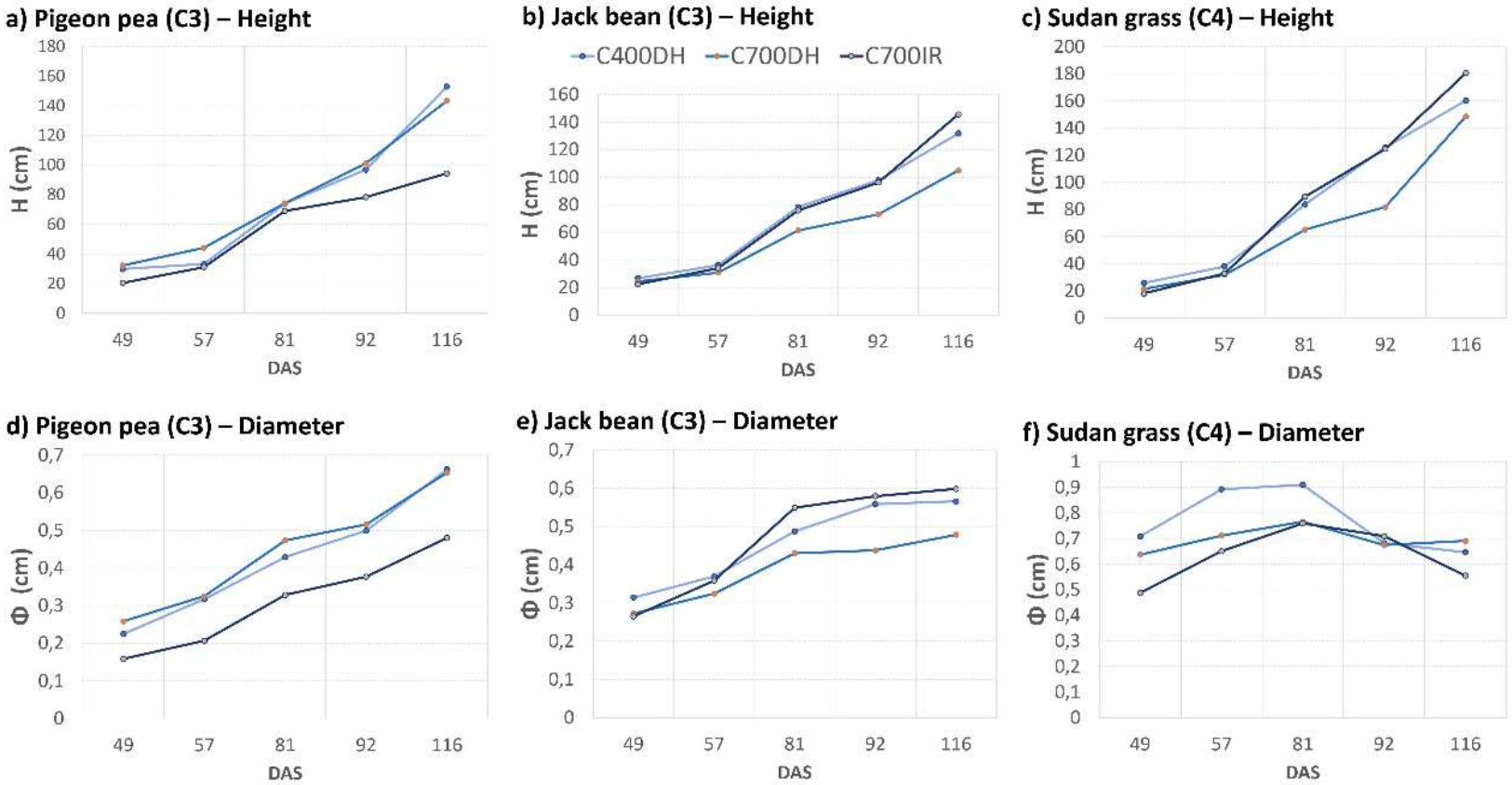

Own authorship

3.4. Dry matter

The results of the analyses of aboveground biomass are in line with those related to plant height, as the treatment with high water availability (C700IR) appears to favor Pigeon Pea while disadvantaging the other species. Conversely, water deficit combined with increased CO_2 (C700DH) tends to hinder aboveground biomass accumulation in Jack Bean and Sudan Grass, while stimulating greater biomass production in Pigeon Pea (Fig.7a).

Fig.7. Mean values of stem, leaf, and total dry matter (a) and number of individuals (b) for respective treatment (TR) and species (SP) combinations

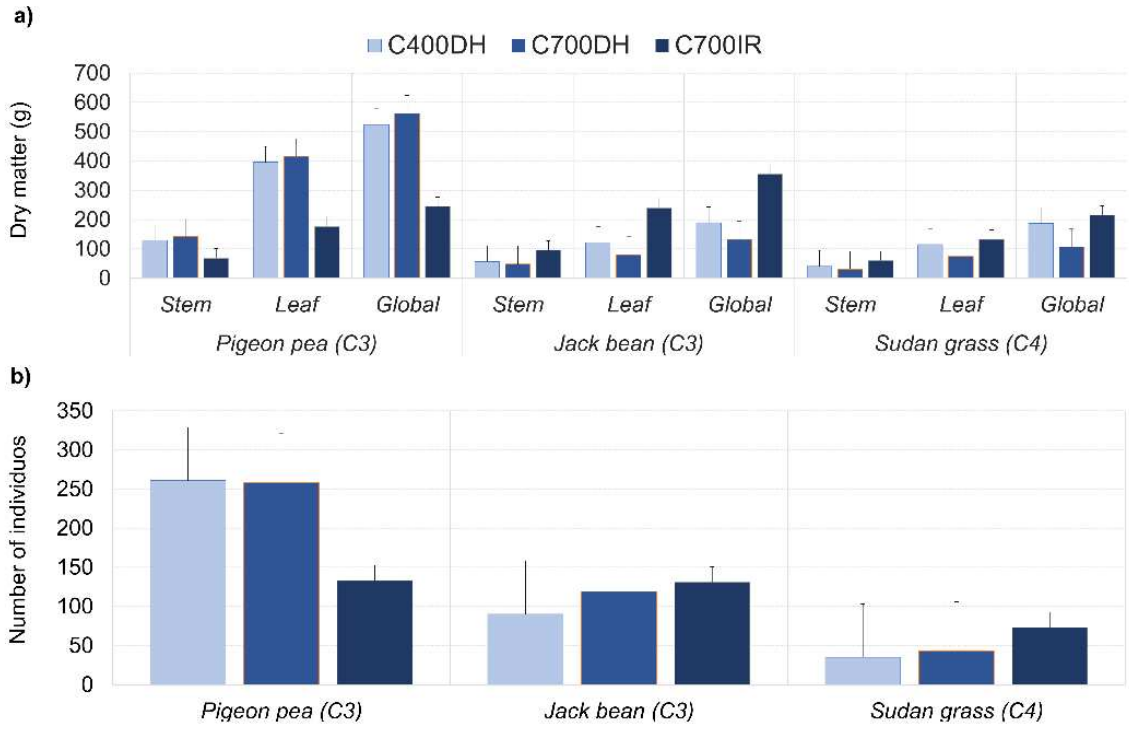

Own authorship

Another interesting observation is that the treatments do not influence carbon partitioning between the stem and leaves of the plants, although it would be more insightful to assess differences in assimilate accumulation between roots and aboveground parts. It is important to note, however, that despite the results indicating a clear trend, the differences are not statistically significant (Table 4). The summary of the Analysis of Variance (ANOVA) for attributes evaluated in this section can be found in the appendix (Table S4 – Appendix).

Once again, a similar response of the analyzed plants to the treatments is observed for the number of emerging individuals (Fig.7b). In this regard, however, the number of Pigeon

Pea individuals that developed under conditions of elevated CO_2 and high water availability (C700IR) was significantly lower compared to the other treatment. Nevertheless, from an ecological perspective, it is important to note that the numerical superiority of this species over the others diminishes with the increase in CO_2 and water concentration.

Table 4 – Mean values of stem dry matter (SDM), leaf dry matter (LDM), total dry matter (TDM) and number of individuals (IND) for respective treatment (TR) and species (SP) combinations

TR	**SDM** (g)			**LDM** (g)		
	Pigeon p.	**Jack b.**	**Sudan g.**	**Pigeon p.**	**Jack b.**	**Sudan g.**
C400DH	128.67 **Aa**	57.12 **Aa**	40.74 **Aa**	395.60 **Aa**	122.04 **Aa**	115.25 **Aa**
C700DH	142.49 **Aa**	48.49 **Aa**	31.03 **Aa**	415.59 **Aa**	80.22 **Aa**	74.70 **Aa**
C700IR	68.33 **Aa**	95.70 **Aa**	60.47 **Aa**	176.15 **Aa**	239.46 **Aa**	132.57 **Aa**
TR	**TDM** (g)			**IND**		
	Pigeon p.	**Jack b.**	**Sudan g.**	**Pigeon p.**	**Jack b.**	**Sudan g.**
C400DH	524.26 **Aa**	189.41 **Aa**	187.29 **Aa**	87.00 **Aa**	30.00 **Ab**	11.67 **Ab**
C700DH	562.14 **Aa**	132.52 **Aa**	106.51 **Aa**	86.00 **Aa**	39.67 **Ab**	14.33 **Ab**
C700IR	244.48 **Aa**	354.76 **Aa**	215.04 **Aa**	44.33 **Ba**	43.67 **Aa**	24.33 **Aa**

[1] C400DH: current atmospheric CO_2 concentration without irrigation; C700DH: elevated CO_2 without irrigation; C700IR: elevated CO2 with irrigation; Pigeon p.: Pigeon pea; Jack b.: Jack bean and Sudan g.: Sudan grass.
[2] The means followed by at least one same uppercase letter in the column and lowercase letter in the row for each variable do not differ from each other at a 5% probability level according to the Tukey test.
Own authorship

4. DISCUSSION

4.1. Microclimate within the chambers

Notably, the microclimate inside the chambers does not resemble the external environment in the experimental area. According to Fernandes et al. (2018), the maximum temperature in Parauapebas is typically around 32ºC. In contrast, in the chambers subjected to the C700IR treatment, the temperature reached 48.5 ºC. At current atmosphere, with CO_2 concentration around 400 ppm and under favorable light and water conditions, the photosynthetic thermal optimum in C_3 species ranges typically between 20-35 °C (SAGE; WAY; KUBIEN, 2008), peaking at approximately 25 °C, whereas it usually occurs between 30-40 °C in C_4 species (MASSAD; TUZET; BETHENOD, 2007). However, species can acclimate, enduring higher temperatures through a change in thermal optimum (SAGE; WAY; KUBIEN, 2008). Although according to Sage and Kubien (2007), for C_3 plants at current CO_2

levels, acclimation is expected within a temperature range 5 to 10°C higher or lower, the limits of acclimation of resilient tropical species, specifically selected to be used in land reclamation, are still not clear. For Maize, a tropical C_4 plant, Crafts-Brandner & Salvucci (2002) reported net photosynthesis inhibition at leaf temperatures above 38°C.

Temperature is indeed a key factor in plant's response assessment. It becomes a stressor when excessively high, impacting their growth in various ways and potentially leading to death (TAIZ et al., 2017). The elevated temperatures recorded within the chambers are linked to the sustained retention of thermal energy originating from sunlight permeating the transparent plastic walls of the chambers. The disparity between the chambers' internal temperature and the external environment is a well-known drawback of the OTC method for assessing plant responses to climate change in the field. Nevertheless, OTC experiments offer a good cost-benefit ratio among options and allow control over soil moisture (SILVA et al., 2020), providing valuable insights into the expected responses of plants utilized in the revegetation of open-pit slopes to the challenges posed by climate change.

The superior observed maximum temperatures in C700IR chambers can be attributed to not only the elevated concentration of CO_2 but also the increased presence of water vapor. This is the primary greenhouse gas with greater radiative flux than carbon dioxide (SHERWOOD; DIXIT; SALOMEZ, 2018). Furthermore, water vapor exhibits a positive feedback effect, as its presence amplifies the warming caused by CO_2. The addition of carbon dioxide, which also raises air temperature, further enhances evaporation rates, warming the air and creating a positive feedback loop (HELD; SODEN, 2000).

Regarding humidity, variations among treatments may be linked to the source of water vapor. The C_3 plants under elevated CO_2 concentrations and water deficit conditions tend to reduce stomatal aperture, consequently minimizing transpiration (SAGE; KUBIEN, 2007; TAIZ et al., 2017). In this context, the humidity observed in the chamber may reflect soil water evaporation, while in chambers under other treatments, plants predominantly consume water, releasing it through transpiration. This assessment becomes feasible through the analysis of plant physiological parameters, which will be addressed in subsequent sections.

4.2. Single leaf response

The physiological parameters of the leaves were measured on the 57th day after sowing (DAS), encompassing species near the end of their vegetative cycle. It is interesting to observe the differences in physiological responses between C_3 and C_4 herbaceous species,

considering their distinct cellular organizations and biochemistry processes (TAIZ et al., 2017), which may influence how they respond to simultaneous changes in diverse abiotic factors (WAND et al., 2001).

Primarily, our findings suggest that severe water deficit has a detrimental impact on photosynthesis in these plants, even when cultivated under elevated atmospheric CO_2 concentrations. This contrasts with the results reported by Silva et al. (2013) for Majestoso-type carioca beans (C_3) and by Fan et al. (2020) for bell pepper (C_3), where plants maintained high photosynthetic rates under high atmospheric CO_2 concentrations, even in the presence of water stress. However, these authors noted some attenuation of positive CO_2 fertilization effect along soil water gradients, indicating that potential benefits of CO_2 fertilization may be somewhat diminished or even counteracted by water availability.

In the case of Jack bean (C_3), the observed lower values in photosynthetic rates could potentially be attributed to an increased occurrence of photorespiration, which reduces photosynthetic efficiency. Photorespiration competes with photosynthesis for the same substrate (RuBP) during the Calvin-Benson cycle and incurs an energy cost (JIANG et al., 2023; TIMM; HAGEMANN, 2020). In C_3 plants, atmospheric carbon is promptly fixed into three-carbon molecules within the chloroplast stroma through the Calvin-Benson cycle. Unlike in C_4 plants, there is no inherent carbon storage within the cellular structure of the plant leaf. Therefore, under conditions of low Ci concentration, RuBisCO may inadvertently fix atmospheric O_2, catalyzing the counterproductive oxygenation reaction of RuBP. This phenomenon underscores the challenges posed by low Ci concentrations in the photosynthetic process of C_3 plants (TAIZ et al., 2017).

Hence, in the current investigation conducted under conditions of current atmospheric CO_2 and water deficit (C400DH), the significantly low Ci levels observed can give rise to photorespiration, consequently diminishing photosynthetic rates. Furthermore, the subdued photosynthetic rates observed in Jack bean under C400DH and particularly in the C700DH treatments are further justified by elevated temperatures, resulting in higher leaf temperatures (Tl) compared to the C400DH treatment. This elevated thermal stress may have exacerbated the adverse effects of water deficit on plants, influencing the photosynthetic response. In warmer environments, the balance tends to shift away from photosynthesis toward photorespiration. Under such conditions, CO_2 solubility significantly decreases, the oxygenase activity of RuBisCo surpasses the carboxylase activity, and stomata close to conserve water, consequently reducing CO_2 concentration around the active site of RuBisCo (TAIZ et al., 2017).

Regarding stomatal conductance, C_3 and C_4 species responded as expected, as the treatments did not yield significant differences in this variable for Sudan grass (C_4), but produced clear effects in Jack bean (C_3). For this species, stomatal conductance was higher under elevated levels of CO_2 and irrigation (C700IR) and lower under conditions of elevated CO_2 and water deficit (C700DH). Species of C_3 plants have a substantial water requirement, particularly in warm and arid environments where they face a functional dilemma: the reduction of stomatal aperture. Apart from controlling CO_2 flux, the stomatal apparatus in plants also regulates water flux. In an effort to minimize water loss through transpiration, C_4 plants employ a mechanism to store CO_2 as malate, allowing for organic synthesis without compromising stomatal conductance. However, C_3 plants lack this mechanism and lose water by keeping stomata open for photosynthesis. Consequently, under water stress, C_3 plants need to decrease the frequency of stomatal opening (TAIZ et al., 2017). Nevertheless, while C_3 plants generally undergo a reduction in stomatal conductance with increasing CO_2 levels, the photosynthetic limitation due to stomatal factors diminishes (ZHANG et al., 2018) owing to the ample availability of atmospheric CO_2. In this study, for instance, Jack bean (C_3) under elevated CO_2 concentration and water deficit (C700DH) exhibited high Ci despite its low stomatal conductance. However, this trend did not hold true under the current CO_2 concentration (C400DH).

Stomata are additionally linked to transpiration, the process by which plants release water vapor into the atmosphere. This occurs primarily through diffusion via the stomatal openings, contributing to the regulation of plant temperature (TAIZ et al., 2017). The cooling effects of transpiration are crucial, considering that photosynthesis is a temperature-dependent process. Additionally, extreme leaf temperatures can adversely affect plant growth and development (SAGE; KUBIEN, 2007). Plants strategically mitigate water loss from leaves by modulating the transpiration rate, especially in response to short-term water stress conditions (FAN et al., 2020). Additionally, the presence of elevated CO_2 concentrations has the potential to alleviate or counteract the adverse effects of water stress on plants by reducing the leaf transpiration rate (CHAVES et al., 2012). Our findings not only support this notion but also reveal lower transpiration rates in plants subjected to water stress. This phenomenon persisted even in the case of Sudan grass, where there were no discernible differences in stomatal conductance values.

As mentioned earlier, transpiration directly influences leaf temperature. Our results demonstrate that higher leaf temperatures were manifested by species grown in chambers with elevated CO_2 concentrations. These chambers also exhibited the highest air temperatures. The

elevated leaf temperatures of species under the C700DH treatment may have been accentuated by the observed lower (compared to C700IR) transpiration rates. Those rates followed a similar pattern to photosynthetic rates, and consequently, no significant difference was observed in Water Use Efficiency (WUE), which represents the relationship between these two variables. This finding contrasts with those reported by Sreeharsha et al. (2019), who noted a significant increase in WUE in Pigeon pea species due to elevated CO_2-induced photosynthetic rates. It also deviates from the findings of Fan et al. (2020), who reported high WUE in bell peppers even under water stress.

4.3. Plants' emergency and growth

The growth and dry matter variables did not exhibit statistically significant differences among the treatments; however, a discernible pattern emerged in plant responses. Notably, the treatment involving irrigation and CO_2 injection beyond current levels appeared to be detrimental to Pigeon pea (C_3) while favoring the development of Jack bean (C_3) and Sudan grass (C_4). Kimani et al. (1994) assessed Pigeon pea development under varying water stress levels in ambient CO_2 and demonstrated its considerable drought resistance. However, they consistently reported lower development of Pigeon pea under stress compared to those developed under full water availability. Moreover, Sreeharsha et al. (2015) reported a significant increase in biomass for growth parameters under elevated atmospheric CO_2 (550 ppm) and temperatures ranging from 21.25 to 31.2°C for the evaluated species. The alleviation of damage resulting from water deficit was also observed with the rise in atmospheric CO_2 levels (SREEHARSHA et al., 2019). Those findings contrasted with the present study. The discrepancy may be explained by the temperature in chambers under the irrigated treatment (C700IR), which reached 48°C.

Extremely high temperatures induce thermal stress, potentially leading to photoinhibition, protein loss and plant damages, compromising their growth and yield (FIRMANSYAH; ARGOSUBEKTI, 2020; SAGE; KUBIEN, 2007). Although the optimal thermal range for C_3 plants is 20-35°C (SAGE; WAY; KUBIEN, 2008), and for C_4 plants it is between 30-40°C (MASSAD; TUZET; BETHENOD, 2007), plants originating from hot climates, like the tropical species evaluated here, typically photosynthesize in the thermal range of 15 to 45°C without apparent issues (SAGE; KUBIEN, 2007). Plants can also acclimate in response to abiotic changes in the environment, maintaining or increasing their development beyond these thermal limits. However, the photosynthetic acclimation limit for tropical species

remains unclear. In the current study, it is plausible that, within the C700IR chambers, the species either did not acclimate completely, which is typically observed in tropical plants (SLOT; KITAJIMA, 2015), or reached the temperature limit for acclimatization, a limit that can be higher for the other evaluated species. The absence of physiological variables for this species precludes drawing definitive inferences in this regard.

From an ecological standpoint, the more vigorous development of other species in the chambers may have hindered Pigeon pea due to interspecific competition. Evidence, such as the significantly lower number of individuals recruited under these conditions, endorses this hypothesis. Climate change is inducing natural species selection beginning with competition amongst individuals (MAGALHÃES; AMOROSO; LARSON, 2021). Studies have revealed differences between the responses of species growing in isolation and those in competition (POORTER; NAVAS, 2003; ZISKA; BUNCE, 2006). Therefore, in addition to efforts to predict the response of individual plants to climate change, it is vital to support and encourage large-scale and more integrative studies.

In this discussion, it is important to highlight that many studies point to the increased growth and productivity of plant species under high concentrations of CO_2, known as the "CO_2 effect". Fan et al. (2020) reported a strong effect of atmospheric CO_2 at elevated concentrations on the biomass production of chili pepper individuals in their study. According to the authors, this effect remains notable under conditions of low and moderate water stress but does not hold under severe water stress. In the present study, although water deficit was associated with poorer results in Jack bean and Sudan grass species, it was not sufficient to produce a significant difference between treatments. It is worth noting that the species evaluated here are native to tropical regions and are recognized for their special adaptability to low-fertility, hot, and dry environments. For this reason, exotic Fabaceae species are commonly selected to be part of the seed mix used for land reclamation in Brazilian mining areas, when their use is technically justified (DAS CHAGAS et al., 2024).

With respect to atmospheric CO_2 increment, it is known that it can be extremely beneficial for C_3 plants as it enhances the CO_2 gradient between air and leaf, ensuring higher intracellular CO_2 concentration (Ci) in these species, thereby reducing photorespiration rates (TAIZ et al., 2017; ZISKA; BUNCE, 2006). Several beneficial effects of CO_2 observed in different studies, including the amplification of C_3 plant growth (ZISKA; BUNCE, 2006). On the other hand, in theory, C_4 species should not benefit from the increase in atmospheric CO_2 concentration since they naturally have a CO_2 concentration system near-saturation around the RuBisCO sites, limiting photorespiration even in situations of lower atmospheric CO_2

concentrations (TAIZ et al., 2017). However, significant effect of increased CO_2 on the development of these species have been disclosed (ZISKA; BUNCE, 2006). Wand et al. (2001), for example, reported a significant increase in total biomass in C_3 (44%) and C_4 (33%) grass species under elevated CO_2 concentrations, with C_3 species exhibiting higher tillering and C_4 species having a larger leaf area.

While there is indeed a discernible positive trend in the growth and dry matter increment for Jack bean and Sudan grass under irrigation and elevated CO_2 (C700IR), it did not reach statistical significance. This results in aligned with those of de Souza et al. (2015), who reported the lack of repose in growth and dry matter parameters of Sorghum (C_4) to elevated CO_2 and drought in an OTC experiment. However, as elucidated in the preceding section, a noteworthy increase in photosynthetic rates was observed in plants subjected to the C700IR treatment, yet this enhancement did not manifest in heightened stature or augmented biomass production. This incongruity may be attributed to the intricate process of photoassimilate partitioning, whereby additional carbon is allocated to structures associated with limiting resources, particularly the root system (LAL et al., 2022).

In an atmosphere enriched with CO_2, where carbon is no longer a constraining factor for photosynthesis and plant growth, the limiting factors shift to nutrients and water availability. Consequently, under such conditions, there is a general tendency for the root-to-shoot ratio to increase (LAL et al., 2022; ZISKA; BUNCE, 2006). However, in the context of the present study, it appears that carbon allocation might not be the sole influencing factor, given the absence of discernible differences in Water Use Efficiency (WUE) (A/E). A more plausible explanation for the observed outcomes could be the imposition of extreme temperatures, subjecting the plants to heat stress. In tropical regions, excessive radiation and elevated temperatures frequently pose constraints on plant growth and yields (FIRMANSYAH; ARGOSUBEKTI, 2020). Under heat stress, plants redirect a significant portion of their energy resources to sustain crucial cellular processes. This includes the synthesis of heat shock proteins, temperature regulation, and the modulation of genes to activate signaling pathways (FIRMANSYAH; ARGOSUBEKTI, 2020; JHA; BOHRA; SINGH, 2014). This reallocation of energy comes at the expense of the plant's own growth.

5. CONCLUSIONS AND RECOMMENDATIONS

In this experiment conducted in the Amazon biome, within the equatorial belt with high incidence of sunlight, the use of open-top chambers was responsible for generating a

microclimate distinct from the external environment, particularly in terms of temperature, which reached extremely high values, causing thermal stress. This represents a drawback of this methodology for assessing the impact of elevated atmospheric CO_2 in the field.

Our study revealed no evidence that some of the fast-growing exotic species typically included in the seed mix used for reclamation of degraded mining areas are deeply affected by the increase in atmospheric CO_2 and intense drought events—at least regarding height growth and biomass production. As known, the evaluated species exhibit significant resistance to water stress and low-fertility soils, characteristics that underlie their selection for land reclamation efforts. Conversely, evidence emerged of the vulnerability of these species to extreme heat, which can also occur due to the climate change and its effects on the frequency of extreme climate events. Beneficial effects of fertilization, potentially stimulated by higher atmospheric CO_2 concentrations and simultaneous irrigation, may have been overshadowed by the extreme chamber temperatures, especially those under the C700IR treatment.

Despite the limited impact of the evaluated environmental factors on plant height and dry matter, attention is drawn to a significant impact on the emergence of Pigeon pea individuals, which halved in resource-rich environments (elevated CO_2 and irrigation). This is likely a result of interspecific competition within the chambers and may signal a change in the developing vegetation composition. It is crucial to note that the three species assessed in this study are just a subset of a diverse seed mix, encompassing numerous other species. In this regard, we also demonstrate the importance of conducting integrated studies that aim to evaluate plant responses at the community or ecosystem level. The growth positive responses, often significant in isolated assessments as reported in the literature, were not held in this study.

Furthermore, we encourage the conduct of similar studies that assess native species included in the seed mix, as well as the root systems of these species. Such research would contribute to even more robust conclusions, thereby collaborating with environmental sustainability efforts in the Amazon Rainforest and worldwide.

REFERENCES

ALLEN, L. H. et al. Elevated CO_2 increases water use efficiency by sustaining photosynthesis of water-limited maize and sorghum. **Journal of Plant Physiology**, v. 168, n. 16, p. 1909–1918, nov. 2011.

ARIAS, P. A. et al. Technical Summary. Em: MASSON-DELMOTTE, V., et al. (Eds.). **Climate Change 2021 – The Physical Science Basis. Contribution of Working Group I to the Sixth Assessment Report of the Intergovernmental Panel on Climate Change**.

Cambridge, United Kingdom and New York, NY, USA: Cambridge University Press, 2023. p. 35–144.

BOCHOW, N.; BOERS, N. The South American monsoon approaches a critical transition in response to deforestation. **Science Advances**, v. 9, n. 40, 6 out. 2023.

CHAVES, M. M. et al. Photosynthesis under water deficits, flooding and salinity. Em: **Terrestrial Photosynthesis in a Changing Environment**. [s.l.] Cambridge University Press, 2012. p. 299–311.

CRAFTS-BRANDNER, S. J.; SALVUCCI, M. E. Sensitivity of Photosynthesis in a **C_4** Plant, Maize, to Heat Stress. **Plant Physiology**, v. 129, n. 4, p. 1773–1780, 1 ago. 2002.

DA CRUZ, D. C. et al. An overview of forest loss and restoration in the Brazilian Amazon. **New Forests**, v. 52, n. 1, p. 1–16, 3 jan. 2021.

DAS CHAGAS, H. S. et al. Plant growth and metabolism of exotic and native Crotalaria species for mine land rehabilitation in the Amazon. **Journal of Forestry Research**, v. 35, n. 1, p. 27, 23 dez. 2024.

DE SOUZA, A. P. et al. Changes in Whole-plant metabolism during grain-filling stage in *Sorghum bicolor L.* (Moench) grown under elevated CO_2 and drought. **Plant Physiology**, p. pp.01054.2015, 2 set. 2015.

FAN, X. et al. Carbon dioxide fertilization effect on plant growth under soil water stress associates with changes in stomatal traits, leaf photosynthesis, and foliar nitrogen of bell pepper (Capsicum annuum L.). **Environmental and Experimental Botany**, v. 179, 1 nov. 2020.

FERNANDES, T. et al. Detecção e análise de focos de calor no município de Parauapebas-PA, Brasil por meio da aplicação de geotecnologia. **Enciclopédia biosfera**, v. 15, n. 28, p. 398, 2018.

FIRMANSYAH; ARGOSUBEKTI, N. A review of heat stress signaling in plants. **IOP Conference Series: Earth and Environmental Science**, v. 484, n. 1, p. 012041, 1 abr. 2020.

GASTAUER, M. et al. Mine land rehabilitation in Brazil: Goals and techniques in the context of legal requirements. **Ambio**, v. 48, n. 1, p. 74–88, 11 jan. 2019.

HELD, I. M.; SODEN, B. J. Water Vapor Feedback and Global Warming. **Annual Review of Energy and the Environment**, v. 25, n. 1, p. 441–475, nov. 2000.

JHA, U. C.; BOHRA, A.; SINGH, N. P. Heat stress in crop plants: its nature, impacts and integrated breeding strategies to improve heat tolerance. **Plant Breeding**, v. 133, n. 6, p. 679–701, 27 dez. 2014.

JIANG, X. et al. The role of photorespiration in plant immunity. **Frontiers in Plant Science**, v. 14, 1 fev. 2023.

KIMANI, P. M.; BENZIONI, A.; VENTURA, M. Genetic variation in pigeon pea (Cajanus cajan (L.) Mill sp.) in response to successive cycles of water stress. **Plant and Soil**, v. 158, n. 2, p. 193–201, jan. 1994.

LAL, M. K. et al. From source to sink: mechanistic insight of photoassimilates synthesis and partitioning under high temperature and elevated [CO_2]. **Plant Molecular Biology**, v. 110, n. 4–5, p. 305–324, 24 nov. 2022.

LUCAS, E. W. M. et al. Trends in climate extreme indices assessed in the Xingu river basin - Brazilian Amazon. **Weather and Climate Extremes**, v. 31, p. 100306, mar. 2021.

MAGALHÃES, J. G. DE S.; AMOROSO, M. M.; LARSON, B. C. What evidence exists on the effects of competition on trees' responses to climate change? A systematic map protocol. **Environmental Evidence**, v. 10, n. 1, p. 34, 11 dez. 2021.

MASSAD, R.-S.; TUZET, A.; BETHENOD, O. The effect of temperature on **C_4**-type leaf photosynthesis parameters. **Plant, Cell & Environment**, v. 30, n. 9, p. 1191–1204, 4 set. 2007.

MATLABA, V. J. et al. Socioeconomic dynamics of a mining town in Amazon: a case study from Canaã dos Carajás, Brazil. **Mineral Economics**, v. 32, n. 1, p. 75–90, 23 abr. 2019.

MU, Y.; JONES, C. An observational analysis of precipitation and deforestation age in the Brazilian Legal Amazon. **Atmospheric Research**, v. 271, p. 106122, jun. 2022.

OMETTO, J. P., et al. Tropical Forests. Em: PÖRTNER, H.-O. et al. (Eds.). **Climate Change 2022: Impacts, Adaptation and Vulnerability. Contribution of Working Group II to the Sixth Assessment Report of the Intergovernmental Panel on Climate Change**. Cambridge, UK and New York, NY, USA: Cambridge University Press, 2022. p. 2369–2410.

POORTER, H.; NAVAS, M. Plant growth and competition at elevated CO_2 : on winners, losers and functional groups. **New Phytologist**, v. 157, n. 2, p. 175–198, 24 fev. 2003.

RAMOS, S. J. et al. Changes in soil properties during iron mining and in rehabilitating minelands in the Eastern Amazon. **Environmental Monitoring and Assessment**, v. 194, n. 4, p. 256, 7 abr. 2022.

SAEG. **Sistema para Análises Estatísticas**. ViçosaFundação Arthur Bernardes - UFV, 2007.

SAGE, R. F.; KUBIEN, D. S. The temperature response of C_3 and C_4 photosynthesis. **Plant, Cell & Environment**, v. 30, n. 9, p. 1086–1106, set. 2007.

SAGE, R. F.; WAY, D. A.; KUBIEN, D. S. Rubisco, Rubisco activase, and global climate change. **Journal of Experimental Botany**, v. 59, n. 7, p. 1581–1595, maio 2008.

SANTOS, J. R. N. et al. TENDÊNCIAS DE EXTREMOS CLIMÁTICOS NA REGIÃO DE TRANSIÇÃO AMAZÔNIA-CERRADO NO ESTADO DO MARANHÃO. **Revista Brasileira de Climatologia**, v. 26, 14 fev. 2020.

SHERWOOD, S. C.; DIXIT, V.; SALOMEZ, C. The global warming potential of near-surface emitted water vapour. **Environmental Research Letters**, v. 13, n. 10, p. 104006, 27 set. 2018.

SILVA, J. B. L. DA et al. Influences of two CO_2 concentrations and water availability on bean crop. **Engenharia Agrícola**, v. 33, n. 4, p. 730–738, ago. 2013.

SILVA, J. B. L. DA et al. Desenvolvimento de estrutura experimental para estudos de mudanças climáticas em culturas agrícolas. **Brazilian Journal of Animal and Environmental Research**, v. 3, n. 3, p. 2258–2264, 2020.

SILVA, R. G. DA; ALVES, R. DE C.; ZINGARETTI, S. M. Increased [CO_2] Causes Changes in Physiological and Genetic Responses in **C_4** Crops: A Brief Review. **Plants**, v. 9, n. 11, p. 1567, 13 nov. 2020.

SLOT, M.; KITAJIMA, K. General patterns of acclimation of leaf respiration to elevated temperatures across biomes and plant types. **Oecologia**, v. 177, n. 3, p. 885–900, 7 mar. 2015.

SREEHARSHA, R. V. et al. Mitigation of drought-induced oxidative damage by enhanced carbon assimilation and an efficient antioxidative metabolism under high CO_2 environment in pigeonpea (Cajanus cajan L.). **Photosynthesis Research**, v. 139, n. 1–3, p. 425–439, 22 mar. 2019.

SREEHARSHA, R. V.; SEKHAR, K. M.; REDDY, A. R. Delayed flowering is associated with lack of photosynthetic acclimation in Pigeon pea (Cajanus cajan L.) grown under elevated CO_2. **Plant Science**, v. 231, p. 82–93, fev. 2015.

TAIZ, L. et al. **Fisiologia e desenvolvimento vegetal**. 6. ed. Porto Alegre: artmed, 2017.
TEIXEIRA, P. C. et al. **Manual de Métodos de Análise de Solo**. 3 rev. e ampl ed. Brasília, DF: Embrapa, 2017.

TIMM, S.; HAGEMANN, M. Photorespiration—how is it regulated and how does it regulate overall plant metabolism? **Journal of Experimental Botany**, v. 71, n. 14, p. 3955–3965, 6 jul. 2020.

TORRES, M. **Painel científico para a Amazônia participa da COP 27**.

WAND, S. J. E. et al. Responses of wild C_4 and C_3 grass (Poaceae) species to elevated atmospheric CO $_2$ concentration: a meta-analytic test of current theories and perceptions. **Global Change Biology**, v. 5, n. 6, p. 723–741, 24 ago. 2001.

ZHANG, J. et al. The Responses of Plant Leaf CO_2/H_2O Exchange and Water Use Efficiency to Drought: A Meta-Analysis. **Sustainability**, v. 10, n. 2, p. 551, 21 fev. 2018.

ZISKA, L. H.; BUNCE, J. A. Plant Responses to Rising Atmospheric Carbon Dioxide. Em: **Plant Growth and Climate Change**. [s.l.] Wiley, 2006. p. 17–47.

APPENDIX

Fig. S1 Dimensions and structural details of the open-top chambers **(a)**; Chamber with a single module and a bell jar at the top **(b)**; Distribution of the nine chambers with two modules each, spaced 2 m apart in the experimental site **(c)**

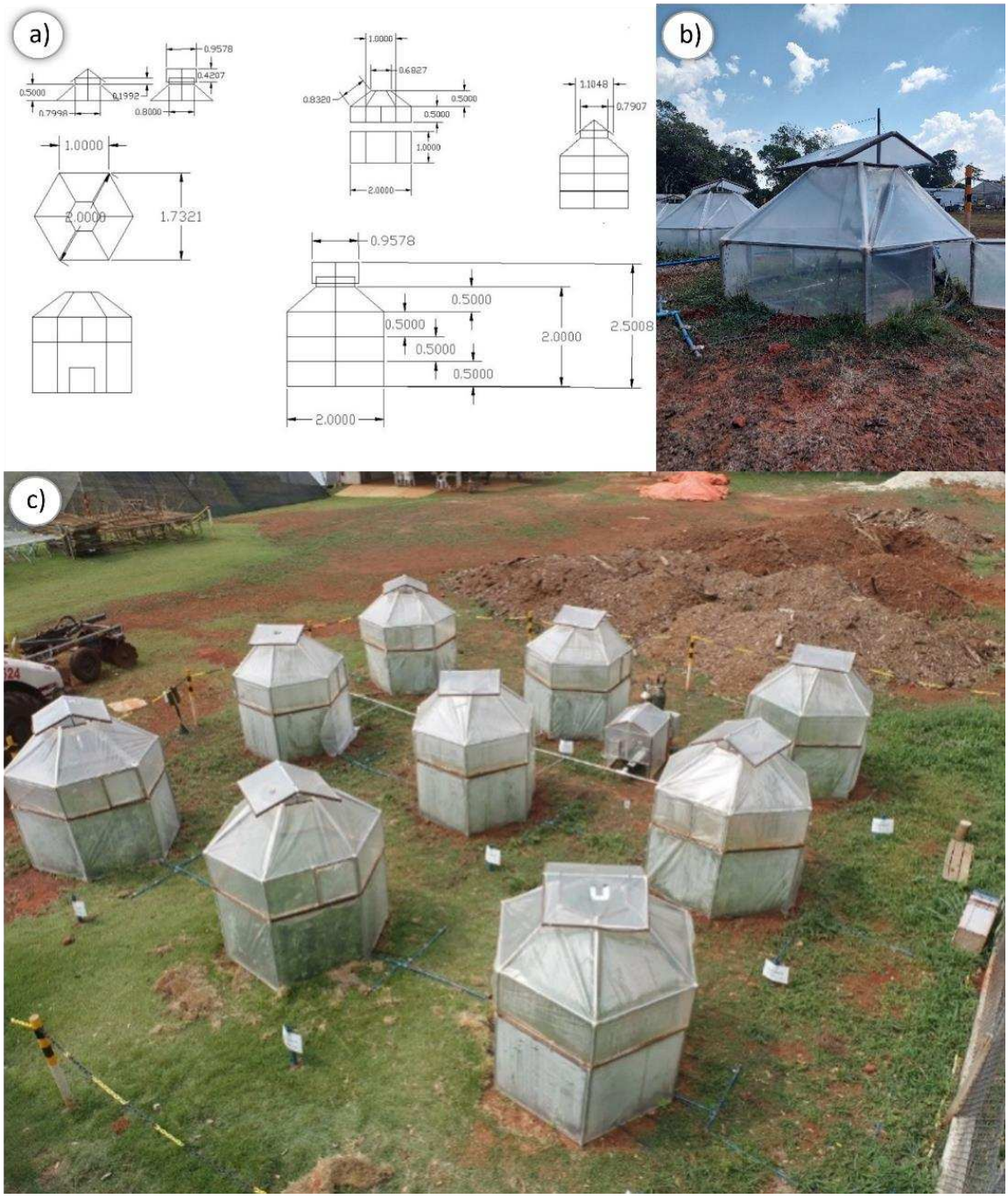

Own authorship

Table S1 – List of species sown in the chambers of the study, segmented into native and exotic categories

Sp. Code	Family	Scientific name	Commom name	Category
1	Asteraceae	*Vernonanthura brasiliana*	Assa-peixe-do-pará	native
2	Asteraceae	*Vernonanthura brasiliana*	Assa-peixe-do-pará	native
3	Fabaceae	*Bauhinia acreana*	Capa-bode	native
4	Verbenacaea	*Lantana camara*	Chumbinho	native
5	Verbenacaea	*Lantana camara*	Chumbinho	native
6	Verbenaceae	*Lantana camara*	Chumbinho	native
7	Verbenaceae	*Lantana camara*	Chumbinho	native
8	Urticaceae	*Cecropia obtusa*	Embaúba-branca	native
9	Urticaceae	*Cecropia obtusa*	Embaúba-branca	native
10	Urticaceae	*Cecropia pachystachya*	Embaúba-do-brejo	native
11	Urticaceae	*Cecropia sp*	Embaúba-fruto-verde	native
12	Urticaceae	*Cecropia sp*	Embaúba-fruto-verde	native
13	Urticaceae	*Cecropia purpuracens*	Embaúba-roxa	native
14	Urticaceae	*Cecropia purpuracens*	Embaúba-roxa	native
15	Urticaceae	*Cecropia purpuracens*	Embaúba-roxa	native
16	Urticaceae	*Cecropia distachya*	Embaúba-vermelha	native
17	Urticaceae	*Cecropia distachya*	Embaúba-vermelha	native
18	Fabaceae	*Senegalia polyphylla*	Espinheiro-preto	native
19	Fabaceae	*Senegalia polyphylla*	Espinheiro-preto	native
20	Fabaceae	*Senegalia polyphylla*	Espinheiro-preto	native
21	Fabaceae	*Senegalia polyphylla*	Espinheiro-preto	native
22	Fabaceae	*Senegalia polyphylla*	Espinheiro-preto	native
23	Fabaceae	*Senegalia polyphylla*	Espinheiro-preto	native
24	Fabaceae	*Senegalia polyphylla*	Espinheiro-preto	native
25	Fabaceae	*Senna alata r*	Fedegoso-gigante	native
26	Fabaceae	*Senna alata r*	Fedegoso-gigante	native
27	Fabaceae	*Senna ungulata*	Fedegoso-pequeno	native
28	Fabaceae	*Senna ungulata*	Fedegoso-pequeno	native
29	Fabaceae	*Senna ungulata*	Fedegoso-pequeno	native
30	Fabaceae	*Senna ungulata*	Fedegoso-pequeno	native
31	Fabaceae	*Senna ungulata*	Fedegoso-pequeno	native
32	Fabaceae	*Senna ungulata*	Fedegoso-pequeno	native
33	Boraginaceae	*Cordia bicolor*	Freijó-branco-folha-grande	native
34	Moraceae	*Ficus catappifollia*	Gameleira	native
35	Moraceae	*Ficus guianensis*	Gameleira-do-alto	native
36	Moraceae	*Ficus guianensis*	Gameleira-do-alto	native
37	Moraceae	*Ficus guianensis*	Gameleira-do-alto	native
38	Moraceae	*Ficus guianensis*	Gameleira-do-alto	native
39	Moraceae	*Ficus insipida*	Gameleira-do-baixo	native
40	Moraceae	*Ouratea castaneifolia*	Gameleira-do-carrasco	native
41	Onagraceae	*Ludwigia tomentosa*	Gengelim-da-canga	native

To be continued

Continuation of Table S1

Sp. Code	Family	Scientific name	Commom name	Category
42	Solanaceae	*Solanum crinitum*	Jurubeba	native
43	Solanaceae	*Solanum crinitum*	Jurubeba	native
44	Solanaceae	*Solanum crinitum*	Jurubeba	native
45	Solanaceae	*Solanum crinitum*	Jurubeba	native
46	Solanaceae	*Solanum crinitum*	Jurubeba	native
47	Solanaceae	*Solanum crinitum*	Jurubeba	native
48	Solanaceae	*Solanum crinitum*	Jurubeba	native
49	Solanaceae	*Solanum crinitum*	Jurubeba	native
50	Solanacea	*Solanum sp*	Jurubeba-fruto-rajado	native
51	Hypericaceae	*Vismia guianensis*	Lacre-vermelho-folha-miuda	native
52	Hypericaceae	*Vismia guianensis*	Lacre-vermelho-folha-miuda	native
53	Fabaceae	*Mimosa camporum*	Maliça-camporum	native
54	Fabaceae	*Aeschynomene americana*	Maliça-da-canga	native
55	Fabaceae	*Aeschynomene americana*	Maliça-da-canga	native
56	Fabaceae	*Aeschynomene americana*	Maliça-da-canga	native
57	Verbanaceae	*Lippia grata*	Malva-da-canga	native
58	Fabaceae	*Mimosa acutistipula var.ferrea*	Mimosa-da-canga	native
59	Fabaceae	*Mimosa acutistipula var.ferrea*	Mimosa-da-canga	native
60	Fabaceae	*Mimosa acutistipula var.ferrea*	Mimosa-da-canga	native
61	Fabaceae	*Mimosa acutistipula var.ferrea*	Mimosa-da-canga	native
62	Fabaceae	*Mimosa acutistipula var.ferrea*	Mimosa-da-canga	native
63	Fabaceae	*Mimosa acutistipula var.ferrea*	Mimosa-da-canga	native
64	Fabaceae	*Dioclea apurensis*	Mucunã-da-canga	native
65	Fabaceae	*Dioclea apurensis*	Mucunã-da-canga	native
66	Fabaceae	*Dioclea apurensis*	Mucunã-da-canga	native
67	Fabaceae	*Dioclea apurensis*	Mucunã-da-canga	native
68	Malpighiaceae	*Byrsonima spicata*	Muricí-da-canga	native
69	Malpighiaceae	*Byrsonima spicata*	Muricí-da-canga	native
70	Fabaceae	*Senna occidentalis*	Pajamarioba	native
71	Fabaceae	*Bauhinia ungulata*	Pata-de-vaca-da-folha-miúda	native
72	Fabaceae	*Bauhinia longipedicellata*	Pata-de-vaca-folha-grande	native
73	Malvaceae	*Apeiba peteumo*	Pente-de-macaco-folha-aspera	native
74	Malvaceae	*Apeiba peteumo*	Pente-de-macaco-folha-aspera	native
75	Malvaceae	*Apeiba peteumo*	Pente-de-macaco-folha-aspera	native
76	Malvaceae	*Apeiba peteumo*	Pente-de-macaco-folha-aspera	native
77	Malvaceae	*Apeiba peteumo*	Pente-de-macaco-folha-aspera	native
78	Malvaceae	*Apeiba peteumo*	Pente-de-macaco-folha-aspera	native
79	Malvaceae	*Apeiba peteumo*	Pente-de-macaco-folha-aspera	native
80	Malvaceae	*Apeiba peteumo*	Pente-de-macaco-folha-aspera	native
81	Malvaceae	*Apeiba peteumo*	Pente-de-macaco-folha-aspera	native
82	Malvaceae	*Apeiba peteumo*	Pente-de-macaco-folha-aspera	native

To be continued

Conclusion of Table S1

Sp. Code	Family	Scientific name	Commom name	Category
83	Malvaceae	*Apeiba peteumo*	Pente-de-macaco-folha-aspera	native
84	Lecythidaceae	*Eschweilera ovata*	Tauari	native
85	Bixaceae	*Bixa orellana r*	Urucum-vermelho	native
86	Bixaceae	*Bixa arborea v*	Urucum-do-baixo	native
87	Asteraceae	*Lepidaploa arenaria r*	Vernônia-da-canga	native
88	Asteraceae	*Lepidaploa arenaria r*	Vernônia-da-canga	native
89	Asteraceae	*Lepidaploa arenaria r*	Vernônia-da-canga	native
90	Asteraceae	*Lepidaploa arenaria r*	Vernônia-da-canga	native
91	Fabaceae	*Cajanus cajan*	Feijão-guandu	exotic
92	Fabaceae	*Canavalia ensiformis*	Feijão-de-porco	exotic
93	Fabaceae	*Crotalaria juncea*	Crotalária	exotic
94	Poaceae	*Avena strigosa*	Aveia-preta	exotic
95	Fabacea	*Cassia occidentalis*	Fedegoso	native
96	Brassicaceae	*Rafhanus sativus*	Nabo-forrageiro	exotic
97	Asteraceae	*Helianthus annuus*	Girassol	exotic
98	Poaceae	*Sorghum sudanense*	Capim-sudão	exotic

Sp. Code: Specie code (identifier)

Table S2 – Summary of the Analysis of Variance (ANOVA) for the physiological variables Net Photosynthesis (A), Stomatal Conductance (gs), CO_2 Concentration in the Sub-stomatal Chamber (Ci), Transpiration (E), Vapor Pressure Deficit (VpdL), Leaf Temperature (T_l), the ratio between Ci and atmospheric CO_2 concentration (Ci/Ca), and Water Use Efficiency (WUE) based on the treatments (TR) and species (SP) evaluated in the experiment. Note that these physiological attributes were exclusively assessed in Jack Bean and Sudan Grass.

SV	df	Mean square							
		A	gs	Ci	E	VpdL	T_l	Ci/Ca	WUE
TR	2	836.06**	0.06*	46.880.30**	56.21**	4.45**	91.00**	0.02^{NS}	0.12^{NS}
Error (a)	15	14.27	0.01	5.141.74	2.06	0.30	3.79	0.02	0.65
SP	1	32.65^{NS}	3.66**	738.214.10**	585.20**	24.69**	169.20**	2.91**	122.12**
TRxSP	2	41.75^{NS}	0.02^{NS}	6.092.48^{NS}	2.41^{NS}	0.27^{NS}	0.64^{NS}	0.01^{NS}	0.75^{NS}
Error (b)	15	27.98	0.02	7.886.50	3.94	0.27	1.77	0.03	0.77
CV Main plot (%)	-	14.76	27.08	25.40	16.99	20.88	6.14	23.56	20.10
CV Subplot (%)	-	20.67	32.10	31.45	23.48	19.85	4.19	28.64	21.99

SV: Source of variation; df: degrees of freedom; TR: Treatments; SP: Species; CV: Coefficient of variation
^{NS} Non-significant at least at 5% by Tukey's test.
* Significant at 5% by Tukey's test.
** Significant at 1% by Tukey's test.

Table S3 – Summary of the Analysis of Variance (ANOVA) for the final height (Hf) and diameter (Φf) variables based on the treatments (TR) and species (ESP) assessed in the experiment

		Mean Square	
SV	**df**	**Hf**	**Φf**
TR	2	580.0648^{NS}	0.01607569 ^{NS}
Error (a)	6	1621.343	0.019
SP	2	3559.419 ^{NS}	0.01587708 ^{NS}
TRxSP	4	2225.502 ^{NS}	0.02072049 ^{NS}
Error (b)	12	1619.881	0.011
CV Main plot (%)		28.724	23.037
CV Subplot (%)		28.712	17.919

SV: Source of variation; df: degrees of freedom; TR: Treatments; SP: Species; CV: Coefficient of variation
^{NS} Non-significant at least at 5% by Tukey's test.

Fig. S2 Stem etiolation observed in different individuals of Sudan grass **(a, b,** and **c)** in the experiment

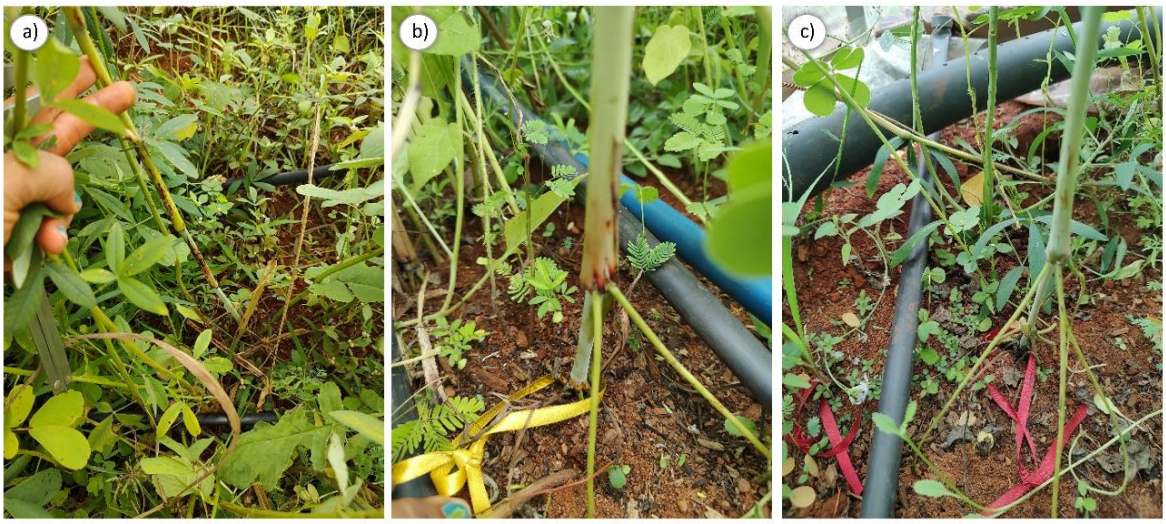

Own authorship

Table S4 – Summary of the Analysis of Variance (ANOVA) for the variables Number of individuals (IND), Stem dry mass (SDM), Leaf dry mass (LDM), Total dry mass (TDM), and Dry mass per plant (DMP) in relation to the treatments (TR) and species (SP) evaluated in the experiment.

		Mean square			
SV	**df**	**TDM**	**SDM**	**LDM**	**IND**
TR	2	2940.513 ^{NS}	5.110693 ^{NS}	1927.613 ^{NS}	193.4444^{NS}
Error (a)	6	34071.23	1604.50	20137.66	431.30
SP	2	188650.7*	11136.54*	125645.6*	7112.333**
TRxSP	4	68444.98 ^{NS}	3615.468 ^{NS}	37056.48 ^{NS}	933.6111^{NS}
Error (b)	12	46328.58	2685.51	26622.50	346.52
CV Main plot (%)		66.02	53.56	72.92	49.06
CV Subplot (%)		76.98	69.30	83.84	43.97

SV: Source of variation; df: degrees of freedom; TR: Treatments; SP: Species; CV: Coefficient of variation
^{NS} Non-significant at least at 5% by Tukey's test.
* Significant at 5% by Tukey's test.
** Significant at 1% by Tukey's test.